



University of Kentucky
UKnowledge

University of Kentucky Doctoral Dissertations

Graduate School

2008

ROLE OF THE REACTIVE OXYGEN SPECIES PEROXYNITRITE IN TRAUMATIC BRAIN INJURY

Ying Deng

University of Kentucky, Yingdeng_vd@hotmail.com

[Right click to open a feedback form in a new tab to let us know how this document benefits you.](#)

Recommended Citation

Deng, Ying, "ROLE OF THE REACTIVE OXYGEN SPECIES PEROXYNITRITE IN TRAUMATIC BRAIN INJURY" (2008). *University of Kentucky Doctoral Dissertations*. 667.
https://uknowledge.uky.edu/gradschool_diss/667

This Dissertation is brought to you for free and open access by the Graduate School at UKnowledge. It has been accepted for inclusion in University of Kentucky Doctoral Dissertations by an authorized administrator of UKnowledge. For more information, please contact UKnowledge@lsv.uky.edu.

ABSTRACT OF DISSERTATION

Ying Deng

The Graduate School

University of Kentucky

2007

ROLE OF THE REACTIVE OXYGEN SPECIES PEROXYNITRITE IN
TRAUMATIC BRAIN INJURY

ABSTRACT OF DISSERTATION

A dissertation submitted in partial fulfillment of the
requirements for the degree of Doctor of Philosophy in the
College of Medicine at the University of Kentucky

By

Ying Deng

Lexington, Kentucky

Director: Dr. Edward D. Hall, Professor of
Anatomy and Neurobiology, Neurology and Neurosurgery

Lexington, Kentucky

2007

Copyright © Ying Deng 2007

ABSTRACT OF DISSERTATION

ROLE OF THE REACTIVE OXYGEN SPECIES PEROXYNITRITE IN TRAUMATIC BRAIN INJURY

Reactive oxygen species (ROS) is cytotoxic to the cell and is known to contribute to secondary cell death following primary traumatic brain injury (TBI). We described in our study that PN is the main mediator for both lipid peroxidation and protein nitration, and occurred almost immediately after injury. As a downstream factor to oxidative damage, the peak of Ca²⁺-dependent, calpain-mediated cytoskeletal proteolysis preceded that of neurodegeneration, suggesting that calpain-mediated proteolysis is the common pathway leading to neuronal cell death. The time course study clearly elucidated the interrelationship of these cellular changes following TBI, provided window of opportunity for pharmacological intervention.

Furthermore, we conducted a pharmacological study to solidify our hypothesis. First of all, we tested the potency of a membrane permeable, catalytic scavenger of PN-derived free radicals, tempol for its ability to antagonize PN-induced oxidative damage. Tempol successfully inhibited PN-induced protein nitration at dosages of 30, 100 and 300mg/kg. Moreover, early single dose of 300mg/kg was administered and isolated mitochondria were examined for respiratory function and oxidative damage level. Our data showed that tempol reduced mitochondrial oxidative damage, and maintained mitochondrial function within normal limits, which suggested that tempol is efficiently permeable to mitochondrial membrane and mitochondrial oxidative damage is essential to mitochondrial dysfunction. Next, we found that calpain-mediated proteolysis is reduced at early treatment with a single dose of tempol. However, the effect of tempol on calpain is short-lived possibly due to systematic elimination. In our multiple dose study, tempol showed a significant inhibitory effect on SBDPs. Consequently, we measured neurodegeneration with the de Olmos aminocupric silver staining method at 7 days post-injury and detected a significant decrease of neuronal cell death.

Together, the time course study and pharmacological study strongly support the hypothesis that PN is the upstream mediator in secondary cell death in the CCI TBI mouse model. Moreover, inhibition of PN-mediated oxidative damage with the antioxidant, tempol, is able to attenuate multiple downstream

injury mechanisms. However, targeting PN alone may be clinically impractical due to its limited therapeutic window. This limitation may be overcome in future studies by a combination of multiple therapeutic strategies.

KEYWORDS: Traumatic brain injury, Peroxynitrite, Tempol, Mitochondrial dysfunction, Calpain-Mediated Proteolysis

Ying Deng

August 27, 2007

ROLE OF THE REACTIVE OXYGEN SPECIES PEROXYNITRITE IN
TRAUMATIC BRAIN INJURY

By

Ying Deng

Edward D. Hall

Director of Dissertation

Jane E. Joseph

Director of Graduate Study

August 27, 2007

RULES FOR THE USE OF DISSERTATION

Unpublished dissertations submitted for the Doctor's degree and deposited in the University of Kentucky Library are as a rule open for inspection, but are to be used only with due regard to the rights of the authors. Bibliographical references may be noted, but quotations or summaries of parts may be published only with the permission of the author, and with the usual scholarly acknowledgements.

Extensive copying or publications of dissertation in whole or in part also requires the consent of the Dean of the Graduate School of the University of Kentucky.

A library that borrows this dissertation for use by its patrons is expected to secure the signature of each user.

Name

Date

DISSERTATION

Ying Deng

The Graduate School
University of Kentucky

2007

ROLE OF THE REACTIVE OXYGEN SPECIES PEROXYNITRITE IN
TRAUMATIC BRAIN INJURY

DISSERTATION

A dissertation submitted in partial fulfillment of the
requirements for the degree of Doctor of Philosophy in the
College of Medicine at the University of Kentucky

By

Ying Deng

Lexington, Kentucky

Director: Dr. Edward D. Hall, Professor of
Anatomy and Neurobiology, Neurology and Neurosurgery

Lexington, Kentucky

2007

Copyright © Ying Deng 2007

谨以此文献给父母图华和问菊对我的养育与栽培。

ACKNOWLEDGEMENTS

This dissertation is the result of wonderful team work and excellent mentorship, and I would like to specially thank my dissertation chair, Dr. Edward D. Hall, Ph.D. for his patience, encouragement, and insightful guidance throughout my graduate work. I deeply appreciate his support for my endeavors and his constant source of wisdom and inspiration. I also would like to thank members of my dissertation committee, Dr. Patrick G. Sullivan, Ph.D.; Dr. James R. Pauly, Ph.D.; Dr. James W. Geddes, Ph.D.; Dr. Nada M. Porter, Ph.D.; and outside examiner Dr. Michael B. Reid, Ph.D, for their valuable comments, constructive critiques, and unwavering commitment to my academic development.

I would like to express my appreciation to the members of the Hall and Sullivan research laboratories who offer excellent expertise and precious friendship. I am also grateful to have wonderful staff members of the Integrated Biomedical Science graduate program, Department of Anatomy and Neurobiology, and Spinal Cord and Brain Injury Research Center, all of whom offer their generous help in my everyday life during my graduate study.

My deep thanks to my parents, Wenju and Tuhua, my Aunt Annie, Anita and Angela, my husband Ben, for their love and support; last, but not least, my friends in Kentucky and in China, for being there for me through the ups and downs of my life and for enriching my life.

The contents of Chapter Two have previously been published as an article in the Journal of *Experimental Neurology* titled, “Temporal Relationship of Peroxynitrite-Induced Oxidative Damage, Calpain-Mediated Cytoskeletal Degradation and Neurodegeneration after Traumatic Brain Injury”, by Ying Deng, Brian M. Thompson, Xiang Gao and Edward D. Hall, et al., 205(1):154-65, Copyright © 2007.

TABLE OF CONTENTS

Acknowledgements.....	iii
List of Figures.....	vii
Chapter One: Post-Traumatic Secondary Injury in Experimental Traumatic Brain Injury.....	1
Free Radicals Production and Oxidative Damage in Traumatic Brain Injury.....	1
Mitochondrial Dysfunction in Traumatic Brain Injury.....	20
Calpain-Mediated Cytoskeletal Proteolysis in Traumatic Brain Injury.....	24
The Relationship of Oxidative Damage, Mitochondrial Dysfunction, Calpain Activation and Neurodegeneration in Traumatic Brain Injury.....	28
Chapter Two: Temporal Relationship of Peroxynitrite-Induced Oxidative Damage, Calpain-Mediated Cytoskeletal Degradation and Neurodegeneration after Traumatic Brain Injury.....	32
Introduction.....	32
Materials and Methods.....	36
Results.....	45
Discussion.....	57
Chapter Three: Tempol in Its Ability to Scavenge Free Radicals, Ameliorate Mitochondrial Dysfunction and Inhibit Calpain Activity.....	68
Introduction.....	68
Materials and Methods.....	72
Results.....	81
Discussion.....	95
Chapter Four: Effect of Tempol on Behavioral Recovery and Neurodegeneration after Traumatic Brain Injury.....	104
Introduction.....	104
Materials and Methods.....	106
Results.....	112
Discussion.....	118
Chapter Five: Summary and Conclusions.....	124
Appendices.....	132
Reference.....	136

Vita.....150

LIST OF FIGURES

Figure 1.1 Simplified schematic of superoxide production from ETC.....	5
Figure 1.2 Biochemistry of ROS formation.....	14
Figure 1.3 Chemistry of initiation and propagation phases of cell membrane LP.....	16
Figure 1.4 Hypothetical interrelationship between mitochondrial PN-induced oxidative damage in neuronal mitochondria and the rest of the neuron, compromise of Ca ²⁺ homeostasis, calpain-mediated proteolysis and neurodegeneration.....	31
Figure 2.1 Slot-blotting studies in ipsilateral cortical traumatic brain injury tissues showing the temporal changes in protein nitration (3-nitrotyrosine; 3NT) and lipid peroxidation.....	47
Figure 2.2 Immunohistochemical (IHC) staining studies showing the time course and spatial extent of PN-induced 3NT and 4HNE at the epicenter (Bregma-2.0mm) of the injury site during the first 12 hrs compared to sham.....	49
Figure 2.3 High power photomicrographs of 3NT and 4HNE immunostaining in the contusion site in a sham, non-injured brain compared to staining at the contusion site at 1 hr after injury.....	50
Figure 2.4 Time course of the post-traumatic increase in calpain-mediated α -spectrin breakdown products in CCI cortical tissues.....	54
Figure 2.5 Time course of post-traumatic neurodegeneration in CCI model as revealed by the de Olmos silver staining technique.....	56
Figure 2.6 Hypothetical interrelationship between PN-induced oxidative damage in neuronal mitochondria and the rest of the neuron, compromise of Ca ²⁺ homeostasis, calpain-mediated proteolysis and neurodegeneration.....	67
Figure 3.1 Chemical structure of tempol.....	71
Figure 3.2 Tempol treatment studies using quantitative slotblotting in ipsilateral cortical traumatic brain injury tissues showing dose-response changes in protein nitration (3-nitrotyrosin, 3NT).....	82
Figure 3.3 Effect of optimal single dose tempol treatment on mitochondrial respiration in ipsilateral cortical traumatic brain injury tissues measured by Clarke-type electrode.....	86
Figure 3.4 Effect of optimal single dose tempol treatment on mitochondrial oxidative damage in ipsilateral cortical traumatic brain injury tissues measured by quantitative slotblotting.....	88
Figure 3.5 Effect of optimal single dose tempol treatment on	

calpain-mediated α -spectrin breakdown in ipsilateral cortical traumatic brain injury tissues measured by quantitative westernblotting.....	90
Figure 3.6 Effect of multiple dose tempol treatment on calpain-mediated α -spectrin breakdown in ipsilateral cortical traumatic brain injury tissues measured by quantitative westernblotting.....	92
Figure 3.7 Therapeutic window study using multiple doses of tempol measured by quantitative westernblotting.....	94
Figure 4.1 Behavioral outcome of multiple dose tempol treatment measured by neuroscore motor test after TBI.....	113
Figure 4.2 Histological evaluation of multiple dose tempol treatment on tissue sparing and silver staining in ipsilateral hemisphere after TBI.....	116
Figure 4.3 Histological evaluation of multiple dose tempol treatment on coronal brain section silver staining in ipsilateral hemisphere after TBI.....	117
Figure 4.4 Hypothetical interrelationship between PN-induced oxidative damage in neuronal mitochondria and the compromise of Ca^{2+} homeostasis, calpain-mediated proteolysis and neurodegeneration.....	123
Figure A.1 Time course of mitochondrial states III & IV respiratory rates in mouse ipsilateral cortex after severe (1.0mm) TBI	132
Figure A.2 Time course of lipid (HNE) and protein (protein carbonyl) oxidative damage in percoll-purified mitochondria from the ipsilateral cortex after a severe (1.0mm) TBI.....	133

Chapter One

Post-Traumatic Secondary Injury in Experimental Traumatic Brain Injury

Free Radicals Production and Oxidative Damage in Traumatic Brain Injury

Introduction

Oxygen is necessary for life. However, only about 85-90% of the O₂ taken up by mammalian cells is effectively utilized by their mitochondria for energy production. The remainder is converted to highly toxic reactive oxygen species (ROS) and their derived oxygen radicals which are damaging to cells. Following acute traumatic brain injury (TBI), oxidative stress leading to the formation of ROS and free radicals and oxidative alteration of brain tissue has been implicated as a common pathway following excitotoxicity. Excitotoxicity begins immediately after TBI, in which excessive excitatory amino acid, such as glutamate, is released into extracellular spaces and over-activates glutamate receptors, thereby inducing abnormal calcium influx (Faden, Demediuk et al. 1989). Moreover, other investigators showed that there is a prompt increase in free radicals that is essentially coincident with the release of glutamate proximate to the injury site, and there is a close correlation between the magnitudes of both events, suggesting that these two processes are part of a common pathways (Globus, Alonso et al. 1995). Furthermore, *in vitro* cortical cell culture studies showed that application of free radical scavengers or antioxidant compounds reduces glutamate-mediated excitotoxicity providing additional support for the

role of oxidative stress and damage mechanisms in excitotoxicity (Monyer, Hartley et al. 1990). However, oxidative stress is not the only component of post-traumatic cell death. Growing evidence has indicated that post-traumatic free radical production is linked to disruption of intracellular calcium (Ca^{2+}) homeostasis, induction of mitochondrial dysfunction and loss of Ca^{2+} buffering capacity and downstream activation of the Ca^{2+} -dependent protease, calpain, which can proteolytically dismantle cellular structure.

Brain tissue is particularly vulnerable to oxidative damage due to its high metabolic requirement for oxygen; its prevalent concentration of oxidizable polyunsaturated fatty acids (PUFAs) in membranes; its enrichment in redox active metals, most notably iron and the presence of potentially phagocytic microglia which can become a major source of ROS and free radicals when activated by injury. The high content of free radical-sensitive PUFAs in the membrane lipids of neurons and myelin provides the target for free radical-induced lipid peroxidation (LP), in which a single free radical can trigger a chain reaction in the lipid bilayer that is potentiated by transition metal ions (Hall and Braugher 1993; Watson 1993).

Experimental TBI models have provided compelling evidence supporting the important role of ROS and LP in the pathophysiology of acute TBI. The first work showing this was provided by Kontos and his colleagues who demonstrated an almost immediate post-injury increase in brain microvascular superoxide radical production in fluid percussion injury (FPI) TBI model (Kontos and Povlishock 1986; Kontos and Wei 1986). Moreover, hydroxyl radical was shown

to increase during the first minutes after injury (Hall, Andrus et al. 1993), followed in close succession by increased LP, blood-brain barrier (BBB) disruption and edema (Smith, Andrus et al. 1994; Nishio, Yunoki et al. 1997; Kasprzak, Wozniak et al. 2001). In addition to that, evidences from addition of exogenous antioxidants and transgenic studies further suggest oxidative damage as a potential therapeutic target (Hall and Smith 1991; Smith, Andrus et al. 1994; Chan, Epstein et al. 1995; Mikawa, Kinouchi et al. 1996; Hall, Kupina et al. 1999).

Definition of Free Radical and ROS

As defined by Halliwell and Gutteridge, a free radical is any species capable of independent existence (hence the “free”) that contains one or more unpaired electrons. Free radicals may be mono- or poly-atomic. It is important to know that not all free radicals are highly reactive. Reactive oxygen species (ROS) is a collective term often used by scientists to include not only the oxygen radicals ($O_2^{\cdot -}$ and $\cdot OH$), but also some non-radical derivatives of O_2 such as hydrogen peroxide (H_2O_2). Therefore, some ROS are not necessarily a free radical themselves, but are molecules that can generate free radicals (Halliwell and Gutteridge et al, 1985). Moreover, some oxides of nitrogen are alternatively termed reactive nitrogen species (RNS), such as nitric oxide ($NO\cdot$) and peroxynitrite anion ($ONOO^-$).

Oxygen as a Source of ROS

After brain injury, ROS and/or free radicals may be generated through several different cellular pathways, such as the free radical leak from mitochondria respiratory chain; nitric oxide synthases (NOSs); conversion of xanthine dehydrogenase (XDH) to xanthine oxidase (XO); phospholipase A₂-cyclooxygenase pathway; Fenton and Haber-Weiss reactions by inflammatory cells (Gutteridge and Halliwell 1989; Kehrer 2000). Moreover, a number of enzymes, such as cytochromes P450, various oxidases, peroxidases, lipoxygenases and dehydrogenases can be sources of ROS.

Oxygen is the most abundant molecule in a biological system. It exists as a di-radical and therefore is very reactive with radicals. Although oxygen can act as an oxidizing agent, its two unpaired electrons remain at most stable state. Thus O₂ normally accepts one electron at a time, reacts sluggishly with non-radicals. As it is partially reduced through normal metabolic processes, oxygen is often the source of free radicals. The escape of the free radicals normally is counteracted by endogenous antioxidant system. However, under pathological conditions, over-production of oxygen-derived ROS and free radicals overwhelms the endogenous antioxidants, inducing "oxidative stress". If the imbalance of the pro- and anti-oxidant system occurs, this leads to degradation or modification of macromolecules (e.g. lipids, proteins, nucleic acids) and irreversible impairment of their function, it is termed as "oxidative damage".

Superoxide Radical

One of the most important sources of superoxide radical ($O_2^{\cdot -}$) *in vivo* is the mitochondrial electron transport chain (ETC). Estimated up to 1% of total mitochondrial oxygen consumption goes toward the production of superoxide or hydrogen peroxide at intermediate steps of the mitochondrial ETC (Ischiropoulos and Beckman 2003). It is believed that mono electron reduction of oxygen into superoxide primarily occurs at ETC complex I (NADH dehydrogenase) level and coenzyme Q level (ubiquinone-cytochrome *b*) (Kowaltowski and Vercesi 1999). (Figure 1.1)

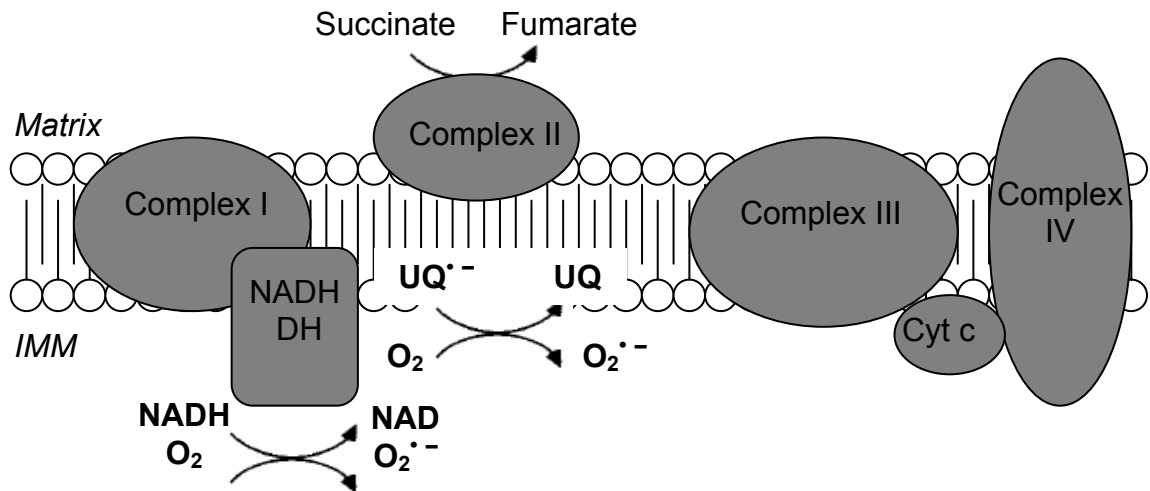
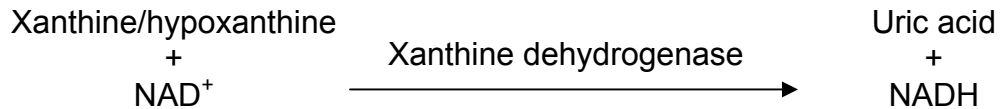


Figure 1.1 Simplified schematic of superoxide production from ETC.

Theoretically, superoxide radical can be generated from oxygen through mono electron reduction at all components of the respiratory chain. However, the NADH dehydrogenase and ubiquinone-cytochrome *b* appear to be the two primary $O_2^{\cdot -}$ generation sites (Turrens and Boveris 1980). Although complex IV catalyses four sequential $1e^-$ additions to molecular oxygen, the intermediates are tightly retained, and there is no leakage of superoxide occurs (Nicholls and Ferguson et al. 2002). Physiologically, electrons are transferred from NADH to the oxidized form of ubiquinone (UQ) to yield the reduced form of ubiquinone and ubiquinol (UQH₂). During the course when UQH₂ transferring the electron to cytochrome *c* oxidase, it is converted to firstly intermediate free radical semiquinone anion species ($UQ^{\cdot -}$), and then back to UQ. This process initially occurs on cytoplasmic face of the inner mitochondrial membrane (IMM), and is then repeated on the matrix face of the IMM. Myxothiazol inhibits UQH₂ at the cytoplasmic face of the IMM, therefore blocks the formation of $UQ^{\cdot -}$, and stimulates $O_2^{\cdot -}$ formation only at the level of NADH dehydrogenase; whereas antimycin A inhibits $UQ^{\cdot -}$ formation at cytoplasmic face, thereby accumulates $UQ^{\cdot -}$ at matrix face of the IMM, resulting in stimulating $O_2^{\cdot -}$ formation at both the level of NADH dehydrogenase and coenzyme Q. Therefore, some hypothesize that mitochondrial generated $O_2^{\cdot -}$ preferably occurs at the level of coenzyme Q (Kowaltowski, Castilho et al. 1995). In contrast to that, complex I level of $O_2^{\cdot -}$ generation is more $\Delta\Psi_m$ dependent. However, the precise nature of the $O_2^{\cdot -}$ production site in complex I remain arguable. Complex I inhibitor rotenone generates $O_2^{\cdot -}$ during electron transport through the complex from NAD⁺-linked

substrates. Even with the absence of endogenous complex I substrates and with succinate (complex II substrate), complex I can still generate $O_2^{\cdot-}$ as a result of reversed electron transfer (Turrens and Boveris 1980). Therefore, NADH dehydrogenase remains a notable site of $O_2^{\cdot-}$ generation.

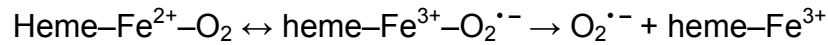
Some $O_2^{\cdot-}$ is also produced by activated phagocytic cells. Activated phagocytic cells are capable of reducing O_2 into $O_2^{\cdot-}$ through the activity of NADPH oxidase (Bianca, Dusi et al. 1999; Gao, Jiang et al. 2002). Another source is the largely endothelial cell-contained xanthine oxidase (McCord 1987). Most of the xanthine/hypoxanthine oxidation *in vivo* is catalysed by xanthine dehydrogenase, which transfers electrons from the substrates onto NAD^+ rather than to O_2 .



However, under ischemic and post-ischemic reoxygenation conditions, xanthine dehydrogenase can be converted into xanthine oxidase by oxidation and therefore produce $O_2^{\cdot-}$ and H_2O_2 while oxidizing xanthine or hypoxanthine. In addition to that, depletion of adenosine triphosphate (ATP) in hypoxic tissues results in accumulation of hypoxanthine. Hypoxanthine can be oxidized by xanthine oxidase when tissue are reoxygenated, causing rapid generation of $O_2^{\cdot-}$ and H_2O_2 .

Superoxide radical can also be produced by heme proteins. Normally, the iron in the heme rings of the hemoglobin or myoglobin remains in the ferrous state (Fe^{2+}) for O_2 binding. However, some delocalization of the electron takes

place and results in an intermediate structure, producing ferric iron (Fe^{3+}) in the heme ring. Ferric iron present in the heme ring is inactive and unable to bind O_2 , thereby releases a molecule of superoxide radical:



Moreover, superoxide can be produced from arachidonic acid cascade through prostaglandin hydroperoxidase (PGH) and 5-lipoxygenase activity as a side-chain reaction depending on the presence of NADH or NADPH (Kukreja, Kontos et al. 1986).

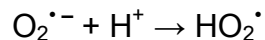
There are several important biological oxidations in the presence of O_2 that result in $\text{O}_2^{\cdot-}$, such as glyceraldehyde, FMNH_2 , FADH_2 , the hormones adrenalin and noradrenalin, L-DOPA (dihydroxyphenylalanine), the neurotransmitter dopamine, tetrahydropteridines and thiol compounds (eg. cysteine) (Davis, Kaufman et al. 1988). Most of these reactions are accelerated by transition metals since O_2 is poorly reactive.

More interestingly, Ca^{2+} influx was suggested to be a source of mitochondrial $\text{O}_2^{\cdot-}$ as well, in which Ca^{2+} leads to IMM alteration and disorganization of the ETC (Kowaltowski, Castilho et al. 1995). Grijalba et al proposed that Ca^{2+} alters the lipid organization of IMM by interacting with the anionic head of cardiolipin, which is an abundant component of IMM. As a result, the function of the ETC was affected, such as coenzyme Q mobility, leading to mono-electronic oxygen reduction at intermediate steps of respiration, which promote the production of $\text{O}_2^{\cdot-}$ (Grijalba, Vercesi et al. 1999).

To this end, superoxide can reduce the endogenous antioxidant enzyme reservoir by direct reaction, such as with catalase and glutathione peroxidase, as well as enzymes involved in energy metabolism (Zhang, Marcillat et al. 1990). Nevertheless, neither $O_2^{\cdot-}$ nor H_2O_2 is sufficiently reactive to account for much of the post-traumatic oxidative damage found *in vivo*. It is known that superoxide-derived species are much more cytotoxic than superoxide itself.

Superoxide-Derived Species

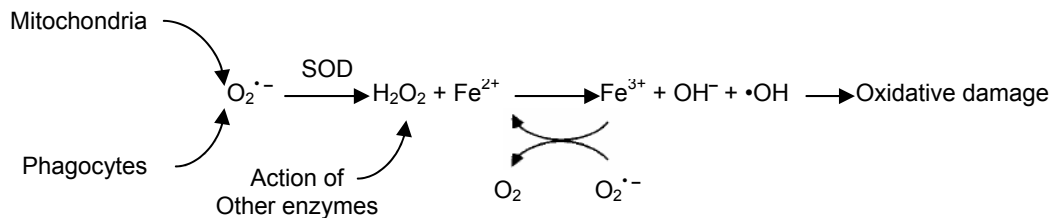
Hydroperoxyl radical: While $O_2^{\cdot-}$ may act as an oxidant or reductant, and is reactive with radicals, for example, reduce Fe^{3+} to Fe^{2+} , it is relatively inert in reaction with non-radicals in aqueous environments. In solution, superoxide exists in equilibrium with its protonated form, hydroperoxyl radical (HO_2^{\cdot}). Under conditions of tissue acidosis occur within severely injured nervous system, $O_2^{\cdot-}$ exists mostly as HO_2^{\cdot} , which is more reactive and capable of initiating LP (Halliwell, Gutteridge et al, 1985). In contrast to the exceedingly slow rate of dismutation of $O_2^{\cdot-}$ to H_2O_2 , HO_2^{\cdot} is much more readily able to generate H_2O_2 (Hall and Braugher 1993).



Hydrogen peroxide: Dismutation of $O_2^{\cdot-}$ by superoxide dismutase (SOD) generates hydrogen peroxide (H_2O_2). SOD is an important antioxidant enzyme and specific for $O_2^{\cdot-}$ as a substrate. However, H_2O_2 is poorly reactive at physiological level. H_2O_2 is usually removed by two types of enzymes: catalases and peroxidases. The catalases directly catalyse decomposition of H_2O_2 to O_2 :

$2 \text{H}_2\text{O}_2 \rightarrow 2 \text{H}_2\text{O} + \text{O}_2$. Peroxidase enzymes remove H_2O_2 by using it to oxidize another substrate: $\text{SH}_2 + \text{H}_2\text{O}_2 \rightarrow \text{S} + 2\text{H}_2\text{O}$. In the case of glutathione peroxidase (GPX), it removes H_2O_2 by coupling its reduction to H_2O with oxidation of reduced glutathione (GSH): $\text{H}_2\text{O}_2 + 2\text{GSH} \rightarrow \text{GSSG} + 2\text{H}_2\text{O}$. Both catalases and GPX enzymes are widely distributed in animal tissues readily to produce H_2O_2 .

Hydroxyl radical: Hydroxyl radical ($\bullet\text{OH}$) is an extremely reactive form of free radicals produced from H_2O_2 by the metal-catalyzed Fenton reaction; or in the presence of $\text{O}_2^{\bullet-}$ and catalytic amounts of transition metals, from the metal-catalyzed Haber-Weiss reaction (Gutteridge and Halliwell 1989).



Hydroxyl radical can also be produced from peroxynitrite (PN), a ROS generated by reaction between nitric oxide ($\text{NO}\bullet$) and superoxide radical ($\text{O}_2^{\bullet-}$) (Radi, Beckman et al. 1991). Hydroxyl radical was detected within half an hour after trauma through the use of trapping agents such as salicylate (Hall, Andrus et al. 1993) or nitron spin traps (Sen and Phillis 1993; Sen, Goldman et al. 1994). The formation of highly reactive $\bullet\text{OH}$ became widely accepted as the primary mechanism of free radical toxicity. Although $\bullet\text{OH}$ is capable of destroying various bio-molecules, the reaction with organic molecules is diffusion rate-limited, ranging from 10^9 to $10^{10} \text{M}^{-1}\cdot\text{s}^{-1}$. Therefore, it will react as fast as it is formed and cannot explain any form of oxidative damage that occurs remote from its site of

formation. Thus, its “non-discriminative” nature makes $\bullet\text{OH}$ attack uncritical targets and quickly be removed from the system (Hall and Braugher 1993; Beckman 1994; Crow and Beckman 1996).

Peroxynitrite: To better understand the toxicity of oxidative damage, an oxidant that is able to out-compete endogenous antioxidant defenses is proposed to be peroxynitrite (Blou 1985; Beckman 1994). Peroxynitrite (PN) refers to peroxynitrite anion (ONOO^-) as well as its conjugate acid, peroxynitrous acid (ONOOH). PN is produced by the very fast reaction of $\text{O}_2^{\bullet -}$ with $\text{NO}\bullet$. Interestingly, $\text{O}_2^{\bullet -}$ is one of the few molecules that reacts with $\text{NO}\bullet$ quickly. PN can generate a wide range of noxious free radical species under physiological conditions. Superoxide radical and nitric oxide react readily at rate of $6.7 \times 10^9 \text{ M}^{-1}\text{s}^{-1}$, which is at least three times faster than SOD reacts with $\text{O}_2^{\bullet -}$, and at least ten times faster than heme compounds react with $\text{NO}\bullet$. Therefore, $\text{NO}\bullet$ and $\text{O}_2^{\bullet -}$ can antagonize each other’s biological actions (Cudd and Fridovich 1982; Huie and Padmaja 1993).



In humans, $\text{NO}\bullet$ is formed from arginine, O_2 and NADPH by nitric oxide synthases (NOSs) and functions as a diffusible messenger to modulate neuronal signaling following excitotoxicity (Garthwaite, Charles et al. 1988), regulate vascular tone, and kill pathogens (Bredt and Snyder 1990; Bredt and Snyder 1994).

hydrolysis to prevent calcium overload (Bringold, Ghafourifar et al. 2000). However, overproduction of intramitochondrial NO•-derived PN was indicated to induce irreversible damage to neuron-mitochondrial complex (Stewart, Sharpe et al. 2000).

PN has relative long half-life compared to other ROS (~1sec), and it can diffuse across membrane, which enable PN to induce oxidative damage remote from its site of formation. The protonated form of PN (around neutral pH), peroxynitrous acid (ONOOH), is a strong oxidizing species. ONOOH is unstable and quickly releases nitrogen dioxide ($\bullet\text{NO}_2$) and hydroxyl radical ($\bullet\text{OH}$). Moreover, PN can also react with carbon dioxide (CO_2) to form nitrosoperoxo carbonate (ONOOCO_2), then breaks down into nitrogen dioxide ($\bullet\text{NO}_2$) and carbonate radical ($\text{CO}_3^{\bullet-}$). PN-derived radicals are extremely potent and react rapidly with bio-molecules (Murphy, Packer et al. 1998; Radi 1998; Hall, Detloff et al. 2004). (Figure 1.2)

One of the most studied reactions involved in PN biochemistry concerns the conversion of 3 position tyrosine to 3-nitrotyrosine (3NT), in which PN-derived $\bullet\text{NO}_2$ nitrates aromatic compounds, which is widely used as a bioassay to detect ONOO^- *in vivo* (Beckman 1996). In addition to that, PN-derived radicals can induce LP which produces various aliphatic aldehydic products which bind to cellular proteins and be measured by immunohistochemistry (Hall, Oostveen et al. 1997; Hall, Detloff et al. 2004). Moreover, 4-hydroxynonenal (4HNE) is the most cytotoxic LP-derived aldehydes (Keller, Mark et al. 1997).

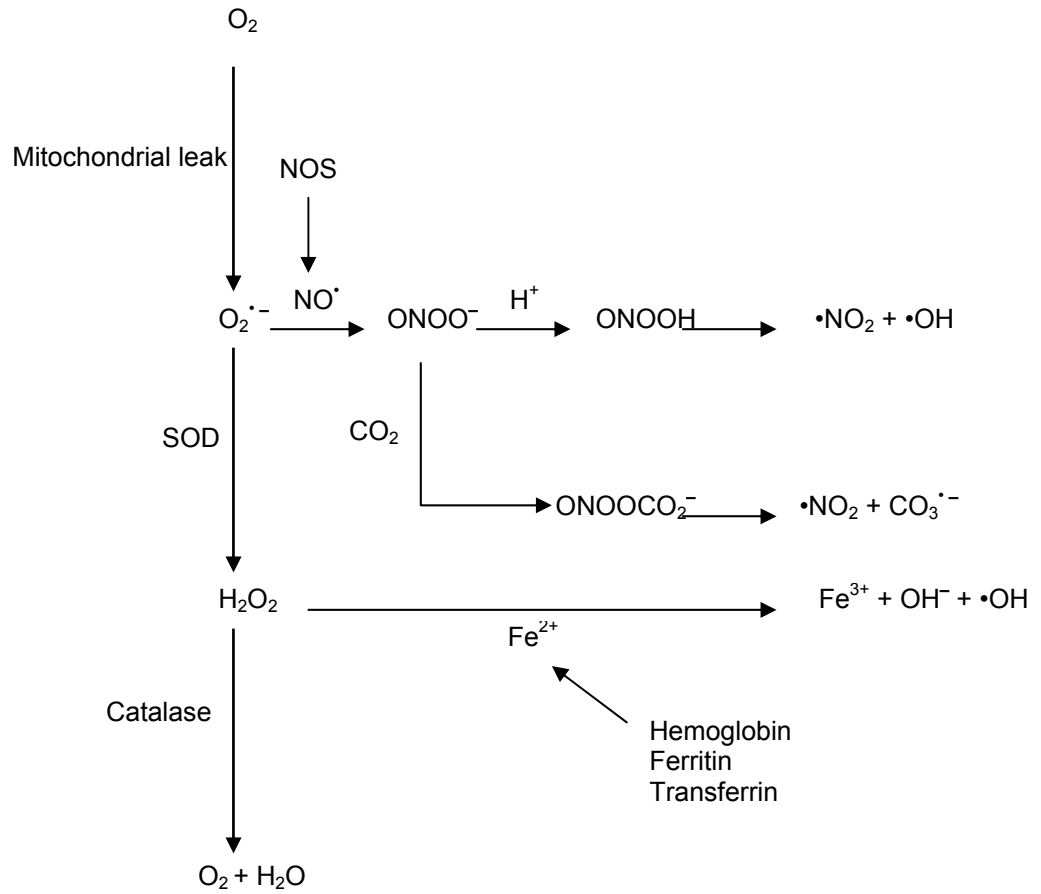


Figure 1.2 Biochemistry of ROS formation.

Neuronal Tissue Oxidative Damage

Oxidative damage to lipids: As noted earlier, due to its high content in PUFAs, brain tissues are very susceptible to LP. A species that can sufficiently react to abstract a hydrogen atom from a methylene ($-\text{CH}_2-$) group can initiate LP. In the case of fatty acids with no or one double carbon-carbon bonds, they are more resistant to such attack. However, in the case of PUFAs, the adjacent double bonds weaken the energy of the attachment of the hydrogen atoms present on the next carbon atom (termed allylic hydrogen), particularly when there is a double bond on both sides of the methylene, giving bis-allylic hydrogen. As a consequence, the commitment of this carbon to bind with the hydrogen atom on it becomes very ambivalent. Therefore, if a free radical comes along, it can easily remove the hydrogen atom and the electron associated with it. As a result, the free radical is quenched, while the PUFA is turned into a free radical, termed alkyl radical (L^\bullet). However, LP is a geometrically progressing process. The allylic radical can then react with molecular oxygen (O_2) and form lipid peroxy radical (LOO^\bullet). If this process is not ceased by endogenous antioxidant compounds or enzymes, the lipid peroxy radical will react with other PUFAs to form a second allylic radical, while becoming a lipid hydroperoxide (LOOH). If there is transition metal ion ($\text{Fe}^{2+}/\text{Fe}^{3+}$) comes along, the LOOH undergoes decomposition to create an alkoxy radical (LO^\bullet) or a peroxy radical (LOO^\bullet). Either lipid radical can attack neighboring fatty acids and thus the process of peroxidation propagates throughout the membrane (Figure 1.3).

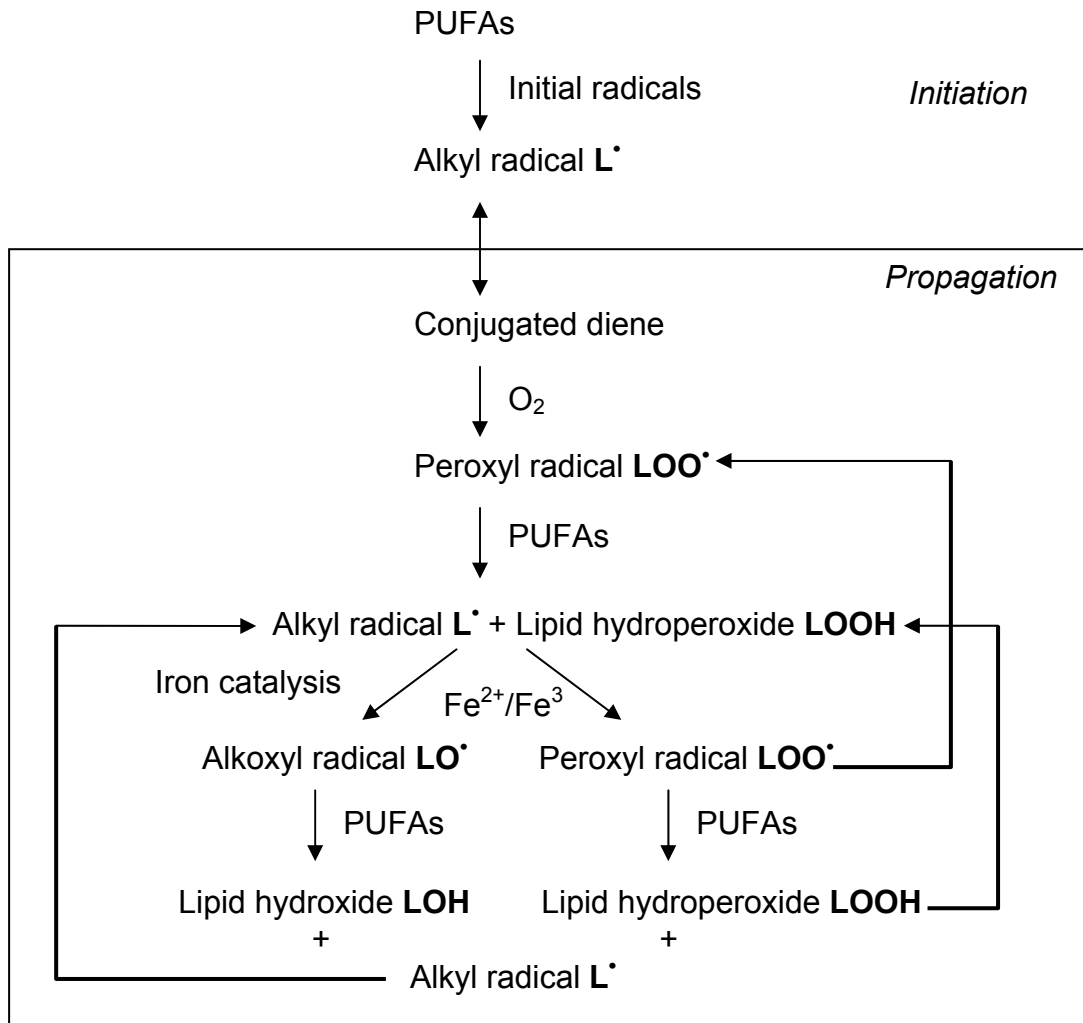
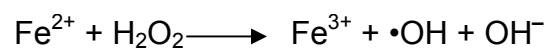


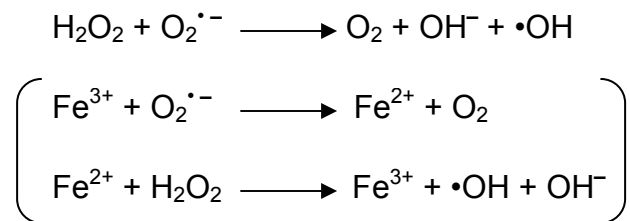
Figure 1.3 Chemistry of initiation and propagation phases of cell membrane LP.

As a result, LP decreases membrane fluidity, increases permeability of the membrane bilayer to various substances that are normally impermeable and inactivates certain membrane-bound enzymes. The continuation of oxidation of fatty acid side chains and their fragmentations to produce aldehydic breakdown products eventually leads to the loss of membrane integrity. Moreover, the products of LP, such as peroxy radicals, alkoxy radicals and aldehydes (especially 4-hydroxynonenal) can induce severe damage to proteins. For example, 4HNE, an end-product of LP, can conjugate onto proteins causing toxic protein aggregates within membranes (Keller, Mark et al. 1997; Kruman, Bruce-Keller et al. 1997).

Varieties of superoxide-derived radicals are capable of inducing LP. Acidic pH conditions, which is known to occur within severely injured neuronal tissues, accelerates superoxide radical to conjugate with H^+ to form hydroperoxyl radical (HO_2^{\bullet}), which is more soluble and much more reactive. As a defense antioxidant mechanism, the rate of $O_2^{\bullet -}$ endogenous dismutation into H_2O_2 is also increased. Normally in brain tissues, low molecular weight forms of redox active iron are retained, as in other tissues, at extremely low or none levels. Although iron storage proteins at neutral pH, such as ferritin and transferrin, have high affinity for iron, they are readily to give up iron under acidic conditions. The irons released from iron-binding proteins participate in catalyzing LP, in which the most studied iron-catalyzed redox reaction is Fenton reaction:



Both $\bullet\text{OH}$ and Fe^{3+} are extraordinary potent oxidants and capable of initiate damage to lipids, proteins and DNAs. On the other hand, Haber-Weiss reaction may also occur in the presence of transition metals to generate oxidizing radicals, though it has a second-order rate constant in aqueous solution of nearly zero.



In addition to iron-dependent radical production, PN-derived $\bullet\text{NO}_2$, $\text{CO}_3^{\bullet-}$ and $\bullet\text{OH}$ (Figure 1.2) are potent oxidants that capable of inducing intensive tissue damages.

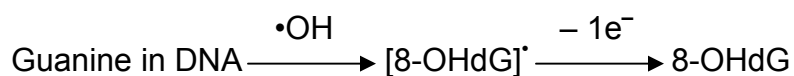
Since LP is a complex process with multiple stages, there are many LP measurement techniques are available for measuring the rate of peroxidation of membrane lipids, lipoproteins or fatty acids. One of the most preferred methods is to measure the aldehyde “end-products” of peroxidation, among which 4HNE is one of the most cytotoxic aldehydes. Reactive aldehyde, such as 4HNE, binds rapidly to proteins, therefore antibody-based immuno-detection of such adducts within cells and tissues is considerable. Moreover, immuno-histochemical procedure can locate the distribution of such adducts in tissue slices subjected to oxidative damage.

Oxidative damage to proteins: Damages to proteins can be induced directly by ROS, as well as indirectly by end product of LP, such as malondialdehyde (MDA) and 4HNE through rapid reaction with thiol ($-\text{SH}-$)

groups at physiological pH. Attack of RNS, such as ONOO⁻, •NO₂ and NO₂Cl, leads to 3NT formation. Moreover, •OH or singlet O₂ can generate multiple end-products upon proteins. By contrast, H₂O₂ and O₂^{•-} at physiological level have little or no direct effect on proteins. Protein oxidation can lead to specific damage to certain amino acid residues. As a result, not only enzymes, but also receptor proteins and transport proteins can become a target of oxidative damage.

The “general” assay of oxidative protein damage is carbonyl assay. The rationale is based on the fact that several ROS attack amino acid residues to generate products with carbonyl groups, which can be measured after reaction with 2,4-dinitrophenylhydrazine (DNPH). The immuno-detection is designed to recognize the protein with carbonyl group that is conjugated to DNPH.

Oxidative damage to DNAs: Oxidative damage to DNAs can lead to strand breakage, damage to the deoxyribose sugar and modification of the purine and pyrimidine bases. However, nuclease activity occurs during DNA repair can also induce strand breakage, but cannot be equated to oxidative DNA damage. The most common assay is to measure 8-hydroxydeoxyguanosine (8-OHdG), 8-hydroxyguanine (8-OH-G) attached to deoxyribose, which is formed by •OH attacking upon DNA followed by mono-electron oxidation of the resulting radical.



However, the intermediate [8-OHdG][•] radical may have alternative fates. Therefore, the measurement of a single product of the amount of hydroxylated guanine in DNA does not sufficiently indicate the amount of initial radical attack.

Moreover, DNA is more susceptible to oxidative damage if it is exposed to H₂O₂ (Schraufstatter, Hinshaw et al. 1986).

Mitochondrial Dysfunction in Traumatic Brain Injury

As noted previously, excitotoxicity is a pathological process results in neuronal cell death through which the over-activation of receptors for the excitatory neurotransmitter, glutamate. *N*-Methyl-D-aspartate (NMDA) receptors are a subclass of glutamate receptors that play an essential role in Na⁺ and Ca²⁺ influx into the cell (Faden, Demediuk et al. 1989). Na⁺ gradient cross the plasma membrane is required for glutamate uptake. NMDA over-activation will exacerbate glutamate accumulation extracellularly and hence Ca²⁺ influx by inducing Ca²⁺ channels. The unique features of mitochondria allow them to accumulate calcium when the intracellular [Ca²⁺]_i reaches a “set-point” of 500nm in order to modulate Ca²⁺ homeostasis in the cytosol (Schinder, Olson et al. 1996; Nicholls and Ferguson et al. 2002). Mitochondrial dysfunction in regards to its Ca²⁺ buffering capability is an essential mediator of excitotoxicity. Specifically, excessive mitochondrial Ca²⁺ accumulation uncouples electron transfer from ATP synthesis leading to mitochondrial dysfunction (Beatrice, Palmer et al. 1980; Gunter and Pfeiffer 1990; Bernardi, Broekemeier et al. 1994).

The disturbance of energy metabolism during Ca²⁺ overload can result in an increase in the mitochondrial leak of oxygen radicals, which can overwhelm the antioxidant defense mechanisms and contribute to cell death (Halliwell and

Gutteridge et al. 1989; Coyle and Puttfarcken 1993; Lang-Rollin, Rideout et al. 2003). Oxidants are constantly generated even during normal metabolism as the intrinsic rate of proton leakage across the IMM increases, such as $O_2^{\cdot-}$, H_2O_2 , $\cdot OH$ (Shigenaga, Hagen et al. 1994). There are array of cellular anti-oxidant defenses that antagonize the production of oxidants. However, in a variety of pathological conditions, such as TBI, the rate of ROS production within mitochondria is exacerbated. The main sites for superoxide production are suggested to be complex I and complex III of the ETC (Turrens and Boveris 1980; Sugioka, Nakano et al. 1988). However, the precise nature of the ROS production sites in complex I remain obscure. It was also indicated that Ca^{2+} influx induces IMM lipid re-organization by interacting with the anionic head of cardiolipin, which is an abundant component in IMM. As a result, mono-electron was delivered to oxygen at intermediate steps of respiration, which result in the production of $O_2^{\cdot-}$ through ETC (Grijalba, Vercesi et al. 1999). In addition to that, $NO\cdot$ production is also detected intramitochondrially through the activation of an isoform of NOS located within the mitochondria. It was suggested that this isoform of NOS is activated upon Ca^{2+} uptake (Giulivi 1998; Tatoyan and Giulivi 1998). Like the three main isoforms of NOS, diversity in its function and location gives it a unique role in mitochondria, such as a feedback signal to prevent overloading of Ca^{2+} and decreasing mitochondrial membrane potential ($\Delta\Psi_m$) (Ghafourifar and Richter 1997). Although $NO\cdot$ is believed to have potential toxic effect, many of them are more likely mediated by PN and its oxidation products rather than $NO\cdot$ by itself, such as PN (Bringold, Ghafourifar et al. 2000; Stewart,

Sharpe et al. 2000). Evidence showed that the NO•-dependent inactivation of iron-sulfur centers was in fact mediated by PN (Castro, Rodriguez et al. 1994; Hausladen and Fridovich 1994). Together, mitochondria provide a favorable environment for PN-induced oxidative damage in response to Ca²⁺ uptake.

Moreover, post-traumatic excessive mitochondrial uptake of Ca²⁺ can lead to a sudden increase in inner membrane permeability to compounds with a molecular mass less than 1.5kD, defined as the formation of mitochondrial permeability transition pore (mPTP). The mPTP formation is believed to be the basis of mitochondrial swelling and metabolic failure and ultimately cell death (Zamzami, Hirsch et al. 1997). Although it is considered to be a non-specific membrane opening, evidence showed that the onset of the mPTP can be prevented by the immunosuppressant cyclosporine A (CsA) suggesting that it is more than a non-specific membrane rupture (Bernardi, Broekemeier et al. 1994; Bernardi 1996; Nicolli, Basso et al. 1996; Sullivan, Thompson et al. 1999). Multiple studies have indicated that the oxidation of mPTP components occurs and may play a major role in promoting mPTP formation. It was shown that mitochondrial Ca²⁺ release could be simulated in response to the oxidation of mitochondrial pyridine nucleotides, and be inhibited (or reversed) by NAD(P)⁺ reduction (Lehninger, Vercesi et al. 1978). Pro-antioxidants that deplete glutathione and promote pyridine nucleotides oxidation also resulted in mPTP formation and cell death; whereas diminishing pyridine nucleotide oxidation and oxidative stress delayed the onset of mPTP and cell death (Nieminen, Byrne et al. 1997). Some evidence has indicated that mPTP occurs when thiol groups of

inner membrane proteins are oxidized, which leads to conformational changes. In studies on PN-induced protein thiol oxidation, mPTP is paralleled by membrane lipid oxidation (Packer and Murphy 1995; Gadelha, Thomson et al. 1997). In addition, thiol-specific antioxidants protect against mPTP (Kowaltowski, Netto et al. 1998). Other research indicated that the oxidation of adenine nucleotide translocator (ANT), an important component of mPTP, through thiol groups cross-linking, can facilitate mPTP formation, probably by enhancing cyclophilin (CypD) binding, and preventing adenosine diphosphate (ADP) binding (McStay, Clarke et al. 2002; Sullivan, Rabchevsky et al. 2004). Skulachev et al hypothesized a reason for mPTP would be to ameliorate or eliminate high ROS producing cells as a defense system in order to prevent further oxidative damage (Skulachev 1996). In this hypothesis, mPTP formation assists maximal O₂ consumption and decreases mitochondrial O₂ concentration through dissipating membrane potential ($\Delta\Psi_m$) and proton force (ΔpH) across the membrane upon Ca²⁺ influx. In other words, it was suggested that elevated mitochondrial ROS production plays a regulatory role of oxidative stress to induce “mild” uncoupling of mitochondrial respiration and phosphorylation by means of increase in proton leak of IMM to promote respiration and ameliorate further ROS production. Nevertheless, complete uncoupling of mitochondrial respiration and ADP phosphorylation or prolonged uncoupling through mPTP will exhaust ADP in the matrix, which increases O₂ concentration because of the inhibition of respiration. Highly oxidized mPTP will not be able to recover and result in disruption of mitochondrial membrane, eventually lead to calcium disturbance as well as

release of pro-apoptotic proteins, such as cytochrome c (Cyt c), Smac/DIABLO and apoptosis inducing factor (AIF), due to rupture of outer mitochondrial membrane (Sullivan, Keller et al. 2002; Halestrap and Brennerb 2003; Green and Kroemer 2004; Sullivan, Springer et al. 2004).

Calpain-Mediated Cytoskeletal Proteolysis in Traumatic Brain Injury

Calpain Isoforms:

Following TBI, excitotoxicity inducing excessive calcium influx was shown to be associated with cell damage. Non-physiological $[Ca^{2+}]_i$ rise can exert adverse effects by over-activating cellular proteases and lipases (Wrogemann and Pena 1976). One of those has been indicated under multiple pathological conditions and contributing to cell damage is calpain. Calpains are family of calcium-activated cysteinyl/thiol (neutral) proteases, in which cysteine residues are present in its active site. The calpain family consists of several tissue-specific isoforms (n-calpains) and two ubiquitous isoforms (μ -calpain and m-calpain). Calpains are expressed in all vertebrates in which they are highly conserved across species. They are also found in various cell types and tissues (Sorimachi, Ishiura et al. 1997). The two ubiquitous calpain isoforms are categorized mainly on the basis of their sensitivity to $[Ca^{2+}]$ upon activation in their purified state *in vitro*. First of all, μ -calpain (aka. calpain I) has micro-molar sensitivity to calcium and is located primarily in the neuronal soma and dendrites. m-Calpain (aka. calpain II) has a millimolar sensitivity to calcium activation and is primarily located

in axons and glia. Moreover, because of the distinct subcellular localization of the calpain subtypes, they may serve specific physiological roles (Hamakubo, Kannagi et al. 1986). More interestingly, μ -calpain, which has higher affinity for calcium binding, has been shown to be located in mitochondria (Garcia, Bondada et al. 2005).

Evidence for a Role of Calpain in TBI:

Growing interests in calpain due to, in many neurodegenerative diseases, etiologic factors such as excitotoxicity, free radical injury and mitochondrial homeostasis all lead to disturbance of intracellular Ca^{2+} level. As one expected effect of disruption of Ca^{2+} homeostasis is the activation of Ca^{2+} -dependent lipases and proteases. Among which, calpain family is believed to be very important since they proteolyse important enzymes, including protein kinases, phosphatases, and modify structure proteins of membrane skeleton (Nixon 1989). In order to detect calpain activity, protease inhibitors that block calpains have been used in experimental TBI models to investigate their activation. These inhibitors have been shown to be neuroprotective *in vivo* as well as *in vitro* in cerebral ischemia (Bartus, Hayward et al. 1994) and TBI models (Saatman, Murai et al. 1996; Posmantur, Kampfl et al. 1997; Kupina, Nath et al. 2001; Kupina, Detloff et al. 2002). However, due to the uncertain selectivity of these inhibitors for calpain proteases, these data have only provided indirect evidence for calpain activity after acute CNS injury. Moreover, subunit autolysis seems to be an early event in the intramolecular activation of μ -calpain (Saido, Nagao et

al. 1992). The ratio of the activated, autolyzed 76kD isoform to the 80kD precursor form has been used as an index for μ -calpain activation. Nevertheless, others reported that μ -calpain activation does not require autolysis (Edmunds, Nagainis et al. 1991). Kampfl et al showed that μ -calpain autolysis was only temporally correlated with calpain-mediated α -spectrin breakdown products (Kampfl, Posmantur et al. 1996)

A more commonly used method of measuring calpain activity is to detect the presence of breakdown products (BDPs). Preferred substrates for calpain include cytoskeletal proteins spectrin, microtubule-associated proteins (MAP2) and neurofilament proteins (NF), which are major components of neuronal cytoskeleton and membrane (Saatman, Graham et al. 1998). Posmantur et al indicated that the occurrence of the loss of neurofilament 68 and low molecular weight BDPs associates with TBI (Posmantur, Hayes et al. 1994). Moreover, unlike other proteases, such as cathepsins and trypsin, calpain produces distinctive breakdown fragments that resemble the patterns observed after TBI. More direct evidence of calpain activity is measured by antibody-based immunodetection of calpain-mediated α -spectrin breakdown and it is widely used in models of TBI (Saatman, Bozyczko-Coyne et al. 1996; Kupina, Detloff et al. 2002; Hall, Detloff et al. 2004). The α -spectrin breakdown products (SBDPs) are produced by both calpain and another cysteine protease, caspase 3. Given that the activation of calpain as well as apoptotic enzymes is implicated in different neuronal cell death cascades, SBDPs became a useful tool to study both proteases in the same model. Calpains are shown to be involved in both necrosis

and apoptosis, while caspases are largely involved in apoptosis (Wang 2000). Spectrin, as a major constituent of the skeletal network, is a common substrate of both calpain and caspase 3, the downstream factor of apoptotic cascade. The breakdown of the 280kD protein α -spectrin by either calpain (145kD product) or calpain and/or caspase 3 (150kD product) can be detected using antibody-based immuno-detection (Wang 2000; Kupina, Detloff et al. 2003; Deng, Thompson et al. 2007). The neuronal cytoskeleton is an important component maintaining cell architecture, as well as axonal transport, and possibly neuronal plasticity (Ludin and Matus 1993). Following experimental acute TBI, evidence has shown significant proteolysis of dendritic MAP2 (Taft, Yang et al. 1992). Immuno-histochemical studies revealed that SBDPs indication of calpain activity occur in apical dendrites following TBI (Saatman, Bozyczko-Coyne et al. 1996). Moreover, it is shown that NF compaction is associated with proteolysis of NF sidearms following traumatic axonal injury (TAI) (Okonkwo, Pettus et al. 1998). However, calpain-mediated proteolysis seemed to be involved more with the axons that are located in areas with the most severe injury sustained from an impact, whereas areas that are with less severity show no calpain-mediated change (Saatman, Bozyczko-Coyne et al. 1996). Above all, increasing evidences point to the important role of calpain in cytoskeletal de-arrangement and degradation, therefore, its possible occurrence in sublethally injured cells.

The Relationship of Oxidative Damage, Mitochondrial Dysfunction, Calpain Activation and Neurodegeneration in Traumatic Brain Injury

TBI is one of the leading causes of serious disability and death in children and adults. Different severities of TBI from mild, moderate to severe cases can all lead to neurological, economical and social burden to not only the patients but also the families and the society as a whole (Thurman, Alverson et al. 1999). The number of treated cases keeps increasing over the years. To this day, there are no clinically proven and FDA approved pharmacological treatments for acute TBI patients. Although improved specialized paramedics and emergency treatments saved lives on scene that otherwise may die, many patients survived the injury continuously suffered from physical, cognitive, emotional and behavioral deficit that severely impair their quality of life. It is now understood that most of the neurological damage is not the immediate result from the acute mechanical impact, but rather an outcome of an evolving pathochemical and pathophysiological process following the initial injury over minutes, hours and days. However, growing evidences from scientific experiments suggests that pharmacological treatments targeting these post-traumatic neurochemical changing may lead to a better neurological and behavioral outcome. This provides hope in the attempt to not only save lives, but also ensure a better quality of life after injury.

In order to examine mechanistic hypothesis and to test preclinical therapeutics, experimental animal models are essential in scientific investigations

(Lighthall, Dixon et al. 1989). In our study, we applied a mouse uni-lateral controlled cortical impact (CCI) model of TBI, which is widely used in scientific studies. This CCI model yields consistent neurochemical, histological and behavioral deficits (Huh, Laurer et al. 2002; Hall, Gibson et al. 2005; Hall, Sullivan et al. 2005; Deng, Thompson et al. 2007; Onyszchuk, Al-Hafez et al. 2007). In this model, a fully anesthetized mouse was placed underneath a computer-controlled pneumatic piston. We firstly produced a craniotomy positioned between bregma and lambda lateral to sagittal suture. Secondly, the pneumatic piston produced a cortical contusion with pre-set parameters. Finally, the skin was sutured and the animals were physiologically monitored until regain consciousness. The mice recovered well with minimal mortality. Furthermore, this model has reproducible gross histological lesions and allows multiple outcome measurements. Also, this model can produce different severity of injury that is easy to use, affordable and sensitive to intervention.

The post-injury secondary cell death cascade is a multi-factorial process. Based on the current state of knowledge, three of the most critically important pathological elements are ROS formation, mitochondrial dysfunction and cytoskeletal degradation. As indicated previously, these injury processes are potentially interwoven: primary injury triggered excitotoxicity inevitably induces abnormal intracellular Ca^{2+} increase; consequently, mitochondria as the cellular Ca^{2+} buffer become the primary effector; meanwhile, mitochondrial NOS and Ca^{2+} -dependent proteases are also closely linked to this cellular response, leading to possible mitochondrial ROS production and cytoskeletal degradation.

Overall, these processes play significant contributory role in the delayed cell death. However, the interwoven relationship of these processes makes it difficult for therapeutic intervention, and pharmacological interpretation flawed without timely assessments.

The central hypothesis underlying the present study is that an initial trauma-induced Ca^{2+} overload, caused by glutamate and depolarization evoked Ca^{2+} entry, elicits the mitochondrial generation of the ROS species PN. PN-derived radical species result in oxidative damage to the mitochondria and other cellular elements leading to an exacerbation of intracellular Ca^{2+} accumulation. This in turn exacerbates calpain activity which mediates cytoskeletal degradation and neurodegeneration. If this scenario is correct, compounds that can penetrate cellular mitochondria and antagonize PN-induced oxidative damage (e.g. PN-derived free radicals scavenger, tempol) should be neuroprotective in that the resulting antioxidant effect will lessen calcium overload, calpain activity and associated cytoskeletal degradation and neurodegeneration as shown in **Figure 1.4.**

This dissertation study began with a thorough assessment of the time course of PN-induced lipid peroxidation and protein nitration, calpain-mediated α -spectrin breakdown and neurodegeneration with the de Olmos aminocupric silver staining method as reported in Chapter 2. Secondly, a detailed pharmacological study was conducted using antioxidant, tempol, to determine its ability to inhibit post-traumatic oxidative damage. Thereafter, the effect of tempol on mitochondrial ROS production and mitochondrial function, as well as calpain

activity was tested. These experiments are described in Chapter 3. Finally, the ability of tempol to improve neurological outcome and lessen post-traumatic neurodegeneration is discussed in Chapter 4. Taken together, these studies provide evidence for a post-traumatic pathological scenario that involves a critical early role of PN and suggests that interruption of PN-mediated oxidative damage is a valid therapeutic strategy. Copyright © Ying Deng 2007.

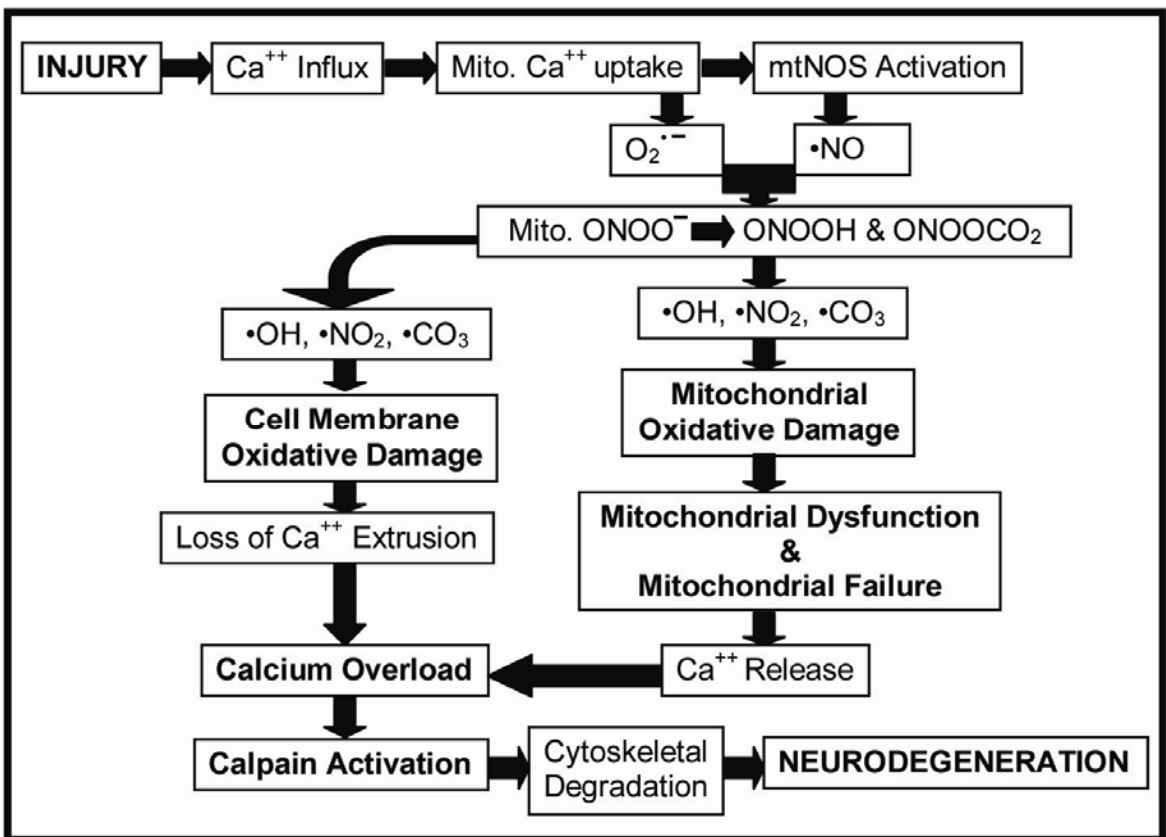


Figure 1.4 Hypothetical interrelationship between mitochondrial PN-induced oxidative damage in neuronal mitochondria and the rest of the neuron, compromise of Ca²⁺ homeostasis, calpain-mediated proteolysis and neurodegeneration.

Chapter Two

Temporal Relationship of Peroxynitrite-Induced Oxidative Damage, Calpain-Mediated Cytoskeletal Degradation and Neurodegeneration after Traumatic Brain Injury

Introduction

There is compelling evidence supporting the role of oxidative damage in the delayed secondary neuronal cell death which is initiated by the primary traumatic brain injury (TBI). The first work in this regard, conducted by Kontos and his colleagues, demonstrated the formation of superoxide radicals in cerebral microvasculature in a cat fluid percussion TBI models (Kontos and Povlishock 1986; Kontos and Wei 1986). Using the salicylate trapping method, Hall and coworkers detected a rapid, but transient rise in brain hydroxyl radical ($\bullet\text{OH}$) in experimental head injury models (Hall, Andrus et al. 1993; Hall, Andrus et al. 1994; Smith, Andrus et al. 1994). This was elegantly confirmed by others using brain microdialysis techniques to monitor salicylate-trapped $\bullet\text{OH}$ over time in the same animals (Globus, Alonso et al. 1995). The increase of $\bullet\text{OH}$ is followed by an increase in lipid peroxidation products (Smith, Andrus et al. 1994). The strongest support for a role of oxidative damage in the acute pathophysiology of TBI is derived from the fact that several antioxidant compounds have been shown to be neuroprotective in TBI models (Hall, Andrus

et al. 1994; Awasthi, Church et al. 1997; Mori, Kawamata et al. 1998; Marklund, Lewander et al. 2001).

The reactive oxygen species (ROS) peroxynitrite (PN), which can produce highly reactive and cytotoxic free radicals, has been suggested to be a key player in post-traumatic secondary brain oxidative damage (Hall, Kupina et al. 1999; Hall, Detloff et al. 2004). Peroxynitrite is formed by the chemical reaction of nitric oxide ($\text{NO}\cdot$), produced by nitric oxide synthase (NOS), with superoxide radical ($\text{O}_2^{\cdot -}$) whenever the two are produced in close proximity (Saran, Michel et al. 1990). All three NOS isoforms (eNOS, iNOS, and nNOS), as a key element in production of PN, have been shown to be up-regulated in brain tissue following TBI (Cobbs, Fenoy et al. 1997; Wada, Chatzipanteli et al. 1998; Gahm, Holmin et al. 2000; Orihara, Ikematsu et al. 2001). In addition, a novel isoform of Ca^{2+} -sensitive NOS (mtNOS), discovered within mitochondria (Bates, Loesch et al. 1995; Lopez-Figueroa, Caamano et al. 2000; Giulivi 2003), has been shown to contribute to mitochondrial production of $\text{NO}\cdot$ and PN (Radi, Cassina et al. 2002). The PN-derived free radicals ($\cdot\text{NO}_2$, $\cdot\text{OH}$, $\cdot\text{CO}_3^-$) can induce extensive oxidative damage to cellular membranes, proteins and DNA (Beckman 1996; Murphy, Packer et al. 1998; Radi 1998). Each of the PN-derived free radicals can initiate lipid peroxidation (LP), or cause protein carbonylation by reaction with susceptible amino acids (e.g. lysine, cysteine, arginine). Moreover, aldehydic LP products (e.g. 4-hydroxynonenal) can bind to cellular proteins compromising their structural and functional integrity (Neely, Sidell et al. 1999). Additionally, $\cdot\text{NO}_2$ can nitrate 3 position of tyrosine residues in proteins. As a result, 3-nitrotyrosine

(3NT) is used as a specific footprint of PN-induced cellular damage (Hall, Oostveen et al. 1997).

In recent work we investigated the role of PN in a mouse model of diffuse closed head injury which demonstrated the spatial and temporal coincidence of PN-induced protein nitration and lipid peroxidation and that this oxidative damage precedes, and therefore may have a causal role in post-traumatic neurodegeneration (Hall, Detloff et al. 2004). However, TBI is a complex disorder that is impossible to fully reproduce in a single model. For example, we have found significant differences between the time courses of neurodegeneration in mouse models of diffuse (Kupina, Detloff et al. 2003) and focal (Hall, Gibson et al. 2005; Hall, Sullivan et al. 2005) TBI. Hence, the magnitude and timing of post-traumatic secondary injury mechanisms probably varies across head injury models. Most importantly, if we are to accurately test the efficacy of novel neuroprotective pharmacological treatments, it is important to first understand the time course of the relevant secondary injury mechanisms in models of focal as well as diffuse TBI.

Thus, the present study was conducted to examine the temporal and spatial characteristics of PN-induced cortical oxidative damage in a model of severe controlled cortical impact (CCI) focal TBI, and its relationship to calpain-mediated cytoskeletal degradation and neurodegeneration. Markers for PN-induced protein nitration (3-nitrotyrosine, 3NT), and lipid peroxidation (4-hydroxynonenal, 4HNE) were measured using immuno-slotblotting and immuno-histochemistry. Secondly, we employed western-blotting methods to look at the

time course of calpain-mediated cytoskeletal degradation in order to assess the temporal relationship of oxidative damage to Ca^{2+} -mediated proteolytic degradation. Finally, we used de Olmos silver staining to measure the evolution of post-traumatic neurodegeneration. The results demonstrate that the PN-mediated oxidative damage is an early event that probably contributes to an exacerbation of neuronal intracellular Ca^{2+} overload, massive calpain activation and cytoskeletal degradation and neurodegeneration.

Materials and Methods

All the surgical, injury and animal care protocols described below have been approved by the *University of Kentucky Institutional Animal Care and Use Committee*, and are consistent with the animal care procedures set forth in the guidelines of the *U.S. Public Health Service Policy on Humane Care and Use of Laboratory Animals*.

Mouse Model of Controlled Cortical Impact (Focal) Traumatic Brain Injury

Young adult male CF-1 mice (Charles River, Portage, MI) weighing 29-31g were used in this study. The mice were anesthetized with isoflurane (3.0%), shaved, and then placed in a stereotaxic frame (David Kopf Instruments, Tujunga, CA). Throughout the surgery, the mice were provided with constant isoflurane (SurgiVet, 100 Series) and oxygen (SurgiVet, O₂ flowmeter, 0-4Lpm). The head was positioned in the horizontal plane of a stereotaxic frame with the nose bar set at zero. We firstly produced a 4mm craniotomy lateral to the sagittal suture, and centered between lambda and bregma. A cortical contusion was produced on the exposed cortex (the anterior-posterior coordinate for the epicenter of the injury was Bregma -2.0mm) using a pneumatically-controlled impactor device (Precision System Instruments TBI-0200 Impactor, Lexington, KY) similar to that previously described (Sullivan, Bruce-Keller et al. 1999; Sullivan, Thompson et al. 1999; Hall, Sullivan et al. 2005) except that the current device utilizes a unique contact sensor mechanism that ensures accurate and

reliable determination of cortical surface prior to initiating the injury sequence. This results in increased accuracy and reproducibility in regards to the CCI injury compared to that produced by earlier CCI impactors. In the present studies, the impactor containing a 3mm diameter rod tip compressed the cortex at 3.5m/sec to a depth of 1mm with a dwell time of 50msec to produce a severe injury. After surgery and injury, a 4mm disk made from dental cement (Dentsply Trubyte) was placed over the craniotomy site and adhered to the skull using cyanoacrylate. In order to prevent immediate post-traumatic hypothermia, following the suturing of the skin, mice were placed in a Hova-Bator incubator (37°C, model 1583, Randall Burkey Co) until they regained consciousness (determined by the regain of the righting reflex and increased mobility). The injured mice were allowed to survive from 30 min to 7 days depending on their experimental group. For the neurochemical studies (measurement of oxidative damage markers and cytoskeletal degradation, see below), the N for each time point group was 8 animals based upon our experience with the variability seen with these measurements in previous studies (Kupina, Detloff et al. 2003; Hall, Detloff et al. 2004; Hall, Sullivan et al. 2005). For each time point, two sham animals were included which were mice that received craniotomy but not cortical contusion. The two sham animals in each group were killed at each of the post-traumatic times along with their brain-injured counterparts. Eight sham mice were randomly selected for comparison with the injured groups.

Tissue Extraction and Protein Assay

At the selected times for the time course analysis (30 min, 1 hr, 3 hrs, 6 hrs, 12 hrs, 24 hrs, 48 hrs, 72 hrs and 7 days), the sham or CCI-injured mice were deeply overdosed with sodium pentobarbital (200mg/kg i.p.). Following decapitation, the ipsilateral cortex were rapidly dissected on an ice-chilled stage and immediately transferred into pre-cooled Triton lysis buffer (1% triton, 20mM tris HCL, 150mM NaCl, 5mM EGTA, 10mM EDTA, 10% glycerol) with protease inhibitors (Complete MiniTM Protease Inhibitor Cocktail tablet). Samples were then briefly sonicated and vortexed at 14,000rpm for 30 min at 4°C, and the supernatants were collected for protein assay. Protein concentration was determined by Bio-Rad DC Protein Assay, with sample solutions diluted to contain 1mg/ml of protein for immunoblotting.

Slot-Immunoblotting Analysis of Oxidative Damage (3NT and 4HNE)

To measure 3-nitrotyrosine (3NT) or 4-hydroxynonenal (4HNE), an aliquot of each ipsilateral cortical sample (2µg) was diluted with 200µl of tris-buffered saline (TBS), and transferred to a Protran (0.2µm) nitrocellulose membrane (Schleicher & Schuell, Dassel, Germany) by a Minifold II vacuum slot blot apparatus (Schleicher & Schuell). After the samples were loaded into the slots, they were allowed to filter through the membrane by gravity (no vacuum). Each slot was then washed with 200µl TBS which was allowed to filter through the membrane again. The membranes were then disassembled from the apparatus, and incubated in a TBS blocking solution with 5% milk for 1 hr at room

temperature. For the detection of 3NT, a rabbit polyclonal anti-nitrotyrosine antibody (Upstate Biotechnology, MA, USA) was used at a dilution of 1:2000 in TBST blocking solution with 5% milk for overnight at 4°C. For the detection of HNE, a rabbit polyclonal anti-HNE antibody (Alpha Diagnostics International) was used at a dilution of 1:5000 in TBST blocking solution with 5% milk for overnight at 4°C. A goat anti-rabbit secondary antibody conjugated to an infrared dye (1:5000, IRDye800CW, Rockland) was applied to the membrane for 1 hr at room temperature. Dry membranes were then imaged and quantified using the Li-Cor Odyssey Infrared Imaging System (Li-Cor[®] Biosciences). Preliminary experiments established protein concentration curves in order to ensure that quantified blots were in the linear range. From the results of these, we selected the 2µg for use based upon that amount giving blots that were well within the linear range. A standardized protein loading control was included on each blot to normalize the band densities so that comparisons could be made across multiple blots. All the samples were run in duplicate which were then averaged. For both the 4HNE and 3NT analyses, no primary antibody controls were run to verify that the oxidative damage staining was specific. In addition, we ran positive controls using both bovine serum albumin and normal brain tissue which were exposed to PN and negative controls in which we pre-absorbed the primary antibodies with either 4HNE or 3NT which resulted in inhibition of the 4HNE and 3NT staining.

Immunohistochemical Analysis of Oxidative Damage (3NT and 4HNE)

A second set of animals was employed for immunohistochemical analysis of 3NT and 4HNE. At the appointed times for the post-traumatic time course analysis (30 min, 1 hr, 3 hrs, 6 hrs, 12 hrs), groups of 5 mice each were overdosed with sodium pentobarbital (200mg/kg i.p.). Two sham, non-injured mice that had craniotomies, but no injury, were included for each time point. The mice were then perfused transcardially with 0.9% sodium chloride (pH7.4) until the venous effluent (sectioned superior vena cava) was cleared of blood, followed by a fixative solution made with 4% paraformaldehyde in 0.2M PBS (pH7.4). The heads were decapitated after fixation and stored in the same fixative solution overnight at 4°C. The brains were removed and equilibrated in the same fixative solution with 15% sucrose overnight at 4°C. The equilibrated brains were sectioned at a thickness of 35µm into the same fixative solution with 15% sucrose at -20°C using a microtome with a freezing stage.

For the 4HNE detection, the free-floating sections were pre-treated with 0.1M NaBH₄ in 0.1M MOPS (pH8.0) for 10 min and rinsed off with 0.2M PBS for three times. The sections were then incubated in 0.3% H₂O₂ for 30 min and rinsed three times with 0.2M phosphate-buffered saline (PBS). Following that, the sections were blocked with a blocking solution (5% goat serum, 0.25% Triton X-100, 1% dry milk, 0.2M PBS) for 2 hrs at room temperature, and then incubated in the primary anti-HNE antibody (rabbit anti-HNE Michael Adducts, Calbiochem) diluted 1:5500 in the same blocking solution overnight at room temperature. The sections were then rinsed with 0.2M PBS six times, and then incubated in

secondary goat anti-rabbit antibody (Vectastain ABC-AP kit) for 2 hrs at room temperature. The sections were then rinsed with 0.1M Tris-HCl (pH8.2) and incubated in Vector blue (Vector blue alkaline phosphatase substrate kit III). They were then rinsed with tap water four times, and mounted onto gelatinized slides. For the 3NT detection, the sections were not pre-treated with 0.1M NaBH₄ in 0.1M MOPS (pH8.0), but were treated the same for the rest of the procedure, except that they were incubated in the primary anti-3NT antibody (rabbit anti-nitrotyrosine, Upstate) diluted 1:1200 in the blocking solution. For both the 4HNE and 3NT analyses, control slides were run without the primary antibodies to verify that the oxidative damage staining was specific. In addition, we ran additional controls in which we pre-absorbed the primary antibodies with either 4HNE or 3NT which resulted in inhibition of the 4HNE and 3NT immunostaining. After the immunohistochemical procedure, all slides mounted with brain sections were counterstained with nuclear fast red (Vector Lot# Q1214), and then cover slipped. The brain sections were photographed on an Olympus Provis A70 microscope at 1.25x, 20× and 40× magnification using an Olympus Magnafire digital camera.

Western-blotting Analysis of Calpain-mediated Cytoskeletal Degradation

To measure calpain-mediated α -spectrin proteolysis, aliquots of each cortical sample (5 μ g) were run on a SDS/PAGE Precast gel (3-8% Tris-Acetate CriterionTM XT Precast gel, Bio-Rad) and then transferred to a nitrocellulose membrane using a semi-dry electro-transferring unit set at 15V for 15 min.

Preliminary experiments established protein concentration curves in order to ensure that quantified bands were in the linear range as measured with the Li-Cor Odyssey Infrared Imaging System. The membranes were incubated in a TBS blocking solution with 5% milk for 1 hr at room temperature. For the detection of α -spectrin and its breakdown products, a mouse monoclonal anti- α -spectrin antibody (Affiniti FG6090) was used at a dilution of 1:5000 in TBST blocking solution with 5% milk for overnight at 4°C. A goat anti-mouse secondary conjugated to an infrared dye (1:5000, IRDye800CW, Rockland) was then applied for 1 hr at room temperature. After drying, the membranes were then imaged and quantified using the Li-Cor Odyssey Infrared Imaging System. A standardized protein loading control was included on each blot to normalize the band densities so that comparisons could be made across multiple blots (Hall, Sullivan et al. 2005). This was made up of pooled brain tissue protein collected from previously run TBI mice which gave strong bands corresponding to the 280kD parent α -spectrin, the 150kD and the 145kD breakdown products. The amount of protein in the loading control had been previously determined and shown to be within the linear range as measured with the Li-Cor Odyssey Infrared Imaging System. Following the transfer, the gels were stained with Coomassie Blue to verify even transfer. All the samples were run in duplicate and averaged.

De Olmos Silver Staining Analysis of Neurodegeneration

Neurodegeneration was examined using the de Olmos aminocupric silver histochemical technique in a third set of 27 mice as previously described (de Olmos, Beltramino et al. 1994; Switzer 2000; Hall, Gibson et al. 2005; Hall, Sullivan et al. 2005). At either 6, 12, 24, 48, or 72 hrs or 7 days the injured mice (N=3-4 per time point) were overdosed with sodium pentobarbital (200mg/kg i.p) and transcardially perfused with 0.9% sodium chloride, followed by a fixative solution containing 4% paraformaldehyde; a sham group of 4 mice that received craniotomy only were sacrificed 24 hrs following surgery. Following decapitation, the heads were stored in a fixative solution containing 15% sucrose for 24 hrs after which the brains were removed, placed in fresh fixative and shipped for histological processing to Neuroscience Associates Inc (Knoxville TN). The 27 brains used for this study were embedded into one gelatin block (Multiblock[®] Technology, Neuroscience Associates). The block was then frozen and thirteen 35 μ m coronal sections were taken 420 μ m apart between 1.1mm anterior and 4.4mm posterior to bregma, were de Olmos silver-stained to reveal degenerating neurons and neuronal processes, and then counterstained with Nuclear Fast Red. The brain sections were photographed on an Olympus Provis A70 microscope at 1.25 \times magnification using an Olympus Magnafire digital camera and the image was analyzed by Image-Pro Plus (4.0). The percentage area of silver staining for each brain section was calculated by dividing the area of silver staining in each section by the area of the total hemispheric section and multiplying by 100. The volume of silver staining in the hemisphere as a

percentage of the overall hemispheric volume was estimated by the equation $\% V = t \times \Sigma \% a(s)$, where $\% V$ is percent silver stain volume, t = the distance between sections analyzed (420 μ m) and $\Sigma \% a(s)$ is the sum of percent area of silver staining in all sections examined (13 for each brain) (Hall, Sullivan et al. 2005).

Statistical Analysis

For all of the time course analyses, we used Statview 5.0 to perform a one-way analysis of variance (ANOVA), followed by Fisher's PLSD post-hoc analysis to determine the significance of differences between individual time points and the non-injured sham group. For the ANOVA, a $p < 0.05$ was required to establish a statistically significant difference across the groups. However, for the post-hoc Fisher's analysis, the program determined significance based upon a correction for multiple comparisons comparing sham to each of the 9 post-injury time points. Differences between pairs of post-injury time points (e.g. 30 min. vs. 1 hr) were also analyzed.

Results

Quantitative Post-Traumatic Time Course of Protein Nitration and Lipid Peroxidation

Figure 2.1 displays the complete quantitative time course study for 3NT and 4HNE in the ipsilateral cortical samples taken from sham or CCI-injured mice. Figure 2.1A indicates schematically the dorsal and coronal view of contusion site and peri-contusional cortical tissue that was collectively sampled for the current study. Figure 2.1B shows the time course of changes in 3NT, a selective marker of PN-mediated damage. As noted in the MATERIALS AND METHODS, two non-injured sham animals corresponding to each post-traumatic time point were run. For the nine time points, this resulted in a total of 18 shams. A comparison of the bands obtained from different pairs of shams, showed little evidence that those animals killed at the later time points had any more 3NT or 4HNE than those sampled at the earlier time points. Therefore, we randomly selected 8 of the 18 shams to use as the sham group for comparison with the different injured groups. The ANOVA showed that there was a highly significant overall difference across the collective sham and post-traumatic groups in regards to 3NT levels [$F(9,70)=2.744$; $p<0.0001$]. Post-hoc analysis revealed a significant increase in 3NT at 30 min after injury compared to the sham group. At 1 hr after injury, the 3NT level reached its peak and was approximately twice as much as that seen in sham, non-injured mice. The 3NT level maintained significantly high until 12 hrs after injury, and at 24 hrs, it returned to baseline

(sham level). However, a small, but statistically significant secondary increase in 3NT was also observed at 48, but not at 72 hrs.

Figure 2.1C displays the time course of post-traumatic changes in 4HNE, a marker for lipid peroxidation, at different time points after injury. As with the 3NT analysis, there was a highly significant overall difference across the collective sham and post-traumatic groups in regards to 4HNE content [$F(9,70)=15.211$; $p<0.0001$]. Post-hoc analysis of between group differences showed that there was a significant increase in 4HNE at 30 min after injury, the 4HNE level reached its peak at 1 hr after injury and it stayed significantly higher than the sham level until 12hr before returning to the baseline levels seen in the sham animals.

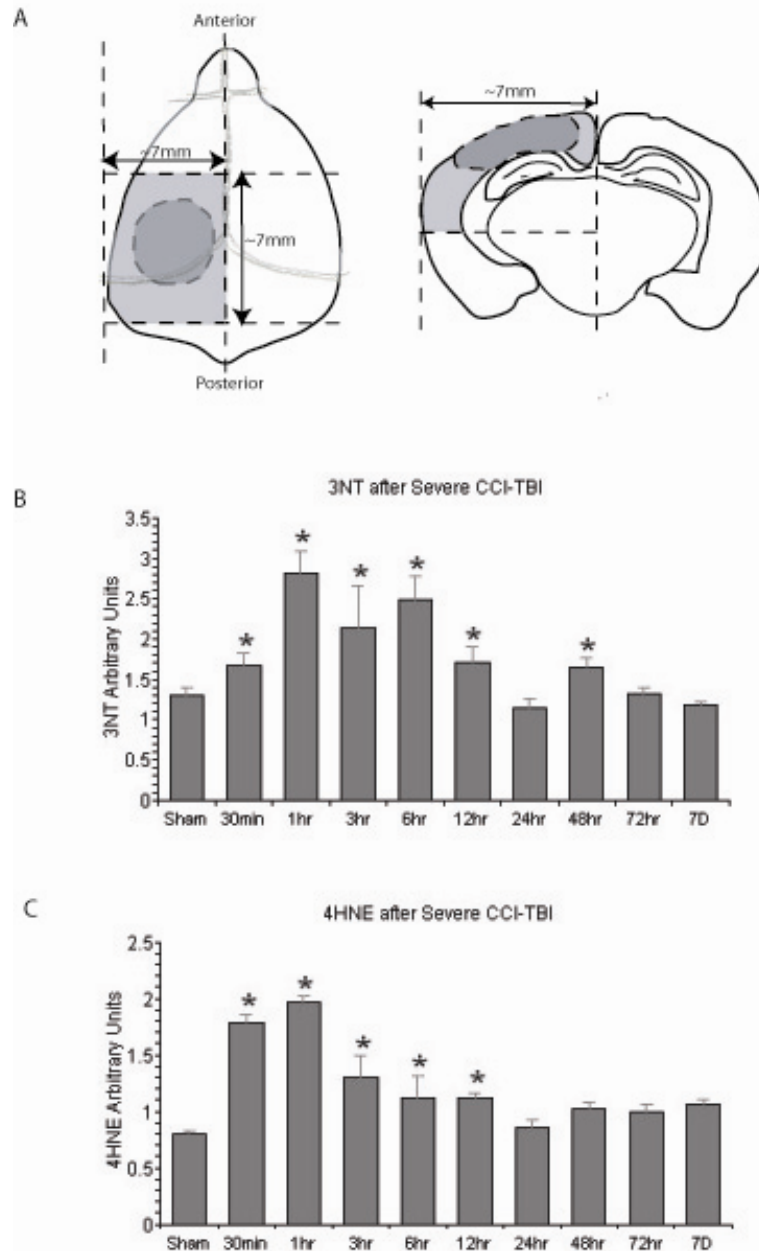


Figure 2.1 Slot-blotting studies in ipsilateral cortical traumatic brain injury tissues showing the temporal changes in protein nitration (3-nitrotyrosine; 3NT) and lipid peroxidation. A. Schematic showing peri-contusional cortical tissue samples; B. time course of changes in 3-NT; C. Time course of LP end product 4HNE. N = 8 animals per timepoint; values = mean + standard error; one-way ANOVA and Fisher's PLSD post hoc test: *P < 0.0001 vs. sham.

Spatial and Temporal Distribution of Peroxynitrite-Induced Protein Nitration and Lipid Peroxidation

Figure 2.2 demonstrates the temporal and spatial characteristics of the immunohistochemical staining related to post-traumatic oxidative damage in the ipsilateral hemisphere of mice after CCI injury. Two adjacent brain sections in the epicenter (Bregma-2.0mm) of the contusion were selected for 3NT staining and 4HNE staining. In Figure 2.2, the staining for 3NT and 4HNE markers were concentrated within and around the contusion area in the ipsilateral cortex, and the 3NT and 4HNE staining was largely overlapping. Staining for both markers was observed as early as 30 min. Staining remained intense up to 6 hrs after injury. At 12 hrs, the staining showed signs of decrease no doubt due to proteolytic degradation of the oxidatively modified proteins. This time course is in good agreement with the quantitative time course for 3NT and 4HNE shown in Figure 2.1.

Figure 2.3 shows high power photomicrographs of 3NT and 4HNE immunostaining within the cortical contusion site in a sham, non-injured brain compared to staining at the contusion site at 1 hr after injury. At 20x and 40x magnification, intense staining for both oxidative damage markers is seen throughout the neuropil. In addition, microvascular staining for both 3NT and 4HNE is seen to clearly outline the microvessels deep within the injured cortex. Although the sham brain shows some light staining in the neuropil, there is no evidence of staining of non-injured microvessels. The pattern of staining in both

the parenchyma and vasculature has also been seen previously after a diffuse brain injury (Hall, Detloff et al. 2004).

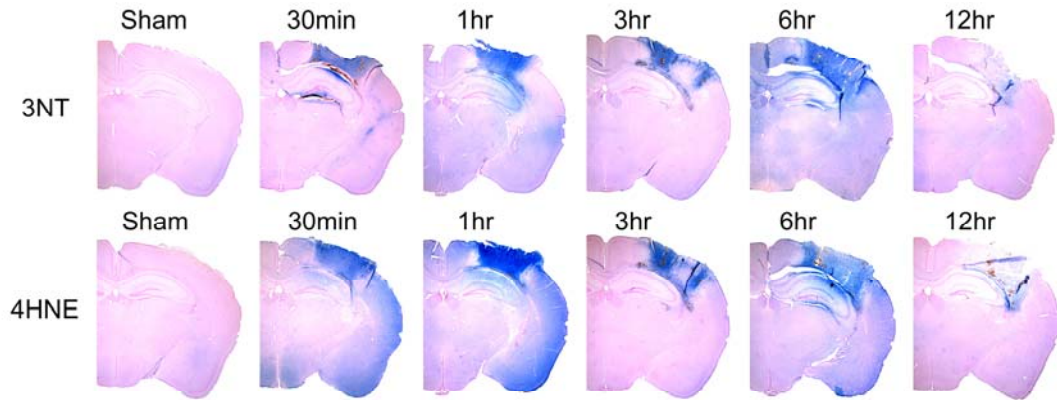


Figure 2.2 Immunohistochemical (IHC) staining studies showing the time course and spatial extent of PN-induced 3NT and 4HNE at the epicenter (Bregma-2.0mm) of the injury site during the first 12 hrs compared to sham. The IHC staining indicated prominent increase of both markers after injury and similar distribution between the two.

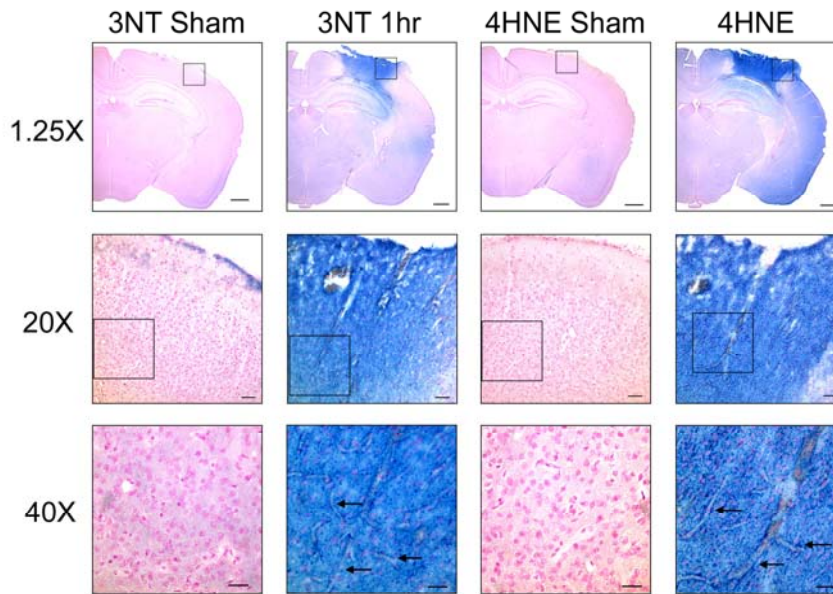


Figure 2.3 High power photomicrographs of 3NT and 4HNE immunostaining in the contusion site in a sham, non-injured brain compared to staining at the contusion site at 1 hr after injury. At 20x and 40x magnification, intense staining for both oxidative damage markers is seen throughout the neuropil. In addition, microvascular staining for both 3NT and 4HNE is seen to clearly outline the microvessels (arrows) deep within the injured cortex. Although the sham brain shows some light staining in the neuropil, there is no evidence of staining of non-injured microvessels. Please note that the 20x and 40x focus was adjusted to emphasize the microvascular staining, and as a result the background tissue appears slightly out of focus. The calibration bar for the 1.25x photomicrographs is 2.0mm; for 20x the calibration bar is 100 μ m; for 40x the calibration bar is 50 μ m.

Quantitative Post-traumatic Time Course of Calpain-Mediated Cytoskeletal Degradation

Figure 2.4 displays the quantitative post-traumatic time course analysis of calpain-mediated cytoskeletal degradation in the ipsilateral cortical tissue in terms of the levels of α -spectrin breakdown products SBDP145 and 150 measured by western-blotting. The spectrin breakdown product 145 (kD) and 150 (kD) in each time group were compared to the sham SBDP145 and the sham SBDP150 respectively. The SBDP150 band can be produced by either calpain or caspase 3, whereas the SBDP145 band is calpain specific. ANOVA showed that there was a significant overall post-traumatic increase in SBDP145 [F(9,70)=9.444; $p<0.0001$] and SBDP150 [F(9,70)=8.857; $p<0.0001$]. Accordingly, post-hoc analysis of the significance of increases seen at individual post-traumatic time points was compared to sham, non-injured animals. At 30 min after injury, the mean SBDP150 level was significantly increased. The levels of this mixed calpain/caspase 3 marker remained significantly higher than sham levels at all subsequent time points out to, and including, 48 hrs post-injury. The maximum increase in SBDP150 was observed at 24 hrs post-injury. The calpain-specific SBDP145 showed a significant increase vs. sham beginning at 1 hr post-injury, and increased slightly more at 3, 6 and 12 hrs.

Between 12 and 24hrs, there was a statistically significant (12 hr vs. 24 hr; $p<0.0004$) 75% jump in SBDP145 levels with the 24 hrs time point manifesting the maximum post-traumatic increase. In parallel, there was an equally significant (12 vs. 24 hr; $p<0.0001$) increase in the SBDP150 levels SBDP150.

The magnitude of the increase in SBDP145 was greater (compared to the sham group) (18-fold) in comparison to the SBDP150 increase (6-fold). The level of SBDP145 remained significantly elevated at 48 hrs before returning to levels at 72 hrs after TBI that were no longer significantly higher than those seen in sham animals. The overall time course patterns were similar for both SBDP150 and SBDP145.

It should be noted that the current post-traumatic time course of α -spectrin degradation, although similar in several respects to a time course study we published earlier (Hall, Sullivan et al. 2005) using the CCI model, shows some differences that are worthy of explanation. In the previous study, the earliest post-traumatic time point examined was 6 hrs at which time we observed a statistically significant increase in SBDP145 and 150 compared to sham, just as in the present study. However, the elevation in SBDPs did not increase further at 24 or 48 hrs, but rather appeared to plateau before returning to the sham baseline level at 1 week. This is in contrast to the significantly higher peak in SBDP 145 and 150 observed in the current study. There are two likely reasons for the discrepancy between the current and the previously published time course (Hall, Sullivan et al. 2005). First of all, in the current study we employed a more sensitive infrared imaging method for performing the densitometric analysis of the blots which has a broader linear range compared to the less sensitive enhanced chemiluminescence (ECL) method that we previously employed which is only semi-quantitative. Consequently, the previous plateau between 6 and 72 hrs post-injury (Hall, Sullivan et al. 2005), in contrast to the current results is

probably due to the less accurate nature of ECL vs. infrared imaging. Secondly, the current study was performed with a newer CCI device than the one used in the previous study. The newer device (PSI TBI 0200 Impactor) utilizes a unique contact sensor mechanism that insures accurate and reliable determination of cortical surface prior to initiating the injury sequence. This results in increased accuracy and reproducibility in regards to the CCI injury. Thus, for these two reasons, we have more confidence in the accuracy of the current results in regards to the time course of post-traumatic cytoskeletal degradation. Furthermore, the current time course of α -spectrin degradation in the CCI-injured cortex is similar in pattern to the time course of α -spectrin degradation we have seen in the injured hippocampus using the same injury device, injury severity and infrared imaging of the blots (Thompson, Gibson et al. 2006)

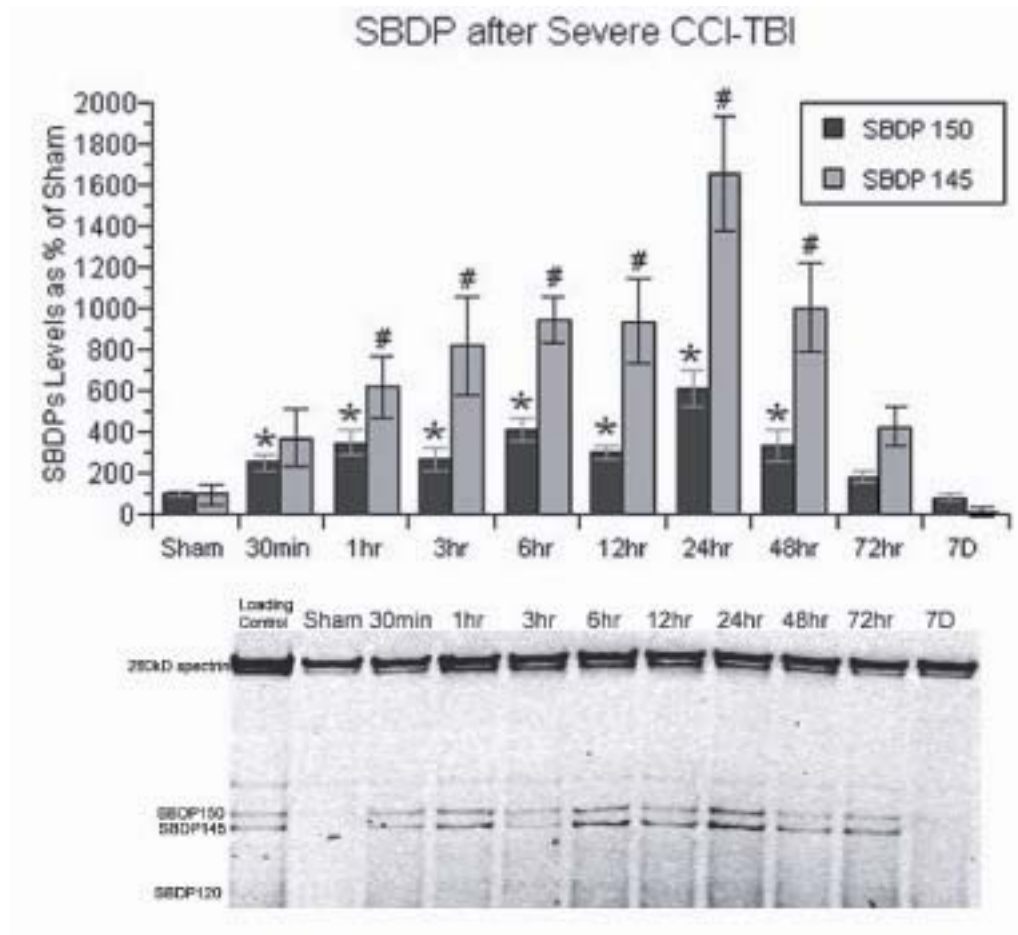


Figure 2.4 Time course of the post-traumatic increase in calpain-mediated α -spectrin breakdown products in CCI cortical tissues. Spectrin breakdown product (SBDP) 145 is specific to calpain activity, whereas SBDP 150 is produced by both calpain and caspase 3. Both SBDPs showed similar patterns, except that calpain-mediated SBDP 145 showed a more prominent increase. Both SBDPs have an immediate increase following injury, and did not reach their peak until 24 hrs. N = 8 animals per timepoint; values = mean + standard error; one-way ANOVA and Fisher's PLSD post hoc test: *P < 0.0001 vs. sham SBDP150; one-way ANOVA and Fisher's PLSD post hoc test: #P < 0.0001 vs. sham SBDP145.

Quantitative Post-Traumatic Time Course of Neurodegeneration

Figure 2.5 shows the quantitative de Olmos aminocupric silver staining analysis of neurodegeneration in the ipsilateral hemisphere of mice subjected to CCI along with histological examples of the spatial and temporal characteristics of silver staining between 6 hrs and 7 days after injury. At 6 hrs after injury, there was a significant increase of silver staining volume compared to minimal level seen in sham, non-injured mouse brains. The silver staining spread over time and peaked at 48 hrs after injury. After 48 hrs, the volume of silver staining slowly waned, but remained significantly higher than the sham level even at 7 days. As shown in the selected brain sections, at 6 hrs, the silver staining was mainly concentrated in all layers in the ipsilateral cortical contusion. A cavitation lesion began to develop at 12 hrs and became evident at 24 hrs. At 24 hrs, the silver staining had spread into and throughout the ipsilateral hippocampus and dorsolateral aspect of the thalamus. At 48 hrs, the silver staining volume reached its greatest extent. Silver staining also extended to the contralateral hippocampus, indicative of the degeneration of CA3 commissural fiber projections to the contralateral dentate gyrus and CA1 region as previously shown (Hall, Sullivan et al. 2005).

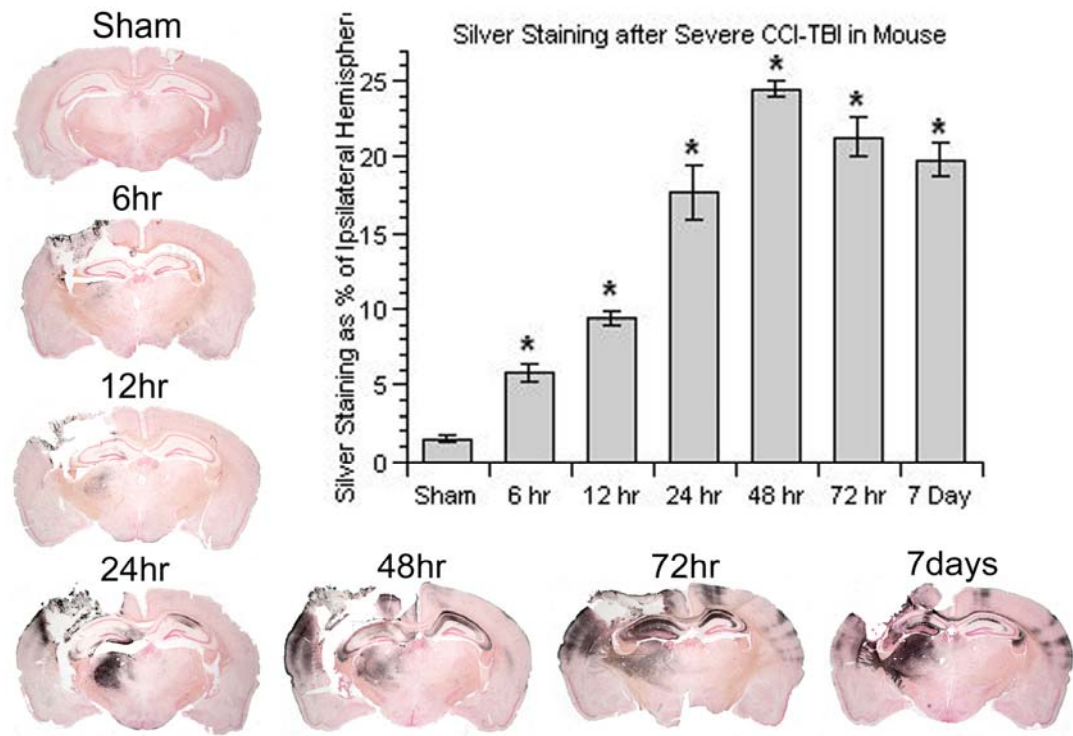


Figure 2.5 Time course of post-traumatic neurodegeneration in CCI model as revealed by the de Olmos silver staining technique. The bar chart provides the quantification of the lesion volume about measurement of the silver staining. An increase in silver staining volume determined by image analysis (see Materials and Methods) occurred as early as 6 hrs and reached its peak at 48 hrs post-injury. N = 3-4 animals per time point; values = mean \pm standard error; one-way ANOVA and Fisher's PLSD post hoc test: *P < 0.0001 vs. sham.

Discussion

The present study in the context of the focal controlled cortical impact (CCI) mouse model has uniquely defined in a parallel fashion the time courses of oxidative damage, calpain-mediated cytoskeletal degradation and neurodegeneration. A careful analysis of these three secondary injury parameters has revealed clues concerning their mechanistic inter-relationships. The following discussion lays out the hypothesis that 1) the potent ROS PN is a key mediator of post-traumatic oxidative damage; 2) a major source of PN is Ca^{2+} -overloaded mitochondria; 3) a major consequence of PN-mediated oxidative damage is exacerbation of intracellular Ca^{2+} overload by impairment of Ca^{2+} homeostatic mechanisms and 4) this leads to an enhancement of calpain-mediated cytoskeletal degradation which is the immediate precursor of post-traumatic neuronal degeneration.

Temporal and Spatial Characteristics of Oxidative Damage and the Role of Peroxynitrite:

The two oxidative markers: tyrosine nitration (3NT) and LP-derived 4HNE modified proteins (see Halliwell and Gutteridge, 1999), increased in unison. Their increase occurred as early as 30 min after injury and peaked at 1hr. The coincidence of the early time course of 3NT and 4HNE suggests that they share a common ROS as their initiating source. The most likely candidate ROS in this regard is PN. The nitration of the 3 position of tyrosine residues in proteins is a

result of PN activity and is used as a selective marker for PN-induced oxidative damage. Therefore, it is generally accepted as evidence of a role of PN in tissue injury models where 3NT elevations are seen (Beckman 1996). Moreover, the indictment of PN as a source of LP (4HNE) is strongly implied by the fact that 3NT and 4HNE share the same early post-traumatic onset (30 min), time to peak (1 hr) and duration (12 hrs). Furthermore, spatial overlap of 3NT and 4HNE seen in the immunohistochemical examples also indicates that nitration and LP are both initiated by PN. Previous work from our laboratory using a mouse model of diffuse TBI, has also shown the spatial and temporal coincidence of 3NT and 4HNE immunostaining leading to a similar conclusion that PN was key player in the post-traumatic oxidative damage (Hall, Detloff et al. 2004). However, in the case of the previously studied diffuse TBI model, the duration of the increase in 3NT and 4HNE was much longer (at least 96 hrs) in contrast to the much shorter expression of oxidative damage in the presently employed focal paradigm. Particularly important is the fact that PN-mediated oxidative damage was observed in both the cortical microvessels and in the neural parenchyma consistent with our earlier studies in the mouse diffuse TBI model (Hall, Kupina et al. 1999; Hall, Detloff et al. 2004)

Sources of Peroxynitrite:

Regarding the sources of PN in the injured brain, NO• is produced by multiple NOS isoforms, and is a mediator of physiological (Garthwaite and Boulton 1995; Bicker 2001) and neuroprotective (Mohanakumar, Hanbauer et al.

1998; Chiueh 1999) actions as well as being an effector of PN formation and oxidative damage (Dawson and Dawson 1996; Vicente, Perez-Rodriguez et al. 2006). An earlier immunocytochemical study revealed the induction of endothelial NOS (eNOS) isoform in microvessels surrounding the cortical contusion post-injury, which may contribute to blood-brain barrier (BBB) breakdown and hyperemia followed by TBI (Cobbs, Fenoy et al. 1997). Other isoforms of NOS, neuronal NOS (nNOS) and inducible NOS (iNOS), have also been shown to be upregulated in TBI models. In a focal brain contusion model, all three isoforms of NOS (nNOS, eNOS, iNOS) have been found to be increased. However, each is expressed in different compartments and cells, and is differentially regulated (Gahm, Holmin et al. 2000). In addition, a possibly novel isoform of NOS (mtNOS) is constitutively present in mitochondria, is Ca^{2+} -dependent (Giulivi 2003) and appears to be involved in mitochondrial respiratory regulation (Elfering, Sarkela et al. 2002). Under hypoxic conditions, mtNOS activity is induced in comparison to that seen in non-stressed mitochondria (Lacza, Puskar et al. 2001). In rat liver mitochondria, mtNOS has been shown to be stimulated by Ca^{2+} influx (Ghafourifar and Richter 1997) and leads to intramitochondrial PN formation (Ghafourifar, Schenk et al. 1999). Furthermore, there is evidence that mitochondria may be the primary target for oxidative damage by PN under a variety of pathological conditions (Radi, Rodriguez et al. 1994). Consistent with this view, recent experiments from our laboratory, using the same mouse CCI model as in the present study, have shown that the early post-traumatic impairment of mitochondrial ultrastructure and bioenergetics are associated with

PN-mediated protein nitration and 4HNE conjugation together with a severe attenuation of Ca^{2+} buffering capacity (Singh, Sullivan et al. 2006a). Furthermore, our in vitro studies with isolated brain mitochondria have demonstrated that application of compounds such as penicillamine, which scavenges PN anion (ONOO^-) and peroxyxynitrous acid (ONOOH) (Hall, Kupina et al. 1999), or tempol, which catalytically scavenges PN-derived oxygen radicals (e.g. $\bullet\text{NO}_2$, $\bullet\text{CO}_3$) (Carroll, Galatsis et al. 2000), can protect against PN-mediated mitochondrial respiratory dysfunction and oxidative damage (Singh et al, 2006b). Both penicillamine (Hall, Kupina et al. 1999) and tempol (Beit-Yannai, Zhang et al. 1996) have been reported to improve neurological recovery in rodent TBI models. Moreover, administration of the NOS inhibitors nitro-arginine methyl ester and 7-nitroindazole have been shown to improve neurological recovery in head-injured mice (Mesenge, Verrecchia et al. 1996) together with a reduction in brain 3NT levels (Mesenge, Charriaut-Marlangue et al. 1998).

Temporal Characteristics of Calpain-Mediated Cytoskeletal Damage:

Several experimental TBI studies from different laboratories have documented the significant contribution of calpain activity to the post-traumatic damage and neurodegeneration (Arrigoni and Cohadon 1991; Posmantur, Kampfl et al. 1996; Saatman, Murai et al. 1996). Pathological calpain activation is known to be triggered by excessive intracellular Ca^{2+} accumulation (Bartus, Elliott et al. 1995; Kampfl, Posmantur et al. 1997), which is associated with the glutamate release and sustained NMDA activation, as well as depolarization-

induced opening of voltage-dependent Ca^{2+} channels immediately after CNS trauma. Preferred substrates for calpain include cytoskeletal proteins, membrane-associated proteins, signaling transduction proteins and transcription factors (Carafoli and Molinari 1998; Wang 2000). As noted earlier, calpain-mediated proteolysis of the major membrane cytoskeletal protein, α -spectrin, results in the appearance of two highly stable breakdown products, calpain-specific SBDP145 and the non-specific calpain/caspase 3-generated SBDP150. Our results showed that there is a rapid accumulation of both SBDPs by 1 hr after injury which further increases at 3 hrs before reaching a plateau at 6 and 12 hrs. Nevertheless, at 24 hrs, both SBDPs showed a significant increase above the level seen at 12 hrs spiked to their peak with a particularly prominent SBDP145 increase. Although a role of caspase 3 cannot be ruled out in regards to the increase in SBDP150, the predominant elevation in the calpain-specific SBDP145 at 24 hrs indicates that the major contribution of calpain to cytoskeletal damage. In addition, the caspase 3 specific SBDP120 (Wang 2000) showed no increase over time which suggests only a very minor role of caspase 3 in post-traumatic spectrin proteolysis. After 24 hrs, the SBDP 145 and 150 levels progressively subsided, and both returned to the baseline level (sham) by 72 hrs after injury.

Interaction of Peroxynitrite-Induced Oxidative and Calpain-Mediated Proteolytic Damage Mechanisms:

Multiple lines of evidence have linked ROS-initiated oxidative damage to the loss of intracellular Ca^{2+} homeostasis and calpain activation. It has been commonly indicated that ROS cause a rapid increase in cytoplasmic Ca^{2+} concentration in diverse cell types (Roveri, Coassin et al. 1992; Chakraborti, Das et al. 1999; Okabe, Tsujimoto et al. 2000), which can contribute to the early transient calpain activation. However, the current study indicated that the full activity of calpain did not occur until a later time point that follows the early wave of oxidative damage and the peak of mitochondrial dysfunction (Singh, Sullivan et al. 2006a). At the point at which mitochondrial functional failure occurs, this results in a loss of mitochondrial Ca^{2+} buffering and release of accumulated Ca^{2+} into the cytoplasm which would be expected to exacerbate calpain activation and spectrin breakdown. It has been shown that mitochondria-derived PN plays a role in mitochondrial Ca^{2+} overload, and can actually promote Ca^{2+} release from intact mitochondria (Bringold, Ghafourifar et al. 2000). Moreover, we have previously demonstrated that the mitochondrial failure is coincident with oxidative damage to mitochondrial proteins and loss of mitochondrial Ca^{2+} buffering capacity (Singh, Sullivan et al. 2006a). In an *in vitro* study, nitric oxide-elicited neuronal apoptosis through excitotoxicity and receptor-mediated intracellular Ca^{2+} overload mechanisms was blocked by calpain inhibitors (Volbracht, Chua et al. 2005). Another *in vitro* study has also indicated that PN-initiated cell death in

human articular chondrocytes is mediated by mitochondrial dysfunction and calpain activity (Whiteman, Armstrong et al. 2004).

In addition to the apparent role of ROS in the post-traumatic impairment of Ca^{2+} homeostasis, ROS also are involved in directly regulating calpain proteolytic activity. As indicated in Figure 2.4, following an immediate and rapid increase of SBDPs at 1 hr after injury, there is essentially a plateau in regards to the SBDP levels between 3 hrs and 12 hrs. Then, between 12 hrs and 24 hrs, both SBDPs exhibited a greater than 75% increase which was highly significant ($p < 0.0004$ for SBDP145 and $p < 0.0001$ for SBDP150). A similar biphasic pattern of calpain-mediated α -spectrin degradation has also been observed by our laboratory in the context of a rat spinal cord injury model (Xiong, Rabchevsky et al. 2007) and by others in a transient ischemic brain injury model (Neumar, Meng et al. 2001). In a recent hippocampal organotypic slice study, stretch-induced injury also showed a biphasic activation of calpain (DeRidder, Simon et al. 2006). This repeatedly demonstrated biphasic time course of calpain-mediated proteolysis can potentially be explained by an initial partial ROS-mediated inhibition of calpain activity in the early post-traumatic hrs during which PN generation and evidence of oxidative damage are at their highest level. Consistent with this hypothesis, it has been shown that ROS can inhibit calpain activity via oxidation of the sulfhydryl groups of cysteine residues at the active site of the enzyme (Benuck, Banay-Schwartz et al. 1992; Guttman, Elce et al. 1997; Guttman and Johnson 1998). Recent work by another group has shown that another cysteine protease caspase 3 in the traumatized brain is similarly inhibited by PN specifically, and

that this is prevented by application of the sulfhydryl reducing agent dithiothreitol (Lau, Arundine et al. 2006). The latter is also relevant since the SBDP150 fragment which also showed a biphasic time course is partially generated by caspase 3 as well as calpain (Wang 2000). Therefore, it is reasonable to speculate that even though intracellular Ca^{2+} overload is triggered immediately after injury (Zhou, Xiang et al. 2001), the peak of calpain- and caspase-mediated cytoskeletal degradation may not be achieved until as much as 24 hrs post-injury after which an initial ROS-mediated calpain and caspase inhibition has subsided. In other words, as the intensity of the PN generation decreases, the oxidative damage-mediated impairment of various Ca^{2+} homeostatic mechanisms and the neurodegenerative consequences of post-traumatic intracellular Ca^{2+} overload and peak calpain activity would have the opportunity to be fully seen. This peak in calpain-mediated damage at 24 hrs closely precedes the progressive increase in post-traumatic neurodegeneration (silver staining) which peaks at 48 hrs.

We have observed the same close association between calpain-mediated cytoskeletal degradation and neurodegeneration in the mouse diffuse TBI model except that the peak of the former is seen at 72 hrs and that of the latter is seen between 72 and 96 hrs (Hall, Detloff et al. 2004). The different time course of PN-mediated oxidative damage and calpain-mediated cytoskeletal degradation seen in focal and diffuse (Kupina, Detloff et al. 2003) TBI models suggests that the therapeutic window and optimum treatment durations for either PN-directed antioxidant agents or calpain inhibitor treatment may differ between the two types of TBI.

Summary:

Our working hypothesis, based upon the findings in this study, is illustrated in Figure 2.6. Initial mechanical trauma to the brain causes membrane depolarization, resulting in the opening the voltage-dependent Na^+ , K^+ and Ca^{2+} channels, and the release of glutamate into the extracellular spaces, which will lead to the activation of NMDA receptors. Both mechanisms directly or indirectly elevate intracellular Ca^{2+} and rapidly initiate the activation of intracellular calpains. However, mitochondria take up the excessive Ca^{2+} in the cell, which subsequently activates mitochondrial NOS and results in overproduction of $\text{NO}\cdot$ radical. Elevated $\text{NO}\cdot$ out-competes superoxide dismutase (SOD) for superoxide radical ($\text{O}_2^{\cdot -}$) leading to the formation of PN. Then, PN-derived free radicals could be expected to initially produce a partial inhibition of calpain and caspase 3 activity. Mitochondria, however, as a major intracellular ROS source not only become a primary location for PN production, but also are susceptible to PN-induced oxidative damage due to their enriched thiol and iron-rich structures within the electron transport chain (ETC). In addition, the biochemical properties of PN enable it to diffuse out of the mitochondria to induce further oxidative damage to the cell membrane and cellular proteins. This increase in oxidative stress during the first 12 hrs, induces cellular oxidative damage by LP, protein oxidation and protein nitration. The calpain-mediated proteolysis displays a biphasic activity probably as a result of an initial partial PN-mediated inhibition of calpain. However, as this subsides, the extensive compromise of Ca^{2+} homeostasis in the mitochondrion and the rest of the cell becomes manifest and

calpain activity is free to reach its peak. In the end, calpain-mediated cytoskeletal degradation becomes a final common pathway leading to neuronal cell death.

The findings of this study strongly support the concept of an important pathophysiological role of PN-mediated oxidative damage following TBI. Peroxynitrite-induced oxidative damage and calpain activation interact and are probably responsible for much of the secondary injury and neurodegeneration that occurs. If so, then PN-targeted antioxidants should be neuroprotective. However, the combination of a PN-targeted antioxidant and a calpain inhibitor might have a better neuroprotective action than either approach alone. Future studies will explore these possibilities. Copyright © Ying Deng 2007.

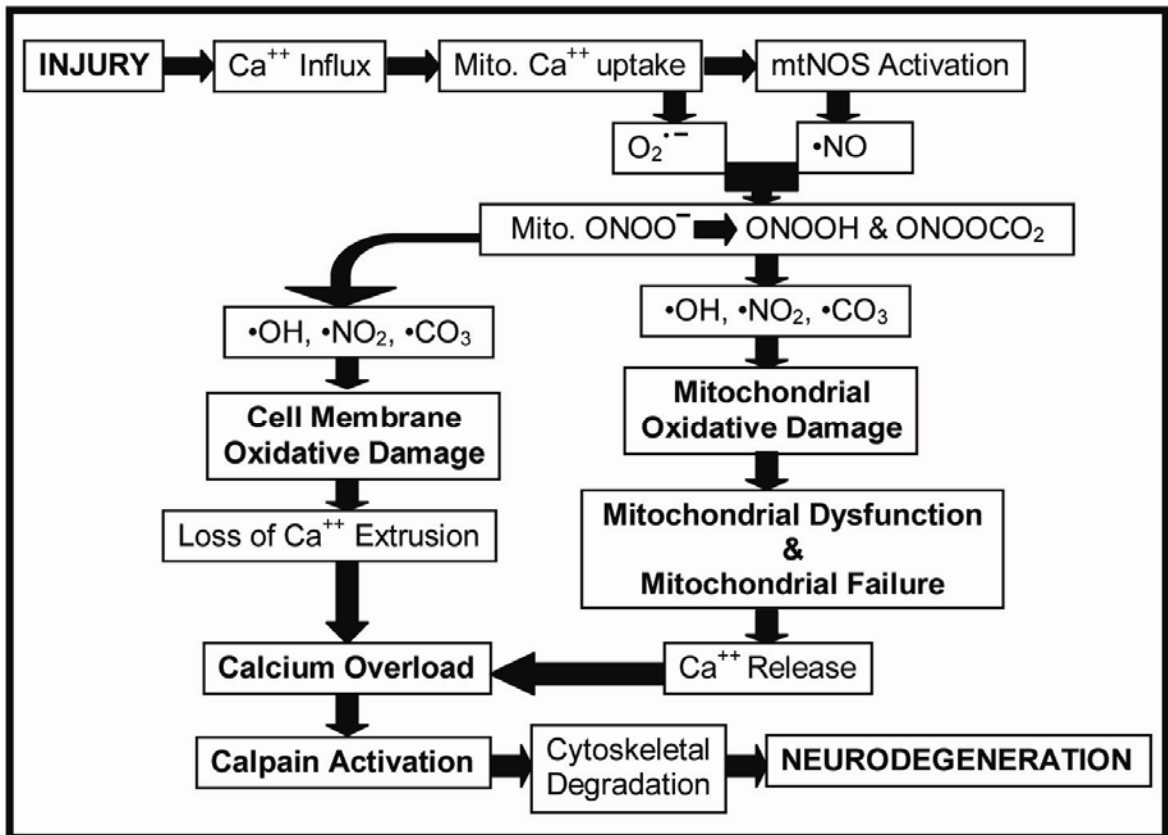


Figure 2.6 Hypothetical interrelationship between PN-induced oxidative damage in neuronal mitochondria and the rest of the neuron, compromise of Ca²⁺ homeostasis, calpain-mediated proteolysis and neurodegeneration. Our results suggest that PN-induced oxidative damage plays a key role in the post-traumatic secondary injury, which leads to exacerbation of Ca²⁺ overload, calpain proteolysis of cytoskeleton and other cellular proteins and neurodegeneration. See **Discussion** for a further description.

Chapter Three

Tempol in Its Ability to Scavenge Free Radicals, Ameliorate Mitochondrial Dysfunction and Inhibit Calpain Activity

Introduction

Nitroxide antioxidants, such as tempol (4-hydroxy-2,2,6,6-tetramethylpiperidine-1-oxyl, see Figure 3.1), are generally described in the literature as potent metal-independent superoxide dismutase (SOD) mimics with better membrane permeability and potency (Samuni, Krishna et al. 1989; Krishna, Russo et al. 1996). Nitroxides have been shown to quench superoxide radical ($O_2^{\cdot -}$) to eventually produce hydrogen peroxide and oxygen just like SOD. Moreover, nitroxides prevent oxidative damage by removing superoxide radical ($O_2^{\cdot -}$) catalytically rather than stoichiometrically. Moreover, six-membered cyclic nitroxides such as tempol react faster as an antioxidant than corresponding five-membered ring nitroxides (Samuni, Krishna et al. 1990). As often studied in biological systems, nitroxides also have the ability to react with lipid peroxidation (LP)-derived intermediates such as alkoxy radical and peroxy radical. Furthermore, they can act as mild oxidizing agents to prevent the cycling of transition metal ions ($Fe^{2+} \rightarrow Fe^{3+}$) and thereby inhibit the production of hydroxyl radicals ($\cdot OH$) via in Fenton-type reaction (Zeltcer, Berenshtein et al. 1997).

More recently, it has been shown that tempol can catalytically decompose the peroxyxynitrite (PN) free radicals nitrogen dioxide ($\cdot NO_2$) and carbonate ($\cdot CO_3$). High-performance liquid chromatography (HPLC) analysis measuring the

intermediates of the reactions between tempol and PN-induced phenolic nitration suggested that oxidized forms of tempol can exchange among themselves without depletion in the reaction with PN-derived free radicals, which makes tempol a potent catalytic antioxidant (Carroll, Galatsis et al. 2000).

Thus, because of its multiple antioxidant properties, and its membrane permeability, tempol or similar compounds may have considerable therapeutic values in protection against cytotoxicity that involves oxidative damage. *In vivo* studies have indicated that tempol provides protection against X-ray-induced DNA damage, or other radiation oncology (DeGraff, Krishna et al. 1992; Hahn, Krishna et al. 1994). Tempol was also suggested to reduce PN-generated nitration, decrease poly ADP-ribose synthetase (PARS) activation, as well as reduce infarct volume and hyperactivity in ischemic experimental models (Cuzzocrea, McDonald et al. 2000; Rak, Chao et al. 2000; Kato, Yanaka et al. 2003). Moreover, tempol was shown to reduce the pathophysiology of acute subdural hematoma (ASDH) (Kwon, Chao et al. 2003). In a Parkinson's disease model, tempol was indicated to attenuate malonate and 1-methyl-4-phenyl-1,2,5,6 tetrahydropyridine (MPTP)-induced neurotoxicity (Matthews, Klivenyi et al. 1999). Furthermore, it has been shown that tempol can improve tissue sparing and locomotor outcome after spinal cord injury (SCI) (Hillard, Peng et al. 2004). Finally, tempol has been shown to limit edema formation, blood-brain barrier (BBB) disruption and to improve functional recovery (Beit-Yannai, Zhang et al. 1996; Zhang, Shohami et al. 1998). In the latter studies, the mechanism of the

neuroprotective antioxidant action was completely attributed by the authors to superoxide scavenging.

The present study was undertaken in the controlled cortical impact (CCI) mouse traumatic brain injury (TBI) model to examine the possibility that tempol's neuroprotective efficacy in acute TBI also involves inhibition of PN-mediated oxidative damage in brain tissue, mitochondria and downstream amelioration of calpain-mediated cytoskeletal breakdown. As demonstrated in our previous study, the early increase of oxidative damage in mitochondrial proteins paralleled to that in the cortical homogenate ipsilateral to the injury, which also coincided with the time course of mitochondrial dysfunction following the injury (Chapter 2; Singh, Sullivan et al. 2006a, see Appendix I and II). This strongly suggests the idea that mitochondria are the primary source and target of PN upon mitochondrial calcium uptake in the CCI model (Singh, Sullivan et al. 2006a). Moreover, as also indicated in our time course study on cellular changes triggered by TBI in the CCI model, the peak of oxidative damage at 1 hr after injury preceded both the peak of calpain activity at 24 hrs and neurodegeneration, measured by silver staining, at 48 hrs (Deng, Thompson et al. 2007). Therefore, the current experiments were conducted to investigate tempol's ability to reduce post-traumatic PN-induced oxidative damage, mitochondrial dysfunction and calpain-mediated cytoskeletal degradation in order to establish a mechanistic linkage between these successive pathophysiological events.

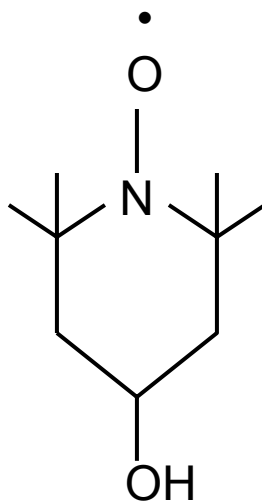


Figure 3.1 Chemical structure of tempol.

Materials and Methods

All the surgical, injury and animal care protocols described below have been approved by the *University of Kentucky Institutional Animal Care and Use Committee*, and are consistent with the animal care procedures set forth in the guidelines of the *U.S. Public Health Service Policy on Humane Care and Use of Laboratory Animals*.

Mouse Model of Controlled Cortical Impact (Focal) Traumatic Brain Injury

Young adult male CF-1 mice (Charles River, Portage, MI) weighing 29-31g were used in this study. The mice were anesthetized with isoflurane (3.0%), shaved, and then placed in a stereotaxic frame (David Kopf Instruments, Tujunga, CA). Throughout the surgery, the mice were provided with constant isoflurane (SurgiVet, 100 Series) and oxygen (SurgiVet, O₂ flowmeter, 0-4Lpm). The head was positioned in the horizontal plane of a stereotaxic frame with the nose bar set at zero. We firstly produced a 4mm craniotomy lateral to the sagittal suture, and centered between lambda and bregma. A cortical contusion was produced on the exposed cortex (the anterior-posterior coordinate for the epicenter of the injury was Bregma -2.0mm) using a pneumatically-controlled impactor device (Precision System Instruments TBI-0200 Impactor, Lexington, KY) similar to that previously described (Sullivan, Bruce-Keller et al. 1999; Sullivan, Thompson et al. 1999; Hall, Sullivan et al. 2005) except that the current device utilizes a unique contact sensor mechanism that ensures accurate and

reliable determination of cortical surface prior to initiating the injury sequence. This results in increased accuracy and reproducibility in regards to the CCI injury compared to that produced by earlier CCI impactors. In the present studies, the impactor containing a 3mm diameter rod tip compressed the cortex at 3.5m/sec to a depth of 1mm with a dwell time of 50msec to produce a severe injury. After surgery and injury, a 4mm disk made from dental cement (Dentsply Trubyte) was placed over the craniotomy site and adhered to the skull using cyanoacrylate. In order to prevent immediate post-traumatic hypothermia, following the suturing of the skin, mice were placed in a Hova-Bator incubator (37°C, model 1583, Randall Burkey Co) until they regained consciousness (determined by the regain of the righting reflex and increased mobility). The injured mice were allowed to survive from 1 hr to 48 hrs depending on their experimental group. For the immunoblotting studies (measurements of oxidative damage marker and cytoskeletal degradation, see below), the N for each treatment group was 8 animals; whereas for the mitochondrial studies, the N for each treatment group was 6 (3 mice were pooled together to create 1 N), based upon our experience with the variability seen with these measurements in previous studies (Kupina, Detloff et al. 2003; Hall, Detloff et al. 2004; Hall, Sullivan et al. 2005).

Tempol Preparation

Tempol was purchased from Sigma-Aldrich (Milwaukee, WI, U.S.A) and freshly prepared in 0.9% saline before abdominal intraperitoneal (i.p.) injection. In our dose-response study we experimented with different dosages at 3mg/kg,

10mg/kg, 30mg/kg, 100mg/kg and 300mg/kg (n=8), which well covered the dosage range that have been explored in related neuropathological studies and pilot studies (Beit-Yannai, Zhang et al. 1996; Mota-Filipe, McDonald et al. 1999; Behringer, Safar et al. 2002). Used as control for the tempol treatment group (injured-tempol), 9% saline was given as vehicle to animals (injured-vehicle). Another control group was composed of sham animal who were subjected to craniotomy but no contusion injury and treated with vehicle (sham-vehicle). Sham animals treated with tempol (n=8) in an initial dose-response study were also tested, and indicated no difference from sham-vehicle group (data not shown). There was zero mortality in the current study.

Tissue Extraction and Protein Assay

At the selected time points for the respective analysis (1 hr, 6 hrs, 12 hrs or 24 hrs), the sham or injured-vehicle, injured-tempol mice were deeply overdosed with sodium pentobarbital (200mg/kg i.p.). Following decapitation, the ipsilateral cortical area of interest as was rapidly dissected on an ice-chilled stage as previously described (Deng, Thompson et al. 2007). Immediately following dissection, samples were transferred into pre-cooled Triton lysis buffer (1% triton, 20mM tris HCL, 150mM NaCl, 5mM EGTA, 10mM EDTA, 10% glycerol) with protease inhibitors (Complete MiniTM Protease Inhibitor Cocktail tablet). Samples were then briefly sonicated and vortexed at 14,000rpm for 30 minutes at 4°C, and the supernatants were collected for protein assay. Protein concentration was

determined by Bio-Rad DC Protein Assay, with sample solutions diluted to contain 1mg/ml of protein for immunoblotting.

Slot-Blotting Analysis of Oxidative Damage (3NT)

To measure 3-nitrotyrosine (3NT), an aliquot of each ipsilateral cortical protein (2µg) or isolated mitochondrial protein was diluted with 200µl of tris-buffered saline (TBS), and transferred to a Protran (0.2µm) nitrocellulose membrane (Schleicher & Schuell, Dassel, Germany) by a Minifold II vacuum slot blot apparatus (Schleicher & Schuell). After the samples were loaded into the slots, they were allowed to filter through the membrane by gravity (no vacuum). Each slot was then washed with 200µl TBS which was allowed to filter through the membrane again. The membranes were then disassembled from the apparatus, and incubated in a TBS blocking solution with 5% milk for 1 hr at room temperature. For the detection of 3NT, a rabbit polyclonal anti-nitrotyrosine antibody (Upstate Biotechnology, MA, USA) was used at a dilution of 1:2000 in TBST blocking solution with 5% milk for overnight at 4°C. Preliminary experiments established protein concentration curves in order to ensure that quantified blots were in the linear range. From the results of these, we selected the 2µg for use based upon that amount giving blots that were well within the linear range. A standardized protein loading control was included on each blot to normalize the band densities so that comparisons could be made across multiple blots. All the samples were run in duplicate which were then averaged. For 3NT analyses, no primary antibody controls were run to verify that the oxidative

damage staining was specific. In addition, we ran positive controls using both bovine serum albumin and normal brain tissue which were exposed to PN and negative controls in which we pre-absorbed the primary antibodies with 3NT which resulted in inhibition of the 3NT staining.

Mitochondrial Percoll Gradient Purification and BCA Protein Assay

Brain cortical mitochondria were extracted as previously described with some modifications (Sullivan, Geiger et al. 2000; Sullivan, Dube et al. 2003). Following decapitation, ipsilateral cortex was quickly removed and pooled from 3 mice. The cortices were placed in a Potter-Elvehjem homogenizer containing five times the volume of ice-cold isolation buffer (5 fold buffer to tissue) with 1 mM EGTA (215mM mannitol, 75mM sucrose, 0.1% BSA, 20mM HEPES, 1mM EGTA; pH adjusted to 7.2 with KOH) and the homogenates were subjected to differential centrifugation at 4°C. First, the homogenate was centrifuged twice at 1300 X g for 3 min in an Eppendorf microcentrifuge at 4°C to remove cellular debris and nuclei. The pellet was discarded and the supernatant further centrifuged at 13,000 X g for 10 min. The crude mitochondrial pellet obtained after differential centrifugation were then subjected to nitrogen decompression to release synaptic mitochondria, using a nitrogen cell disruption bomb, cooled to 4°C under a pressure of 1200 psi for 10 min (Sullivan, Dube et al. 2003; Brown, Sullivan et al. 2004; Kristian, Hopkins et al. 2006). Following nitrogen disruption the mitochondria were suspended in 3.5ml of 15% percoll and further laid on a two preformed layers consisting of 3.5ml of 24% percoll and 3.5ml of 40% Percoll

in 13ml ultra-clear tubes. The gradient was centrifuged in fixed angle rotor at 30,400 X g for 10 min at 4°C. The fraction accumulated at the interphase of 40% and 24% percoll was carefully removed and diluted with isolation buffer without EGTA, then centrifuged at 12,300 X g for 10 min at 4°C. The supernatants were carefully removed, the pellet resuspended in isolation buffer without EGTA and centrifuged at 13,000 X g for 10 min at 4°C. The mitochondrial pellets at the bottom were then transferred to microcentrifuge tubes and topped off with isolation buffer without EGTA and centrifuged at 10,000 X g for 5 min at 4°C to yield a tighter pellet. The final mitochondrial pellet was resuspended in isolation buffer without EGTA to yield a concentration of ~10mg/ml. The protein concentration was determined using the BCA protein assay kit measuring absorbance at 562 nm with a BioTek Synergy HT plate reader (Winooski, Vermont).

Mitochondrial Respiration Measurement

Mitochondrial respiratory rates were measured using a Clark-type electrode in a continuously stirred, sealed thermostatically-controlled chamber (Oxytherm System, Hansatech Instruments Ltd) maintained at 37°C as previously described (Sullivan, Geiger et al. 2000; Jiang, Sullivan et al. 2001; Sensi, Ton-That et al. 2003; Sullivan, Dube et al. 2003). Twenty five to 40µg of isolated mitochondrial protein was placed in the chamber containing 250µl of KCl-based respiration buffer (125mM KCl, 2mM MgCl₂, 2.5mM KH₂PO₄, 0.1% BSA, 20mM HEPES at pH 7.2) and allowed to equilibrate for 1 min. This was

followed by the addition of complex-I substrates, 5mM pyruvate and 2.5mM malate, to monitor state II respiratory rate. Two boluses of 150 μ M ADP were added to the mitochondria to initiate state III respiratory rate for 2 min followed by the addition of 2 μ M oligomycin to monitor state IV respiration rate for an additional 2 min. For the measurement of uncoupled respiratory rate, 2 μ M *p*-trifluoromethoxy carbonyl cyanide phenyl hydrazone (FCCP) was added to the mitochondria in the chamber and oxygen consumption was monitored for another 2 min. This was followed by the addition of 10mM succinate to monitor complex II-driven respiration. The respiratory control ratio (RCR) was calculated by dividing state III oxygen consumption (defined as the rate of respiration in the presence of ADP, second bolus addition) by the state IV oxygen consumption (rate obtained in the presence of oligomycin). Fresh mitochondria were prepared for each experiment and used within 4 hr.

Western-Blotting Analysis of Calpain-Mediated Cytoskeletal Degradation

To measure calpain-mediated α -spectrin proteolysis, aliquots of each cortical sample (5 μ g) were run on a SDS/PAGE Precast gel (3-8% Tris-Acetate CriterionTM XT Precast gel, Bio-Rad) and then transferred to a nitrocellulose membrane using a semi-dry electro-transferring unit set at 15V for 15min. Preliminary experiments established protein concentration curves in order to ensure that quantified bands were in the linear range as measured with the Li-Cor Odyssey Infrared Imaging System. The membranes were incubated in a TBS blocking solution with 5% milk for 1 hr at room temperature. For the

detection of α -spectrin and its breakdown products, a mouse monoclonal anti- α -spectrin antibody (Affiniti FG6090) was used at a dilution of 1:5000 in TBST blocking solution with 5% milk for overnight at 4°C. A goat anti-mouse secondary conjugated to an infrared dye (1:5000, IRDye800CW, Rockland) was then applied for 1 hr at room temperature. After drying, the membranes were then imaged and quantified using the Li-Cor Odyssey Infrared Imaging System. A standardized protein loading control was included on each blot to normalize the band densities so that comparisons could be made across multiple blots (Hall, Sullivan et al. 2005). This was made up of pooled brain tissue protein collected from previously run TBI mice which gave strong bands corresponding to the 280kD parent α -spectrin, the 150kD and the 145kD breakdown products. The amount of protein in the loading control had been previously determined and shown to be within the linear range as measured with the Li-Cor Odyssey Infrared Imaging System. Following the transfer, the gels were stained with Coomassie Blue to verify even transfer. All the samples were run in duplicate and averaged.

Statistical Analysis

For all of the time course analyses, we used Statview 5.0 to perform a one-way analysis of variance (ANOVA), followed by Student-Newman-Keuls (SNK) post-hoc analysis to determine the significance of differences between the non-injured sham group and injured vehicle treated vs. injured tempol treated groups. For the ANOVA, a $p < 0.05$ was required to establish a statistically

significant difference across the groups. However, for the post-hoc SNK analysis, the program determined significance based upon a correction for multiple comparisons.

Results

Dose-Response Study of the Effect of Tempol on Protein Nitration

The level of protein nitration in cortical tissue homogenate was assessed by quantitative antibody-based immuno-slotblotting. Figure 3.2 shows the results of a dose-response analysis examining ipsilateral cortical protein nitration level following TBI (n=8). Five different single i.p. dosages were administered abdominally to the mice 15 min after cortical contusion. All mice were euthanized 1 hr after when PN-induced oxidative is at its peak (Deng, Thompson et al. 2007). The ANOVA showed a significant difference across the experimental groups [F(6,49)=3.397; p<0.01]. Post-hoc analysis revealed that the injured mice treated with vehicle (0.9% saline) showed about 90% of increase in 3NT (a specific marker for PN) level (p=0.007). In comparison to that, three highest dosages of tempol (30mg/kg, 100mg/kg and 300mg/kg) significantly reduced the 3NT level comparing to injured mice treated with vehicle mice. However, there was no significant difference among different dosage groups. The highest dose of tempol treatment in the current study (300mg/kg) was able to completely prevent any post-traumatic increase in 3NT level over the sham baseline level. Therefore, this dosage was chosen in the following studies. Another control group, in which sham was treated with tempol (n=8) showed no difference from sham vehicle-treated group (data not shown).

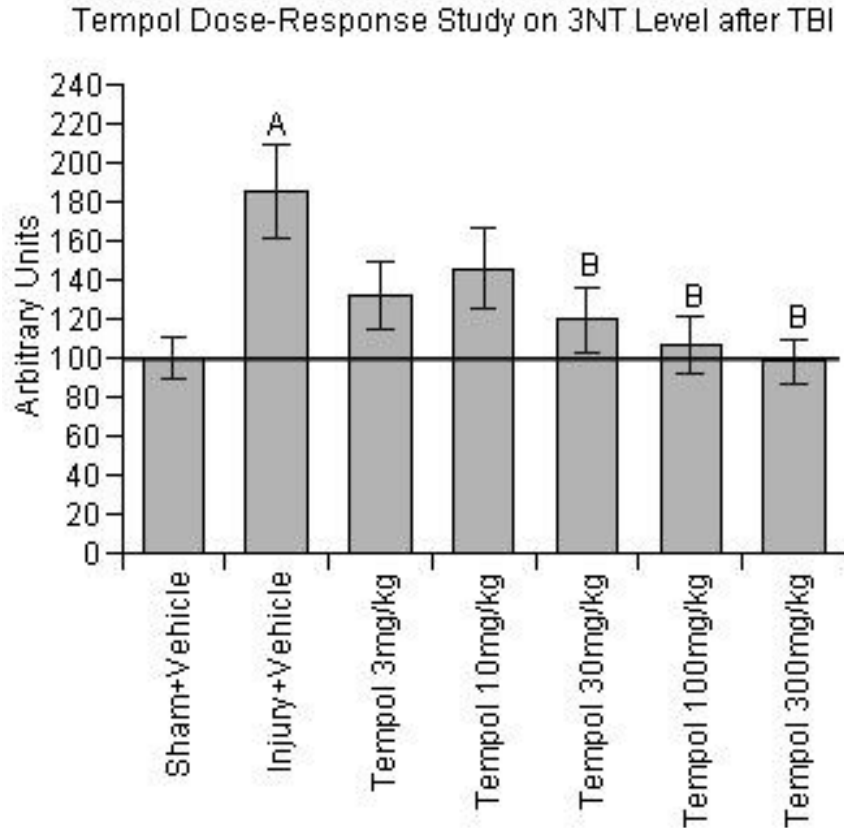


Figure 3.2 Tempol treatment studies using quantitative slotblotting in ipsilateral cortical traumatic brain injury tissues showing dose-response changes in protein nitration (3-nitrotyrosin, 3NT). Single dose of tempol was administrated i.p. to animals 15 min followed by sacrifice at 1 hr after TBI. The three highest doses at 30mg/kg, 100mg/kg and 300mg/kg significantly reduced 3NT level, a specific marker for PN-induced oxidative damage, in ipsilateral cortical tissues. N = 8 animals per treatment group; values = mean + standard error; one-way ANOVA and Student-Newman-Keuls post hoc test: A $p < 0.01$ vs. sham; one-way ANOVA and Student-Newman-Keuls post hoc test: B $p < 0.01$ vs. vehicle.

Effect of Tempol on Mitochondrial Respiration

Isolated cortical mitochondrial protein measured by BCA protein assay was divided to run for mitochondrial respiratory assay and quantitative immunoblotting respectively (see **Materials and Methods**). Mitochondrial oxygen consumption was measured by a Clarke-type electrode. In this study, mice (n=6) were treated with a single i.p. dose either vehicle or tempol (300mg/kg) 15 min after injury, followed by euthanasia 12 hrs after TBI. This time point was selected since it we had previously shown that it represents the peak of mitochondrial dysfunction in the CCI model (Singh, Sullivan et al. 2006a, see Appendix I). Cortical mitochondria were isolated and purified followed by incubation in the constantly-stirred sealed chamber. The oxygen consumption rate of each step was recorded by the slope of the oxygen respiration trace upon substrates addition. Figure 3.3A indicates the respiratory rates comparison among sham vehicle-treated, injured vehicle-treated and injured tempol-treated groups. Two doses of ADP after pyruvate and malate initiated the respiration of mitochondria. There was a significant difference across the sham, injured vehicle and injured tempol-treated groups [$F(2,15)=4.339$; $p<0.05$]. Post-hoc analysis showed that injured vehicle-treated mitochondria displayed significantly decreased complex I-driven state III respiration compared to sham, indicating impaired mitochondrial respiratory function. In contrast, the mitochondria isolated from the tempol-treated mice showed a complete maintenance of normal state III respiration which was significantly higher than the vehicle-treated mice. There was no significant difference detected in state IV respiration among groups upon

oligomycin addition. The inhibition of ATP synthase generally eliminated most of the respiratory activity.

A mitochondrial uncoupler, FCCP, was added to initiate maximal mitochondrial respiration state V by inducing mild proton leak into mitochondria. This analysis also showed a significant difference across the treatment groups [F(2,15)=6.894; p<0.001]. Post-hoc testing showed that the injured vehicle-treated group displayed significantly reduced respiration rate comparing to the sham group, suggesting impairment of the electron transport chain (ETC). However, mitochondria isolated from tempol-treated mice were able to show significantly improved state V respiration compared to the vehicle-treated group. Complex II-driven state VI respiration was tested by adding the complex II substrate succinate. There was no significant difference observed among three treatment groups, suggesting that complex II and the downstream complexes were relatively healthy, in contrast to complex I which was impaired.

Figure 3.3B displays the respiratory controlled ratio (RCR) of isolated mitochondria from the three different treatment groups which the ANOVA showed was significantly different [F(2,15)=11.910; p<0.001]. The RCR indicates how well oxygen consumption is coupled to ATP generation and is often used as the index of mitochondrial function (healthy: RCR>5). In Figure 3.3B, mitochondria from injured mice without drug treatment shows a mean RCR=3.7, which was significantly lower than the sham group, RCR=7.3. The tempol-treated group demonstrated a mean RCR=5.6, suggesting that the mitochondria remain on average within the healthy range (i.e. >5.0). The tempol treated mean was

significantly higher than vehicle-treated group. However, although tempol treatment was able to improve mitochondrial function to healthy level, the RCR in the injured tempol-treated group was significantly lower than that in the sham group, suggesting that mitochondrial function was not fully recovered.

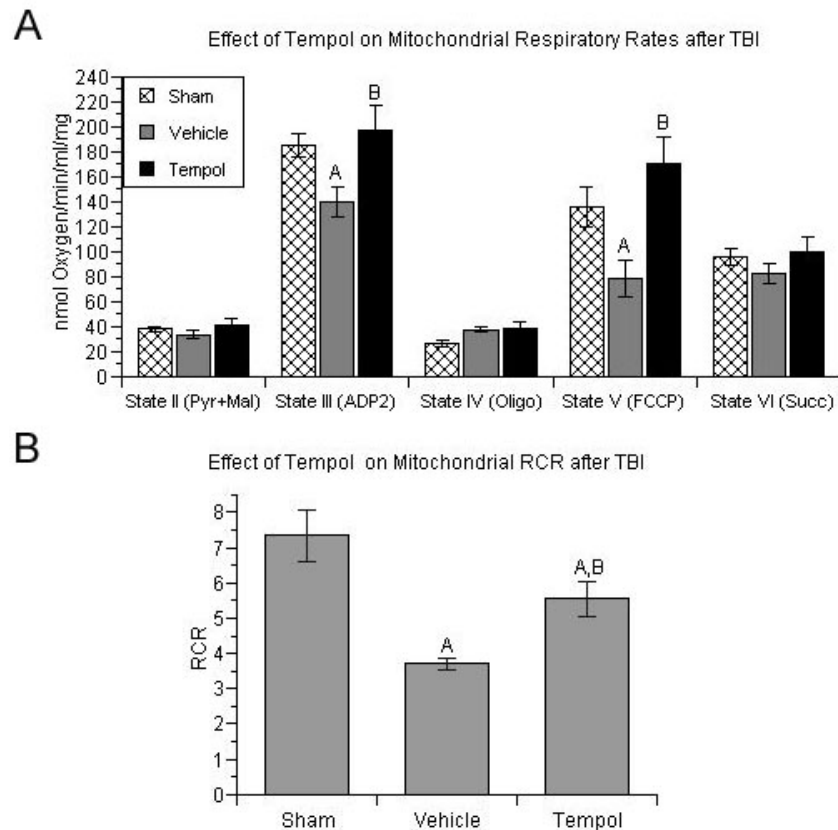


Figure 3.3 Effect of optimal single dose tempol treatment on mitochondrial respiration in ipsilateral cortical traumatic brain injury tissues measured by Clarke-type electrode. A. Single i.p. abdominal dose of tempol (300mg/kg) significantly improved state III (ADP) and state V (FCCP) respiration comparing to vehicle-treated group. B. Tempol treated group showed significant recovery of respiratory controlled ration (RCR) comparing to vehicle-treated group. N = 6 animals per treatment group; values = mean + standard error; one-way ANOVA and Student-Newman-Keuls post hoc test: A $p < 0.05$ vs. sham; one-way ANOVA and Student-Newman-Keuls post hoc test: B $p < 0.05$ vs. vehicle.

Effect of Tempol on Mitochondrial Oxidative Damage

Isolated cortical mitochondrial protein was measured by BCA protein assay and 2 μ g of each sample was run on quantitative antibody-based immunoblots. Figure 3.4 demonstrates mitochondrial 3NT level at 12 hrs after injury subjected to different treatments (n=4). The ANOVA revealed a significant difference across the treatment groups [F(2,9)=4.843; p<0.05]. Post-hoc analysis showed that even though the 3NT level in the injured vehicle-treated group was increased comparing to sham group, this increase was not significant. Consistent with this observation, we had previously found that while a significant increase in 3NT level in mitochondrial proteins is seen as early as 30 min after injury, and out to at least 3 hrs, the persistent mean increase in 3NT at 12 hrs after TBI loses significance in comparison to sham (Singh, Sullivan et al. 2006a). Nevertheless, in the injured tempol-treated group, 3NT level was significantly lower than the injured vehicle-treated group by 55%. Moreover, the mean 3NT level in the injured tempol-treated group was also lower than that seen in the sham group, but this difference was not significant.

Effect of Tempol on Mitochondrial 3NT Level after TBI

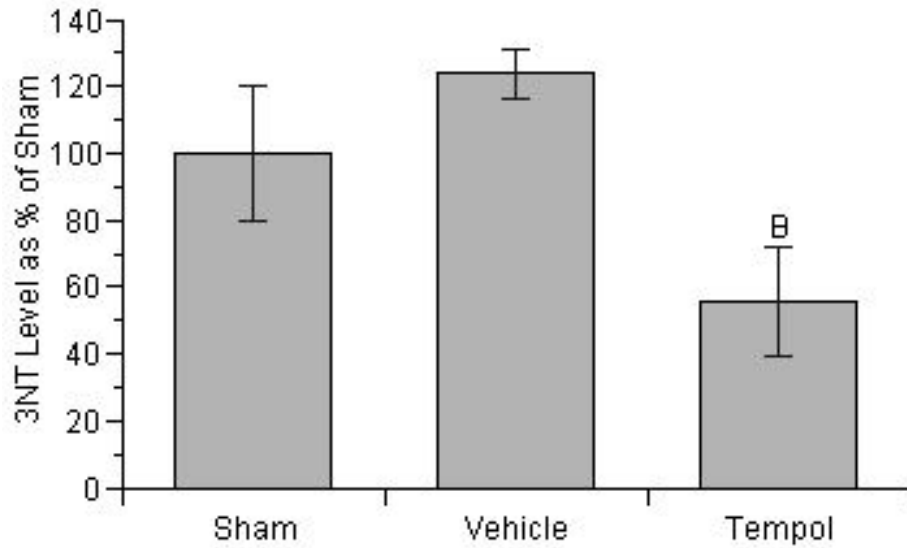


Figure 3.4 Effect of optimal single dose tempol treatment on mitochondrial oxidative damage in ipsilateral cortical traumatic brain injury tissues measured by quantitative slotblotting. Single i.p. abdominal injection of tempol (300mg/kg) significantly decreased 3NT level in comparison to vehicle-treated group in cortical mitochondrial proteins. N = 4 animals per treatment group; values = mean + standard error; one-way ANOVA and Student-Newman-Keuls post hoc test: A $p < 0.05$ vs. sham; one-way ANOVA and Student-Newman-Keuls post hoc test: B $p < 0.05$ vs. vehicle.

Effect of Single Dose of Tempol on Calpain-Mediated α -Spectrin Breakdown

Post-traumatic cytoskeletal degradation was measured by antibody-based immuno-westernblotting detecting α -spectrin breakdown products in cortical tissues ipsilateral to the injury. Mice were treated with a single dose of vehicle or tempol (300mg/kg) 15 min after TBI, and were killed at 1 hr or 6 hrs post-injury (n=8/group). Figure 3.5A shows that there was statistically significant difference across the three groups for the calpain-specific SBDP145 analysis [$F(2,21)=5.590$; $p<0.05$], but not in the case of the SBDP150 which is generated by both calpain and caspase 3 (Wang 2000). Post-hoc testing revealed that there was a significant increase in SBDP145 at 1 hr post-injury in the injured vehicle-treated group compared to the sham vehicle-treated group. However, tempol treatment significantly reduced SBDP145 compared to vehicle treatment by 45%.

Figure 3.5B displays the level of SBDPs at 6 hrs after TBI with or without tempol treatment. Both SBDPs showed significant increase compared to the sham group. Although there was a slight decline of both SBDPs in the injured tempol-treated group compared to vehicle-treated group, the decrease was not significant ($p<0.01$). The magnitude of both SBDPs in injury groups at 6 hrs post-injury was higher than that at 1 hr post-injury, which indicated there is progressive increase of calpain activity over time following TBI until it reaches its peak at 24 hrs in the CCI model (Deng, Thompson et al. 2007). The short term effect of tempol in reducing SBDP145 at 1 hr but not 6 hrs post-injury encouraged us to explore a tempol treatment regimen involving repeated doses administered over the course of the oxidative damage.

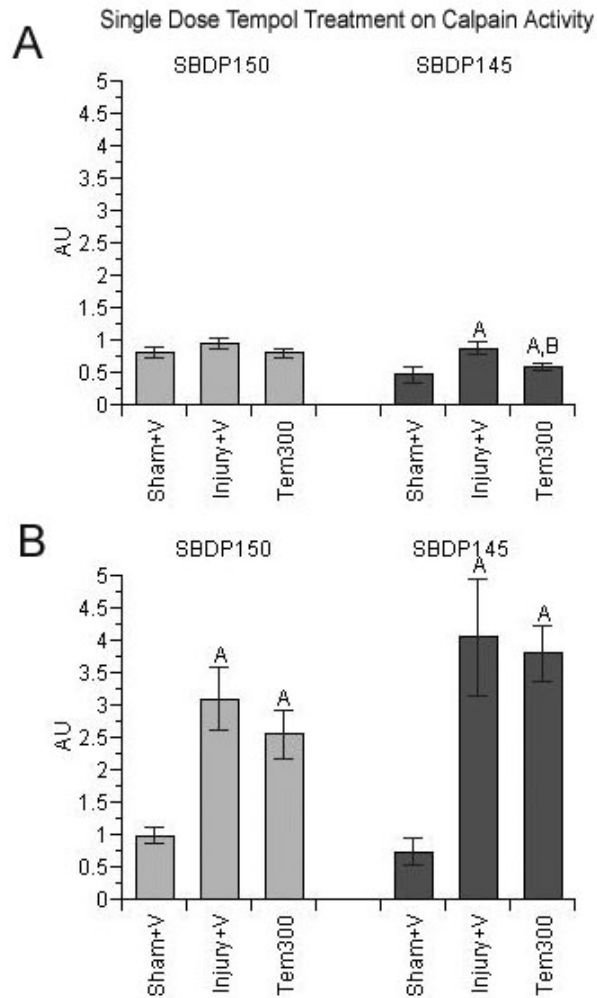


Figure 3.5 Effect of optimal single dose tempol treatment on calpain-mediated α -spectrin breakdown in ipsilateral cortical traumatic brain injury tissues measured by quantitative western blotting. A. Tempol treatment significantly reduced SBDP145 comparing to vehicle treatment, but here was no change in SBDP150 at 1 hr post-injury. B. Tempol treatment was not able to decrease SBDPs at 6 hrs after TBI. N = 8 animals per treatment group; values = mean + standard error; one-way ANOVA and Student-Newman-Keuls post hoc test: A $p < 0.05$ vs. sham; one-way ANOVA and Student-Newman-Keuls post hoc test: B $p < 0.05$ vs. vehicle.

Effect of Multiple Dose of Tempol on Calpain-Mediated α -Spectrin Breakdown

In this study, multiple doses of vehicle or tempol (300mg/kg) were administered i.p. to mice at 15 min, 3 hrs, 6hrs, 9 hrs and 12 hrs post-injury followed by euthanasia at 24 hrs when calpain-mediated SBDPs reach their peak in the CCI model (Deng, Thompson et al. 2007). As indicated in Deng et al, at 24 hrs post-injury, the magnitude of calpain-specific SBDP145 is more than twice as much as that of calpain/caspase 3-produced SBDP150, suggesting a the dominant role of calpain in post-traumatic proteolysis. However, at 24 hrs post-injury the difference across groups for both SBDPs is significant; for SBDP145 [F(2,20)=16.513; p<0.0001] and for SBDP150 [F(2,20)=5.241; p<0.05] In Figure 3.6, tempol treatment decreased both SBDPs significantly compared to vehicle treatment. The effect on SBDP150 was essentially complete since the magnitude of non-specific SBDP150 is much lower than that of calpain-specific SBDP145. However, although tempol treatment also reduced SBDP145 by 45% compared to the injured vehicle-treated group, the SBDP145 level in the injured tempol-treated group remained significantly elevated compared to the sham level, suggesting that proteolytic damage induced by calpain was not fully inhibited even with this repeated dose treatment regimen.

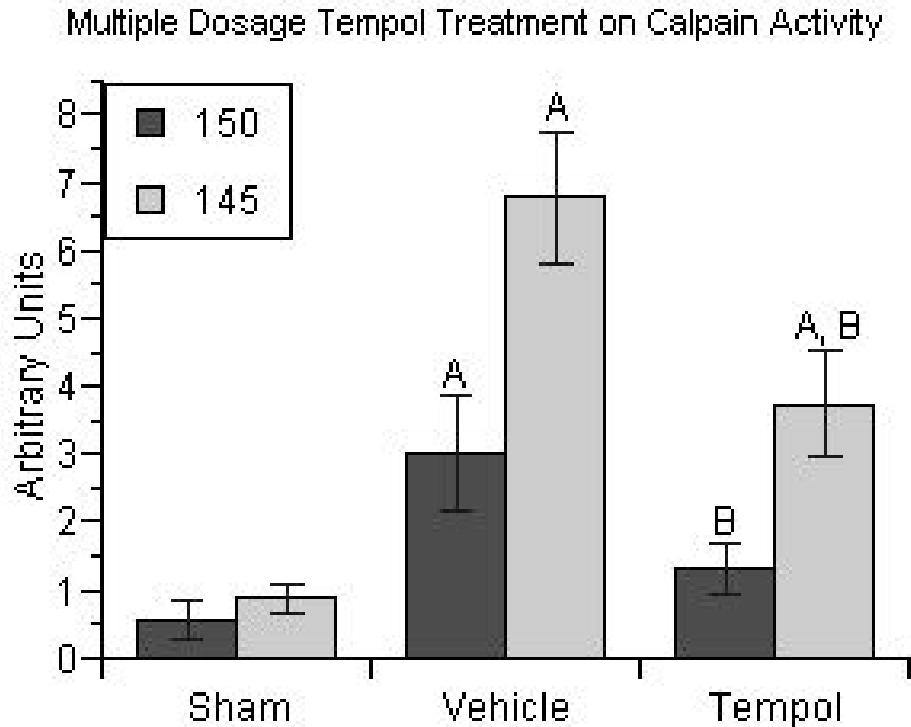


Figure 3.6 Effect of multiple dose tempol treatment on calpain-mediated α -spectrin breakdown in ipsilateral cortical traumatic brain injury tissues measured by quantitative westernblotting. Multiple doses of tempol were administrated at 15 min, 3 hrs, 6 hrs, 9 hrs and 12 hrs before sacrifice of the animals. In injured vehicle-treated group, both SBDPs were significantly increased than sham group with higher magnitude of SBDP145 elevation. Multiple i.p. injection of tempol (300mg/kg) significantly reduced both SBDPs in comparison to vehicle-treated group. N = 8 animals per treatment group; values = mean + standard error; one-way ANOVA and Student-Newman-Keuls post hoc test: A $p < 0.05$ vs. sham; one-way ANOVA and Student-Newman-Keuls post hoc test: B $p < 0.05$ vs. vehicle.

Therapeutic Window of Multiple Dose of Tempol Treatment Measured by Calpain-Mediated α -Spectrin Breakdown

A therapeutic window study next conducted in which the onset of tempol multiple dose treatment was delayed from the 15 min post-injury tested earlier (Figure 3.6 above) to either by 1 hr or 2 hrs. We administered multiple i.p. doses treatment starting at 1 hr or 2 hrs post-injury, with four additional bolus i.p. injections every 3 hrs. Animals were then studied at 24 hrs after the first injection. In Figure 3.7A, a 1 hr delay in treatment with tempol showed no effect in both SBDP145 and SBDP150. Both SBDPs remained at similar level as the injured vehicle-treated group. Figure 3.7B displayed 2 hrs delay treatment of tempol, which showed similar outcome. Although postponing the tempol treatment did not show any protection, it did not exacerbate the post-traumatic cytoskeletal proteolysis measured by calpain-mediated SBDPs.

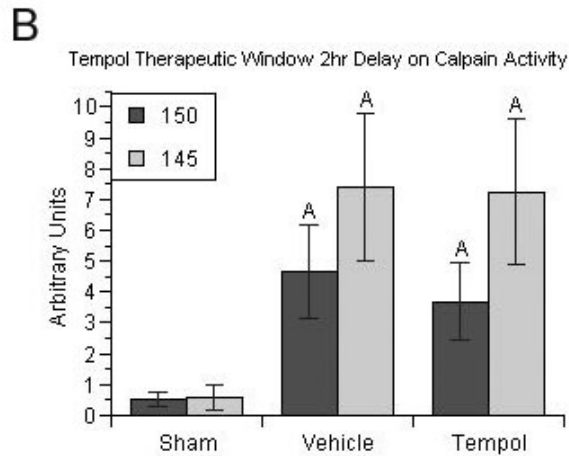
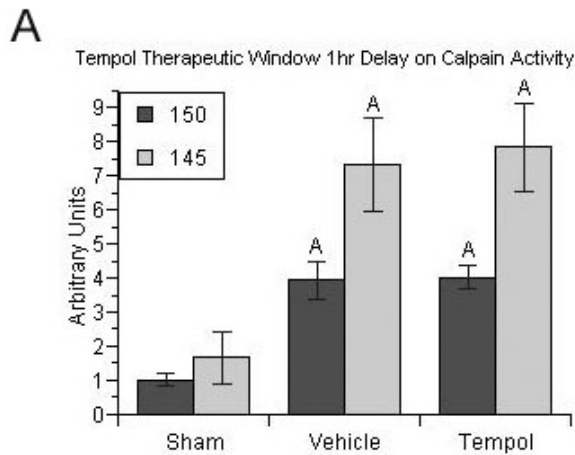


Figure 3.7 Therapeutic window study using multiple doses of tempol measured by quantitative westernblotting. A. The multiple i.p. tempol treatment regimen was postponed by 1 hr after injury, and animals were sacrificed at 25 hrs. B. The multiple i.p. tempol treatment regimen was postponed by 2 hrs after injury, and animals were sacrificed at 26 hrs. N = 8 animals per treatment group; values = mean + standard error; one-way ANOVA and Student-Newman-Keuls post hoc test: A $p < 0.05$ vs. sham; one-way ANOVA and Student-Newman-Keuls post hoc test: B $p < 0.05$ vs. vehicle

Discussion

The current study applied a pharmacological approach in elucidation of the pathophysiological relationship of PN-induced oxidative damage, mitochondrial dysfunction and calcium-activated, calpain-mediated cytoskeletal degradation by testing the ability of the multi-mechanistic nitroxide antioxidant tempol, to inhibit these secondary injury events in the CCI TBI mouse model. Our previous time course study defined the dynamic changes of PN production, oxidative mitochondrial damage, calpain-mediated proteolysis and neurodegeneration, and their temporal inter-relationship (Singh, Sullivan et al. 2006a, see Appendix I; Deng, Thompson et al. 2007). The time course study strongly indicates that PN has a pivotal role in the secondary injury following TBI, and suggests that scavenging of PN or its derived free radicals is a plausible neuroprotective therapeutic target. A thorough analysis was conducted to evaluate the therapeutic effect of tempol in regard to its ability to ameliorate mitochondrial dysfunction and to preserve cytosolic Ca^{2+} homeostasis and as a result to reduce calpain-mediated proteolysis.

Tempol Effect on PN-Mediated Oxidative Damage in the CCI-TBI Mouse Model

The neuroprotective effect of tempol was previously explored in a closed head rat TBI model. Tempol showed cerebroprotective effects by limiting edema formation, ameliorating blood-brain barrier (BBB) disruption and improving functional recovery (Beit-Yannai, Zhang et al. 1996; Zhang, Shohami et al. 1998).

In these studies, it was suggested that the neuroprotective effects of tempol was due to its catalytic scavenging of superoxide radicals. However, oxidative damage markers were not examined, and more recent experiments have suggested that an important antioxidant property that may contribute significantly to the inhibition of post-traumatic oxidative damage in brain tissue involves a catalytic scavenging of the PN-derived radicals $\bullet\text{NO}_2$ and $\bullet\text{CO}_3$.

A stable biomarker of PN oxidative damage to proteins involves the nitration of protein tyrosine residues which produces the product 3-nitrotyrosine (3NT). Although it was previously suggested that nitric oxide ($\text{NO}\bullet$) could give rise to tyrosine nitration, subsequent analyses have shown that this is probably caused by PN-derived $\bullet\text{NO}_2$. Alternatively, PN is able to react with SOD to form nitronium ion (NO_2^+)-like intermediate which may also cause tyrosine residue nitration (Ischiropoulos, Zhu et al. 1992). In the current study, we used antibody-based quantitative immuno-slotblotting detection of the PN-specific marker 3-nitrotyrosine (3NT) to investigate the effect of tempol on PN-induced oxidative damage. Animals were administered with single dose of tempol i.p. at 15 min and sacrificed at 1 hr after injury when PN-induced oxidative damage is at its peak (Deng, Thompson et al. 2007). A significant increase in cortical 3NT level in vehicle treated group compared to sham was observed. Comparing to vehicle treated group, tempol treatment 30mg/kg, 100mg/kg and 300mg/kg significantly decreased 3NT level in the cortical tissue ipsilateral to the injury showing that tempol has a wide range of antioxidant potency, and that scavenging of PN-derived $\bullet\text{NO}_2$ may be key aspect of tempol's antioxidant mechanism *in vivo*.

Tempol Effect on Mitochondrial Respiration and Oxidative Damage in the CCI-TBI Mouse Model

Mitochondria have long been suggested to be a main resource for ROS. The mono-electron transport through the mitochondrial ETC spins off oxidants (mainly $O_2^{\bullet -}$) as by-products during metabolism (Shigenaga, Hagen et al. 1994; Herrero and Barja 1997). Unknown components of ETC complex I and ubiquinone of complex III are indicated to be the major sites of ROS generation. It has been proposed that the complex I flavin mononucleotide (FMN) group was the major ROS generating site (Liu, Fiskum et al. 2002), whereas others hypothesize that mitochondrial generated $O_2^{\bullet -}$ preferably occurs at the level of coenzyme Q (Kowaltowski, Castilho et al. 1995). More recently, a novel Ca^{2+} -dependent isoform of nitric oxide synthase (NOS) was identified within mitochondria which is activated upon mitochondrial Ca^{2+} uptake (Giulivi 1998; Tatoyan and Giulivi 1998). Although NO^{\bullet} has been suggested to itself be toxic, most investigators now believe that the damaging effects of NO^{\bullet} are mediated by PN, which is formed by the diffusion rate-limited reaction of NO^{\bullet} with $O_2^{\bullet -}$ (Beckman and Koppenol 1996). Evidence has been obtained that the NO^{\bullet} -dependent inactivation of iron-sulfur centers was in fact mediated by PN (Castro, Rodriguez et al. 1994; Hausladen and Fridovich 1994). PN-derived radicals are extremely reactive with bio-molecules, including lipids, proteins and DNAs (Murphy, Packer et al. 1998; Radi 1998; Hall, Detloff et al. 2004). The discovery of the mitochondrial isoform of NOS exposes mitochondria as the major source

and therefore a target for PN-mediated oxidative damage (Packer and Murphy 1994).

Mitochondrial membrane integrity and compartmentalization is important in maintaining normal respiratory function. However, high in content in polyunsaturated fatty acids (PUFAs) makes brain mitochondria a vulnerable target for free radicals attack and lipid peroxidation (LP). PN was reported to increase mitochondrial proton leak but was irreversible by mPTP blocker, cyclosporine A (CsA) (Brookes, Land et al. 1998). Echtay et al proposed that 4HNE, the end product of LP, acts as secondary messenger to induce proton leak through uncoupling proteins (UCPs) and adenine nucleotide translocator (ANT) (Echtay, Esteves et al. 2003). In addition to lipid damage, mitochondrial proteins were indicated to be inactivated by oxidative damage in various neurodegenerative diseases (Butterfield and Lauderback 2002; Gibson and Huang 2004; Martin, Rosenthal et al. 2005). In a study in which mitochondria were exposed to PN toxicity as well as Ca^{2+} , the investigators observed the PN-induced membrane protein thiol cross-linking correlated to mitochondrial swelling (Gadelha, Thomson et al. 1997). Moreover, proteomic identification of specific rat mitochondrial fraction proteins demonstrated highly oxidized key components of electron transport chain (ETC) 3 hrs after CCI (Opii, Nukala et al. 2007). In our previous study, quantitative slotblotting measurement of post-injury mitochondrial LP and protein nitration levels showed immediate increase of PN-induced oxidative damage which persists for hours after injury (Singh, Sullivan et al. 2006a, see Appendix II). Although the level of 3NT in injured brain mitochondria

is still elevated, it has lost significance by 12 hrs after injury due perhaps to its decreased production and its possibly increased proteolytic removal (Grune, Reinheckel et al. 1997). In the current study, we demonstrated that the early (15 min post-injury) tempol treatment largely reduced the 12 hrs post-injury cortical mitochondrial 3NT level to below baseline, and significantly lower than the vehicle-treated injured mitochondria. In correlation to reduced mitochondrial oxidative damage, mitochondrial respiration was almost completely preserved (Figure 3.3). Specifically, state III respiration in tempol-treated group shows full preservation compared to the sham group, and the RCR (state III/state IV) showed maintenance to within normal limits

The complex II-driven succinate respiration showed no significant decrease after injury. Therefore, complex I-driven respiration possibly accounted for most of the impaired respiratory function observed. Complex I is a very large complex member with FMN redox center and many iron-sulfur centers. Hence it is vulnerable to oxidative inactivation. Moreover, complex I contains seven mtDNA-encoded subunits out of the thirteen peptides encoded by mtDNA. mtDNA is also a susceptible target for oxidative damage due to its proximity to PN production and lack of histone protection. A recent study on CNS mitochondria showed a correlation between the level of oxidized mtDNA bases and post-traumatic impairment of respiration (Sullivan, Rabchevsky et al. 2004). In any event, uncontrolled oxidative damage to mitochondrial membranes, proteins and DNA can be detrimental to their function. Our studies showed that

administration of the membrane permeable tempol protects mitochondria against oxidative damage and improves mitochondrial function at 12 hrs post-injury.

Tempol Effect on Calpain-Mediated α -Spectrin Breakdown in the CCI-TBI Mouse Model

Calpain-mediated proteolysis has been implicated in many pathological conditions. Evidences for mitochondrial damage and cytoskeletal proteolysis coincide with calpain activity have been demonstrated in TBI models (Chan and Mattson 1999; Wang 2000). Calpain, a cysteine protease, is activated in response to cytosolic Ca^{2+} elevation. It was suggested that calpain plays a role in dendritic remodeling, membrane repair and resealing and after injury (Faddis, Hasbani et al. 1997). However, the disruption of neuronal Ca^{2+} homeostasis may result in excessive activation of calpain (Saito, Elce et al. 1993; Bartus, Elliott et al. 1995). In addition to that, a rat CCI model RT-PCR study revealed increased mRNA expression of calpain and cysteine proteases within minutes after injury that persisted for days post-injury (Ringger, Tolentino et al. 2004). Moreover, calpain has a similar temporal profile as caspases, and responses to different injury severities even though calpain responds to a greater degree (Thompson, Gibson et al. 2006; Deng, Thompson et al. 2007). Because of its extensive involvement in ischemia and traumatic neuronal injuries, calpain-mediate proteolysis is proposed as a final common pathway of neuronal cell death following various insults (Bartus, Elliott et al. 1995; Bartus, Dean et al. 1998).

Dramatic upregulation of calpain activity progresses for hours after injury, which provides a broad temporal opportunity for neuroprotection (Saatman, Graham et al. 1998; Deng, Thompson et al. 2007). Our previous work (Chapter 2 and Deng, Thompson et al. 2007) showed that post-traumatic calpain activation and cytoskeletal proteolysis is preceded by PN-mediated oxidative damage, mitochondrial dysfunction, impairment of Ca^{2+} homeostasis and presumably intracellular Ca^{2+} overload and is then followed by neurodegeneration. If these processes are indeed linked as a series of events, then tempol treatment, which is known to interfere with the initiating PN-induced oxidative damage and mitochondrial dysfunction, should also attenuate the downstream calpain-mediated proteolytic damage to cellular elements. We first tested this hypothesis through single i.p. dose tempol treatment administered immediately after CCI which showed an inhibitory effect on calpain activity at 1 hr post-injury. We accordingly conclude that the membrane permeable tempol is rapidly taken up by mitochondria where it prevents their oxidative damage and loss of Ca^{2+} buffering capacity leading to an attenuation of intracellular Ca^{2+} overload and prevention of calpain over-activation. However, when we waited until 6 hrs after injury, this protective effect observed at 1 hr was no longer apparent in the case of early single dose tempol treatment. This is probably due to the fact that tempol has a very short half-life in mice (<30 min) (Kamatari, Yasui et al. 2002). Furthermore, the high blood flow in cortical tissue will hasten its elimination from the injured brain tissue following a single dose.

Subsequently, we administered multiple dosages of tempol at 3 hrs intervals up to 12 hrs and measured its effect at 24 hrs after injury. This experiment showed that this more aggressive multiple dose tempol treatment had a partial inhibitory effect on calpain-mediated proteolysis. However, the therapeutic window for the achievement of this effect is disappointingly short since delayed initiation of tempol treatment until 1 or 2 hrs post-injury failed to attenuate the 24 hrs peak of calpain-mediated α -spectrin degradation. This result may indicate that even though PN-induced oxidative damage is a critical early event in post-TBI injury, the potential therapeutic practicality of its inhibition is limited by a short therapeutic time window.

Alternatively, it is now well known that oxidative stress has inhibitory effects on both calpain (Benuck, Banay-Schwartz et al. 1992; Guttman, Elce et al. 1997; Guttman and Johnson 1998) and caspase 3 (Lau, Arundine et al. 2006) via oxidation of cysteine residues at the active site. Accordingly, total inhibition of ROS may remove the protective aspect of free radicals which may serve to reduce post-traumatic calpain activation together with the attenuation in oxidative damage to the mitochondria. This dual effect of ROS in this case, may be seen in the biphasic increase time course of α -spectrin degradation we observed which is similar to that seen in different experimental models *in vitro* and *in vivo* neural injury (Neumar, Meng et al. 2001; DeRidder, Simon et al. 2006; Xiong, Rabchevsky et al. 2007). As shown by our previous study, there was a biphasic increase of SBDPs connected by a plateau phase between 3 hrs and 12 hrs. Between 12 hrs and 24 hrs, both SBDPs exhibited a greater than

75% elevation (Deng, Thompson et al. 2007). The sudden and significant increase in SBDPs began at 12 hrs which represented the outer limit of the measurable increase in PN-mediated 3NT (Figure 2.4). Thus, the wave of oxidative damage occurring between 30 min and 12 hrs post-injury while detrimental to the injured tissue overall may at the same time serve to limit the full expression of calpain activation. This two-edged sword in regards to the influence of PN on calcium-induced activation of calpain may explain why at best tempol is only partially effective at attenuating cytoskeletal degradation even when given soon after TBI. It may also help explain why tempol has an apparently very short therapeutic window in relation to inhibiting downstream proteolytic damage. In other words, if tempol is delayed until calpain activation is more established, the removal of the oxidative attenuation of calpain activity may lead to an exacerbation of calpain activity that may offset the benefits of the tempol reduction in mitochondrial oxidative damage. Further experiments are needed to investigate this notion. In any event, it seems clear that antioxidant treatment may need to be combined with other agents that more directly target calpain activation in order to achieve a more pronounced and practical neuroprotective approach. Copyright © Ying Deng 2007.

Chapter Four

Effect of Tempol on Behavioral Recovery and Neurodegeneration after Traumatic Brain Injury

Introduction

Every year in the United States an estimated 1.5 to 2 million people sustain traumatic brain injury (TBI). Despite the progress in diagnostics and surgical treatments and rehabilitation care, most patients suffer from persistent physical and psychological impairments. An efficacious neuroprotective compound is yet to be developed in TBI clinical trials to prevent secondary neurodegeneration and chronic neurological functional impairment. The primary mechanical TBI leads to secondary neural cell damage and cell death which is proportional to the degree of cognitive or sensory and motor dysfunction. Immediate post-traumatic neurochemical changes begin immediately after injury. (Katayama, Becker et al. 1990) which include widespread cellular depolarization and massive release of the excitatory neurotransmitter, glutamate, resulting in calcium (Ca^{2+}) influx through ion channels associated with glutamate receptors. Moreover, the disruption in cellular Ca^{2+} homeostasis leading to intracellular overload is to multiple cytotoxic events including ROS production, mitochondrial dysfunction, and Ca^{2+} -dependent protease activation as indicated in experimental TBI models (Young 1992; Azbill, Mu et al. 1997). As indicated in our previous experiments study using the CCI mouse model, the production of

the reactive oxygen species (ROS) peroxynitrite (PN), is an early immediate post-traumatic event that appears to lead to mitochondrial damage and functional failure and calpain over-activation (Chapter2; Deng et al, 2007). Moreover, we have shown that early administration of the multi-mechanistic nitroxide antioxidant tempol within the first 15 min post-injury can reduce post-traumatic PN-mediated oxidative damage, maintain mitochondrial function and lessen calpain-mediated cytoskeletal degradation. In the current study, we investigated the effect of early tempol to improve neurological recovery and reduce neurodegeneration during the first 7 days in the mouse severe controlled cortical impact (CCI) TBI model.

Materials and Methods

All the surgical, injury and animal care protocols described below have been approved by the *University of Kentucky Institutional Animal Care and Use Committee*, and are consistent with the animal care procedures set forth in the guidelines of the *U.S. Public Health Service Policy on Humane Care and Use of Laboratory Animals*.

Mouse Model of Controlled Cortical Impact (Focal) Traumatic Brain Injury

Young adult male CF-1 mice (Charles River, Portage, MI) weighing 29-31g were used in this study. The mice were anesthetized with isoflurane (3.0%), shaved, and then placed in a stereotaxic frame (David Kopf Instruments, Tujunga, CA). Throughout the surgery, the mice were provided with constant isoflurane (SurgiVet, 100 Series) and oxygen (SurgiVet, O₂ flowmeter, 0-4Lpm). The head was positioned in the horizontal plane of a stereotaxic frame with the nose bar set at zero. We firstly produced a 4mm craniotomy lateral to the sagittal suture, and centered between lambda and bregma. A cortical contusion was produced on the exposed cortex (the anterior-posterior coordinate for the epicenter of the injury was Bregma -2.0mm) using a pneumatically-controlled impactor device (Precision System Instruments TBI-0200 Impactor, Lexington, KY) similar to that previously described (Sullivan, Bruce-Keller et al. 1999; Sullivan, Thompson et al. 1999; Hall, Sullivan et al. 2005) except that the current device utilizes a unique contact sensor mechanism that ensures accurate and

reliable determination of cortical surface prior to initiating the injury sequence. This results in increased accuracy and reproducibility in regards to the CCI injury compared to that produced by earlier CCI impactors. In the present studies, the impactor containing a 3mm diameter rod tip compressed the cortex at 3.5m/sec to a depth of 1mm with a dwell time of 50msec to produce a severe injury. After surgery and injury, a 4mm disk made from dental cement (Dentsply Trubyte) was placed over the craniotomy site and adhered to the skull using cyanoacrylate. In order to prevent immediate post-traumatic hypothermia, following the suturing of the skin, mice were placed in a Hova-Bator incubator (37°C, model 1583, Randall Burkey Co) until they regained consciousness (determined by the regain of the righting reflex and increased mobility). The injured mice were allowed to survive from 7 days. The N for each time point group was 12 animals based upon our experience with the variability seen with these measurements in previous studies (Kupina, Detloff et al. 2002; Hall, Sullivan et al. 2005).

Tempol Preparation

Tempol was purchased from Sigma-Aldrich (Milwaukee, WI, U.S.A) and freshly prepared in 0.9% saline before abdominal intraperitoneal (i.p.) injection. Animals were administered five i.p. dosages of tempol at 300mg/kg according to our dose-response study at 15 min, 3 hrs, 6 hrs, 9 hrs and 12 hrs. Used as control to tempol treatment group (injured-tempol), 9% saline was given as vehicle to animals (injured-vehicle). Another control group involved sham animal with craniotomy but no contusion injury, which was as well treated with vehicle

(sham-vehicle). Sham animals treated with tempol (n=12) in the dose-response study was tested, and indicated no difference from sham-vehicle group (data not shown). There was zero mortality in the current study.

Neuroscore Behavioral Test

The neuroscore test was used to assess the neurological status of the sham and TBI mice at 48 hrs and 7 days post-injury. This test is modified from previously described series of tests used for assessing the effects of TBI in the rat (McIntosh, Vink et al. 1989), and adapted for mouse (Murai, Pierce et al. 1998; Raghupathi, Fernandez et al. 1998). In the present study, we employed the neuroscore with three components: grid walk (front limb and hind limb), cagetop (front limb and hind limb) and lateral pulsion. In preliminary experiments we documented that the neuroscore test was able to detect motor deficit induced by injury after either moderate (0.5 mm) or severe (1.0 mm) CCI TBI. In each component, the animal can receive a total of 4 points for a maximum high of 12 points. Gridwalk: In this component, the mice are forced to walk on a metal gridwalk and timed for 1 min. An observer, who is unaware of the mouse treatment groups, observes the left vs. the right limb 1) for a greater number of slips on the right side than the left; 2) for more profound slips on the right side as apposed to the left. The animal can lose a maximum of 1 point for the front and 1 point for the hind limb for this portion of the motor assessment. Cagetop: In the second neuroscore component, there are total of 3 points that the mice can lose for visible deficits in hind limb and front limb function each. For hind limb

functional assessment, the animal is held by the head and the tail above the grid and then slowly moved down toward the grid as the observer assesses the hind limbs for toe splay as well as hind limb extension. For front limb functional impairment measurement, the animal is suspended by the tail and lowered toward the cage top until he can grab the rungs of the cage top during which he is determined how well he extends his arms. Lateral pulsion: For the third component of the neuroscore test, the animal is placed on a rubber mat, making sure its body is parallel to the corrugations on the mat. He is then slowly pushed back and forth the entire width of the mat. This is done twice slowly to prime the animal. After these two practice trials, the first trial is started with a slow push (same speed as for the practice trials) and then accelerated for each subsequent trial up to 4 trials. Four points are deducted if the animal rolls at the 1st trial, 3 points at the 2nd trial, 2 points at the 3rd trial and 1 point at the 4th trial. The animal gains all points if he does not roll after 4 trials.

De Olmos Silver Staining Analysis of Neurodegeneration

Following the completion of the 7 days post-injury neuroscore test, neurodegeneration was examined using the de Olmos aminocupric silver histochemical technique as previously described (de Olmos, Beltramino et al. 1994; Switzer 2000; Hall, Gibson et al. 2005; Hall, Sullivan et al. 2005). At 7 days the mice (N=12) were overdosed with sodium pentobarbital (200mg/kg i.p) and transcardially perfused with 0.9% sodium chloride, followed by a fixative solution containing 4% paraformaldehyde. Following decapitation, the heads

were stored in a fixative solution containing 15% sucrose for 24 hrs after which the brains were removed, placed in fresh fixative and shipped for histological processing to Neuroscience Associates Inc (Knoxville TN). The brains used for this study were embedded into one gelatin block (Multiblock[®] Technology, Neuroscience Associates). The block was then frozen and thirteen 35 μ m coronal sections were taken 420 μ m apart between 1.1mm anterior and 4.4mm posterior to bregma, were de Olmos silver-stained to reveal degenerating neurons and neuronal processes, and then counterstained with Nuclear Fast Red. The brain sections were photographed on an Olympus Provis A70 microscope at 1.25 \times magnification using an Olympus Magnafire digital camera and the image was analyzed by Image-Pro Plus (4.0). The percentage area of silver staining for each brain section was calculated by dividing the area of ipsilateral hemispheric silver staining in each section by the area of the contralateral hemispheric area and multiplying by 100. The volume of silver staining in the ipsilateral hemisphere as a percentage of the contralateral hemispheric volume was estimated by the equation $\% V = t \times \Sigma \% a(s)$, where $\% V$ is percent silver stain volume, t = the distance between sections analyzed (420 μ m) and $\Sigma \% a (s)$ is the sum of percent area of silver staining in all sections examined (13 for each brain) (Hall, Sullivan et al. 2005).

Lesion Volume Measurement

In addition to measuring the volume of neurodegeneration with the DeOlmos silver staining method, the brain sections were photographed on an

Olympus Provis A70 microscope at 1.25× magnification using an Olympus Magnafire digital camera and the lesion volume was analyzed by ImageJ 1.37v (NIH) (Michel and Cruz-Orive 1988; Sullivan, Thompson et al. 2000; Pandya, Pauly et al. 2007). The percentage area of ipsilateral cortical tissue spared for each brain section was calculated by dividing the area in each section by the area of the contralateral cortex and multiplying by 100. The volume of the ipsilateral cortical spared tissue as a percentage of the contralateral cortical volume was estimated by the sum of percent area of spared tissue of all sections multiplied by the distance between sections analyzed.

Statistical Analysis

For treatment group analyses, we used Statview 5.0 to perform a one-way analysis of variance (ANOVA), followed by Student-Newman-Keuls (SNK) post-hoc analysis to determine the significance of differences between individual the non-injured sham group and injured vehicle treated vs. injured tempol treated groups. For multiple section analyses, we used Statview 5.0 to perform an ANOVA repeated measurement, followed by Student-Newman-Keuls (SNK) post-hoc analysis to determine the significance of differences between individual sections in the non-injured sham group and injured vehicle treated vs. injured tempol treated groups. For the ANOVA, a $p < 0.05$ was required to establish a statistically significant difference across the groups. However, for the post-hoc SNK analysis, the program determined significance based upon a correction for multiple comparisons comparing among groups.

Results

Behavioral Outcome Measured by Neuroscore Motor Test after Tempol Treatment

Five i.p. dosages of tempol (300mg/kg each; last dose at 12 hrs after injury) were administered to the animals at a three hours intervals beginning at 15 min following the CCI injury. Behavioral outcome was assessed at 48 hrs and 7 days after TBI respectively measured by neuroscore. We divided the scores into fore limb and hind limb two categories. At 48 hrs after injury (Figure 4.1), the ANOVA revealed a significant difference across the treatment groups in both fore limb [$F(2,33)=3.610$; $p<0.05$] and hind limb [$F(2,33)=3.927$; $p<0.05$] motor function. Post-hoc analysis showed that the motor function in injured vehicle-treated group was significantly impaired compared to the scores of the sham group. Although the 48 hrs fore limb and hind limb scores for the injured tempol-treated group were not significantly different from the injured vehicle-treated group, the scores of the tempol-treated group were also not significantly lower than the sham group implying some improvement in the 48 hrs neurological status as a result of tempol treatment started at 15 min post-injury. At 7 days after injury, both fore limb [$F(2,33)=2.668$; $p=0.0843$] and hind limb [$F(2,33)=2.797$; $p=0.0755$] motor function showed no significant difference among treatment groups. Although injured vehicle-treated animals showed decreased scores comparing to sham group, this slight deficit was not statistically significant.

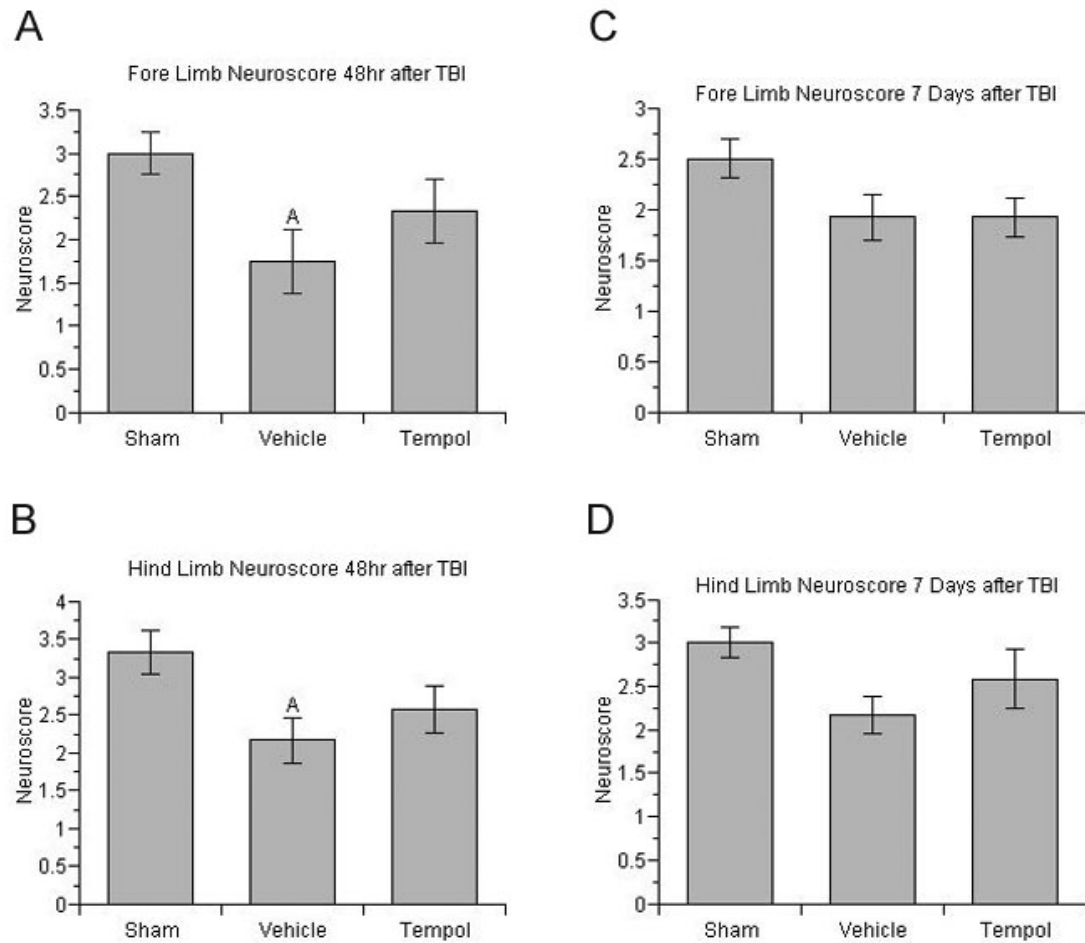


Figure 4.1 Behavioral outcome of multiple dose tempol treatment measured by neuroscore motor test after TBI. Neuroscore was accessed at 48 hrs and 7 days after injury. N = 12 animals per treatment group; values = mean + standard error; one-way ANOVA and Student-Newman-Keuls post hoc test: A p < 0.05 vs. sham; one-way ANOVA and Student-Newman-Keuls post hoc test:

Histological Evaluation of Neurodegeneration Measured by de Olmos Aminocupric Silver Staining after Tempol Treatment

Following the 7 day neuroscore test, the brains were harvested for histopathological analysis of neurodegeneration. Figure 4.2 displays the degrees of cortical tissue sparing (4.2A) and hemispheric neurodegeneration (4.2B) in injured, vehicle-treated and injured tempol-treated animals. Figure 4.2A measured the spared tissue in vehicle-treated vs. tempol-treated animals. The area of spared tissue in ipsilateral cortex was outlined and calculated as percentage of the area of contralateral cortex. In Figure 4.2A, tempol-treated group showed 5% improvement in spared cortical tissue volume compared to vehicle-treated group, however, the increase was not quite significant. Using the de Olmos aminocupric silver staining method, we are able to measure degenerating tissue in the entire ipsilateral hemisphere plus the ipsilateral lesion volume. In Figure 4.2B, both injured groups displayed a significant increase in neurodegeneration silver staining volume compared to sham group. However, the injured tempol-treated group showed significantly reduced neurodegeneration compared to injured vehicle-treated group [$F(2,33)=125.864$; $p<0.05$]. In Figure 4.2C, selected coronal brain section in the epicenter displayed the improvement in tissue sparing as well as the reduction in the volume of neurodegeneration-related silver staining with tempol treatment vs. vehicle treatment.

Figure 4.3 shows the percentage of silver staining in coronal brain sections from the anterior hemispheric boundary of the post-traumatic neurodegeneration to the posterior boundary. Injured groups at all sections

showed a significant increase of silver staining compared to the sham group. The injured, tempol-treated group displayed significantly less silver staining than injured vehicle-treated group at section 28, which is in the epicenter of the injury.

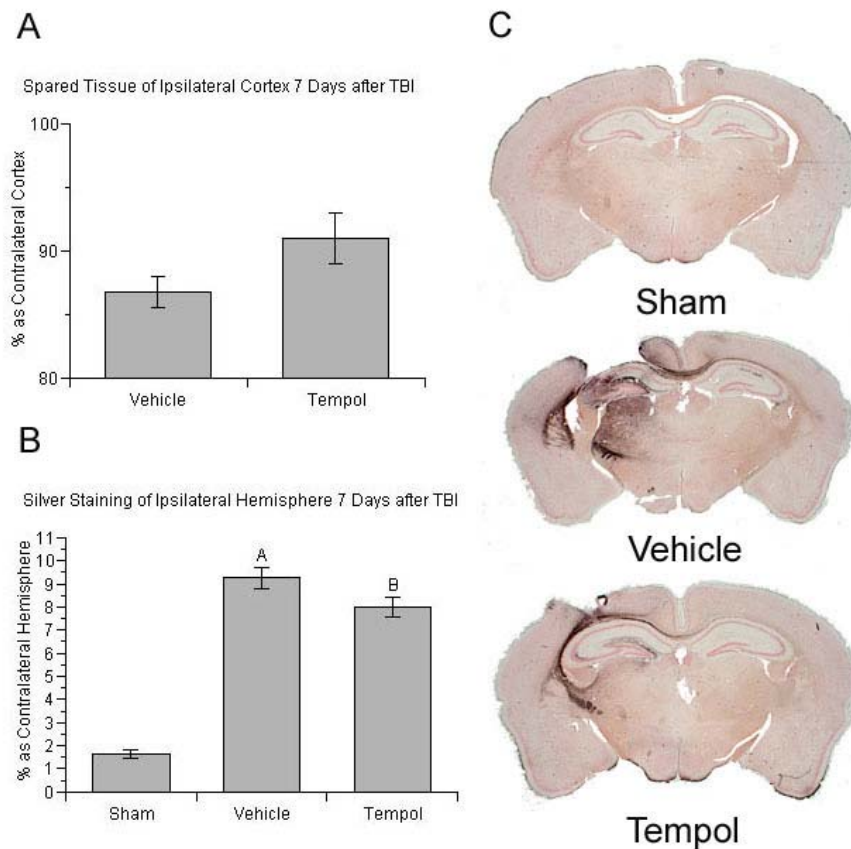


Figure 4.2 Histological evaluation of multiple dose tempol treatment on tissue sparing and silver staining in ipsilateral hemisphere after TBI. A. Tissue sparing at 7 days after injury showed slight increase in tempol treatment group, however, not significant. B. Silver staining at 7 days after injury indicated significant reduction of silver staining in tempol treatment group. C. Selected coronal brain sections in the epicenter from different treatment groups. N = 12 animals per treatment group; values = mean + standard error; one-way ANOVA and Student-Newman-Keuls post hoc test: A $p < 0.05$ vs. sham; one-way ANOVA and Student-Newman-Keuls post hoc test: B $p < 0.05$ vs. vehicle.

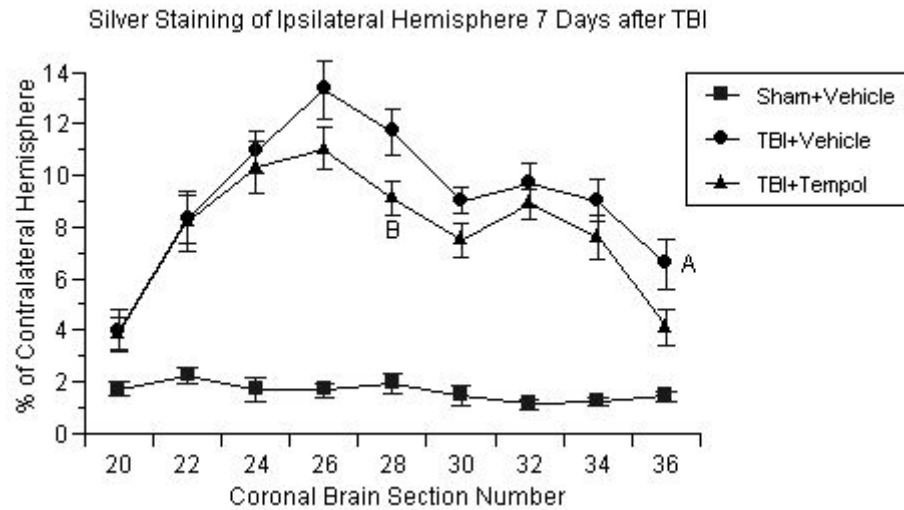


Figure 4.3 Histological evaluation of multiple dose tempol treatment on coronal brain section silver staining in ipsilateral hemisphere after TBI. Silver staining at 7 days after injury indicated significant reduction of silver staining in tempol treatment group at coronal section 28. N = 12 animals per treatment group; values = mean + standard error; repeated measures ANOVA and Student-Newman-Keuls post hoc test: A $p < 0.05$ vs. sham; repeated measures ANOVA and Student-Newman-Keuls post hoc test: B $p < 0.05$ vs. vehicle.

Discussion

In the current study, we tested the hypothesis that tempol, by scavenging ROS, preserving mitochondrial function and reducing calpain-mediated proteolysis (Chapter 3) could reduce post-traumatic neurological impairment and neurodegeneration. There is compelling evidence for the key role of ROS-induced oxidative damage in the secondary injury in TBI models (Kontos and Povlishock 1986; Kontos and Wei 1986; Hall, Andrus et al. 1993; Hall, Andrus et al. 1994; Smith, Andrus et al. 1994; Globus, Alonso et al. 1995). Most convincing is the fact that several antioxidant compounds have been shown to be neuroprotective in TBI models (Hall and Smith 1991; Marshall, Maas et al. 1998; Mori, Kawamata et al. 1998; Marklund, Lewander et al. 2001). However, most antioxidants are targeting one specific free radical and react stoichiometrically.

As indicated in our first study (Chapter 2), PN is probably the key mediator in post-traumatic oxidative damage, which is the main source for both lipid peroxidation and protein nitration (Deng, Thompson et al. 2007). Tempol, a PN-derived free radical scavenger, is a membrane permeable, catalytic antioxidant, which was shown to react promptly with hydroxyl radical, nitrogen dioxide and carbonate radical (Carroll, Galatsis et al. 2000; Bonini, Mason et al. 2002). Moreover, PN as an upstream factor in the secondary injury cascade, we proved that tempol was able to inhibit oxidative damage, ameliorate mitochondrial dysfunction and decrease calpain-mediated cytoskeletal degradation at least when administered during the first 15 min post-injury. Therefore, in the present

study, we further examined the ability of tempol to exert a definitive neuroprotective effect in terms of a reduction in neurological impairment and neurodegeneration.

We applied de Olmos aminocupric silver staining in this study to measure neurodegeneration. Comparing to conventional histological staining used in many pathohistological studies, the silver staining method is much more sensitive in detection of injured neurons and axons in response to TBI (de Olmos, Beltramino et al. 1994; Switzer 2000). At 7 days after injury, severe cavitation has developed at the epicenter of the contusion. However, silver staining revealed subcortical tissue damage widespread to ipsilateral hippocampus and dorsolateral thalamus. Moreover, silver staining disclosed commissural fiber damage extended to the contralateral site to the injury. Therefore, silver staining is able to detect cellular damage that is not measured by conventional histological staining. Spared tissue volume showed no significant difference between vehicle and tempol treatment. However, measurement of silver staining revealed a significant, but rather modest reduction in neurodegeneration after tempol treatment.

Despite the improvement in overall neurodegeneration, there was no significant functional recovery after the tempol treatment measured by neuroscore at 7 days after injury. The current neuroscore motor test was examined in a pilot study. At 48 hrs and 72 hrs after severe (1.0mm) and moderate (0.5mm) CCI in mouse, animals showed significant deficit comparing to sham animals (data not shown). At 48 hrs, severe TBI mice displayed further

impairment than moderate TBI mice. However, at 72 hrs, both severe and moderate TBI mice scored similarly. In the current study, we assessed the neuroscore of the mice at 48 hrs and 7 days respectively. The deficit was detectable in both fore limb and hind limb motor function at 48 hrs after injured with vehicle treatment, but not at 7 days. Nevertheless, the tempol treatment did appear to exert some improvement in neurological recovery at the 48 hrs time point. Although the tempol group did not manifest a significant difference compared to the neuroscore of the vehicle treatment group, neither the fore limb nor the hind limb functional scores were significantly differently from sham group in contrast to the significantly lower scores in the injured, vehicle-treated mice compared to the sham group. This suggested that motor function was somewhat improved with the tempol treatment. At 7 days after injury, we accessed the neuroscore again. However, scores in all groups were similar and there was no significant difference among groups. We suspect that the current neuroscore test may not be suitable for long-term behavioral evaluation. In any event, the beneficial effects of tempol also demonstrated previously in a rat TBI model (Beit-Yannai, Zhang et al. 1996; Zhang, Shohami et al. 1998) and in cerebral ischemia models (Rak, Chao et al. 2000; Leker, Teichner et al. 2002) are consistent with the view that the compound possesses demonstrable neuroprotective properties in CNS injury models, in general.

There may be multiple reasons for the modest effect of tempol. First of all, the testing of tempol for its ability to reduce calpain-mediated cytoskeletal degradation which was assessed at 24 hrs after injury (Chapter 3), showed a

statistically significant 45% reduction in calpain-mediated cytoskeletal degradation. We suspect that the partial inhibition of calpain-mediated proteolysis is part of the reason why tempol did not have more pronounced effect in preserving neuronal tissue. Secondly, in the present experiments, neurodegeneration was not examined until 7 days after injury rather than at its peak which is 48 hrs post-injury (Chapter 2; Deng, Thompson et al. 2007). This was done so that we could assess neurological status out to 7 days before performing histopathology. However, the 7 day time point where less silver staining is seen compared to the 48 hrs peak may make it more difficult to observe a more robust neuroprotective effect. Thirdly, as noted in Chapter 3, the half life of tempol in mice is fairly short (i.e. <30 min) (Kamatari, Yasui et al. 2002) and therefore even repeated dosing with the compound is unable to maintain therapeutic levels adequately during the first 12 hrs post-injury. Other longer-acting PN-directed antioxidants may be more effective due to the ability to maintain a steady, non-fluctuating radical scavenging effect. Lastly, even though PN-mediated oxidative damage is an important player in the secondary injury process, a more complete neuroprotective effect may require simultaneously blocking the secondary injury cascade at multiple points downstream from the early oxidative damage with a mitochondrial protective agent and/or a direct inhibitor of calpain.

Concerning the latter option, the principle pathological role of calpain-mediated proteolysis is demonstrated in secondary neuronal cell death (Buki, Siman et al. 1999; Povlishock, Buki et al. 1999; Kupina, Detloff et al. 2003; Hall,

Sullivan et al. 2005). Calpain is a calcium-dependent protease and is triggered in response to massive calcium influx following TBI (Saatman, Graham et al. 1998; Kupina, Detloff et al. 2003; Serbest, Burkhardt et al. 2007). Immuno-detection of structural protein spectrin, which is a substrate for calpain, showed calpain-mediated proteolysis in damaged axons (Roberts-Lewis, Savage et al. 1994). In addition to spectrin, other structural proteins, such as microtubule associated proteins (MAPs) and neurofilaments (NFs) are also substrates for calpain, and are associated with axonal damage (Maxwell, Povlishock et al. 1997; Okonkwo, Pettus et al. 1998). Therefore, calpain is a logical therapeutic target for pharmacological inhibition in combination with an antioxidant in order to more completely prevent post-traumatic neurodegeneration. Indeed, several calpain inhibitors administered either prior to or after CNS injury (Saatman, Murai et al. 1996; Kupina, Nath et al. 2001; Kupina, Detloff et al. 2002; Buki, Farkas et al. 2003) have been shown to improve post-traumatic neurological recovery and tissue sparing.

In conclusion, despite the possibly limited therapeutic potential of tempol by itself, the protective efficacy of the compound is at least adequate to support our original hypothesis that PN-mediated oxidative damage is an upstream post-traumatic event that contributes to mitochondrial dysfunction, intracellular Ca^{2+} overload, calpain-mediated cytoskeletal degradation and neurodegeneration as illustrated in Figure 4.4. Copyright © Ying Deng 2007.

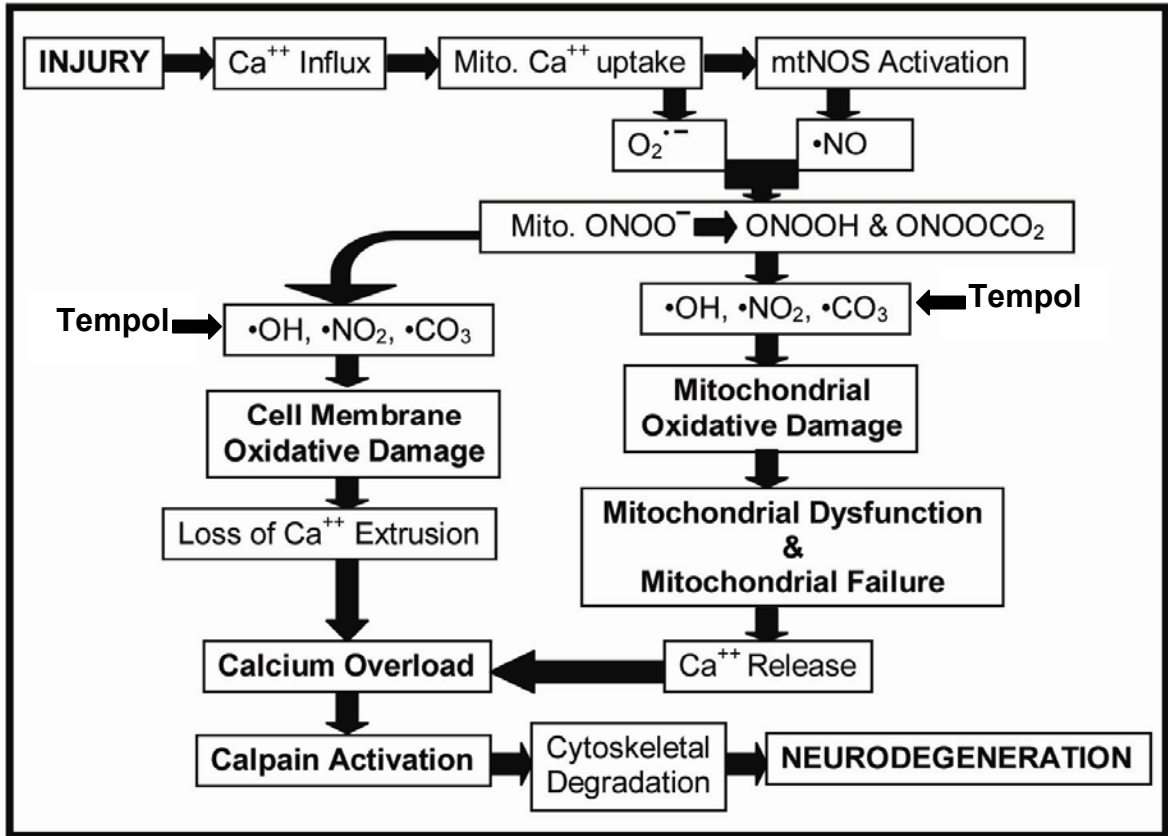


Figure 4.4 Hypothetical interrelationship between PN-induced oxidative damage in neuronal mitochondria and the compromise of Ca^{2+} homeostasis, calpain-mediated proteolysis and neurodegeneration. Our results suggest that the potent antioxidant, tempol, by targeting the upstream PN-derived free radicals, produces cascades of effects on the downstream cellular elements, such as preserve mitochondrial function, ameliorate Ca^{2+} overload, reduce calpain-mediated proteolysis and neurodegeneration.

Chapter Five

Summary and Conclusions

Traumatic brain injury (TBI) is comprised of the primary injury and secondary injury. The initial mechanical assault to the head induces instant tissue damage, which is termed the primary injury. However, the primary injury induces cascades of neurochemical changes, which lead to further neuronal cell loss, microvascular damage and dysfunction and impairment in behavioral function. Secondary injury begins immediately after injury, and this post-injury phase may last for days and weeks depending on the severity of the initial injury. Although little can be done to reduce the primary injury apart from decreasing the risk of TBI, it is feasible to ameliorate post-TBI secondary injury by timely pharmacological intervention. Thus, understanding pathological mechanisms responsible for post-traumatic neuronal damage will shed light on neuroprotective pharmaceutical approaches.

Successful pharmacological interventions for TBI patients are not available to this day due in large part to the complexity of the neurological changes initiated by the primary injury. In this series of studies, we employed a widely used focal TBI model, controlled cortical impact (CCI) mouse model. The current project has identified peroxynitrite (PN) as an important therapeutic target for pharmacological intervention. Moreover, we explored the effect of PN-derived radical scavenger, tempol, on PN-induced oxidative damage, mitochondrial

dysfunction, calpain-mediated proteolysis, neurodegeneration and neurological outcome.

The first study is a thorough comparative time course assessment of PN-induced oxidative damage, calpain-mediated α -spectrin breakdown and neurodegeneration measured by de Olmos aminocupric silver staining in ipsilateral cortex in the CCI mouse model. Both quantitative slotblotting and immunohistochemical studies indicate that PN is the main source of lipid peroxidation and protein nitration, suggesting that PN is an important mediator of post-traumatic oxidative damage. The onset of PN-mediated oxidative damage measured in cerebral cortical tissue begins immediately after injury and peaks at 1 hr after injury. This is coincident with an increase of oxidative damage in cortical mitochondria, suggesting that mitochondria are perhaps the main source and target of post-traumatic production of PN. Furthermore, quantitative westernblotting measured calpain-mediated cytoskeletal degradation which is also increased within the first hours after injury. The increased appearance of calpain-mediated spectrin breakdown (SBDPs) progresses over time and reaches its peak at 24 hrs. Calpain-specific SBDP145 shows a much higher magnitude than non-specific calpain/caspase 3-generated SBDP150, indicating that calpain is the main mediator in post-traumatic proteolysis. Moreover, the peak of calpain-mediated cytoskeletal breakdown precedes the peak of neurodegeneration, which is at 48 hrs after injury.

The time course study elegantly illustrated the interrelationship of several key mediators following TBI. The early increase of PN production correlates with

mitochondrial dysfunction. As a key calcium buffer in the cell, the loss of mitochondrial function exacerbates Ca^{2+} -dependent calpain activity, and eventually neuronal cell loss. The quantitative measurement of the end products of oxidative damage and calpain-mediated proteolysis also provides measurable index for therapeutic studies. More importantly, the complete temporal profile of oxidative damage, calpain activity and neurodegeneration defines the probable time windows for pharmacological intervention. These results reveal that PN is an upstream event that precedes mitochondrial dysfunction, calpain over-activation and neurodegeneration. Therefore, targeting PN-induced oxidative damage may have multiple beneficial effects through inhibition of several key mediators in the secondary injury process. However, the extremely early peak of oxidative damage also makes it a difficult target. Timely treatment is critical in therapeutic interventions. Based on the time course study, we chose the optimal time point of each end point for neuroprotective effect evaluation.

To test the hypothesis that blockade of upstream PN-induced oxidative damage will produce a neuroprotective effect, we pharmacologically targeted PN using a potent antioxidant, tempol, in the CCI model. Tempol is a membrane permeable, catalytic scavenger of PN-derived free radicals. In an initial study, we examined the dose-response of tempol in regards to an inhibitory effect on PN-induced oxidative damage across a three log range of dosages (3, 10, 30, 100 and 300mg/kg i.p.). We chose the PN-specific marker, 3-nitrotyrosine (3NT), as an index to examine the effect of tempol on PN-induced oxidative damage. In order to achieve maximal effect, tempol was administered i.p. at 15 min and

tissue was harvested at 1 hr post-injury when oxidative damage is at its peak. Our results show that tempol inhibited PN-mediated oxidative damage in a dose-related manner with the highest dose levels of 30, 100 and 300mg/kg each producing a statistically significant effect. Moreover, quantitative slotblotting measurement of 3NT indicated that at 300mg/kg, tempol reduces 3NT to sham level. This study demonstrated that tempol is an effective inhibitor of PN-mediated oxidative damage in the injured brain.

Following the success of tempol in inhibition of PN-induced oxidative damage, we chose the optimal dose (300mg/kg) of tempol in the subsequent studies to confirm our hypothesis that oxidative damage is the upstream element in the secondary injury cascade. We hypothesizes that mitochondria are the main source of PN production based upon previous studies in our laboratory showing that PN-mediated damage occurs in mitochondria from the injured brain which parallels the loss of respiratory function and Ca^{2+} -buffering capacity. Indeed, in response to glutamate-induced excitotoxic calcium influx, mitochondrial Ca^{2+} uptake induces superoxide and nitric oxide radical production, which can combine with a diffusion rate-limited rate constant to produce PN. To test the association between mitochondrial PN oxidative damage and respiratory dysfunction, we administered tempol 15 min after injury and isolated the mitochondria from the injured cerebral cortex at 12 hrs post-injury. Using Clarke-type electrode measurement of mitochondrial respiration, tempol-treated mitochondria show improved maintenance of respiratory function together with reduced oxidative protein damage. The protective effect of tempol on

mitochondrial function reveals that: 1) tempol is membrane permeable and effective in penetrating into mitochondrial matrix; 2) mitochondria are a main source for PN production as well as the primary target of PN-mediated oxidative damage. Moreover, the success of using tempol *in vivo* to preserve mitochondrial function, strongly suggests that PN plays a significant role in mediating mitochondria calcium influx-induced functional impairment.

Moving downstream in the hypothesized secondary injury cascade, we examined the effect of tempol on calcium-dependent calpain activity. Calpain is activated upon calcium influx and is shown to play an important role in cytoskeletal degradation, which is considered as a final common pathway to cell death. Because of the close relationship of calpain and cytosolic calcium level, we hypothesize that tempol, by preserving mitochondrial function and maintaining calcium homeostasis, will indirectly attenuate calpain activity. To test this hypothesis, we administered single i.p. dose of tempol 15 min after injury and evaluated calpain-mediated SBDPs at 1 hr and 6 hrs post-injury measured by quantitative slotblotting. The results demonstrate that tempol significantly reduces calpain-specific SBPD145 at 1 hr but not at 6 hrs after injury. The inhibitory effect of antioxidant tempol on calpain-mediated cytoskeletal proteolysis strongly confirms that PN-induced oxidative damage is upstream to calpain over-activation. However, the effect of tempol on calpain activity is short-lived possibly due to the high elimination rate of tempol in the mouse brain. Therefore, we explored the effect of a multiple dose regimen with tempol on calpain-mediated cytoskeletal degradation. In the tempol multiple dose

experiment, we administered tempol 300 mg/kg i.p. to animals at 15 min, 3 hrs, 6 hrs, 9 hrs and 12 hrs post-injury and harvested the tissue at 24 hrs, when calpain-mediated SBDPs are at their peak. This dosing regimen was designed to maintain an inhibition of PN-mediated oxidative damage over its full time course of 12 hrs based upon our original time course studies. Our results show tempol significantly reduces SBDPs by 45% at 24 hrs post-injury. Although the prolonged treatment with tempol may have successfully inhibited most of the oxidative damage, the inhibition of calpain activity was only partial. A possible explanation is that PN itself has inhibitory effect on both calpain and caspase 3 by oxidizing cysteine residues on their active site. Therefore, the complete inhibition of PN may partially antagonize the full expression of its protective benefits via a removal of an oxidative break on calpain activity.

We then did a tempol therapeutic window study by measuring calpain-mediated SBDPs. We used the same multiple dosing regimen, but delayed treatment by 1 hr and 2 hrs. In this study, we are not able to observe any beneficial effect of tempol on calpain inhibition. It is possible that the first hour window is crucial for PN-induced oxidative damage and tempol alone may not be able to induce maximal inhibition on calpain activity.

We have successfully proven that by preventing upstream PN-induced oxidative damage, we can ameliorate mitochondrial dysfunction and attenuate calpain-mediated cytoskeletal degradation, which is linked to cell injury and death. Therefore, we applied the multiple dosing regimen and examined the neurodegeneration at 7 days after injury. In this study, we measured ipsilateral

cortical tissue spared volume and ipsilateral hemispherical silver staining volume. Tempol treatment increases cortical tissue sparing. However, this effect is not significant compared to vehicle-treated group. In contrast, silver staining detected a significant decrease in neurodegeneration in tempol-treated group. In the tempol-treated group, the extent of the silver staining is reduced. We believe that silver staining is a much more sensitive technique that more accurately reveals the degree of post-traumatic tissue damage and more sensitively shows the efficacy of neuroprotective agents.

In this last study, we examined the behavioral outcome in parallel with the neurohistological study. Specifically, we measured motor function of the TBI mice at 48 hrs and 7 days post-injury. At 48hrs, we observed a deficit in motor function in the injured vehicle-treated animals. However, the mean score of the tempol-treated animals is not significantly different from either the non-injured sham group or vehicle-treated group. At 7 days, the neuroscore is not able to detect any difference among the groups suggesting that future studies should focus on the earlier 48 hrs time point. Moreover, a more sensitive functional test, or a combination of different behavioral assessment, such as cognitive as well as motorsensory testing, should be considered in the future.

In summary, the complete time course study and the pharmacological study compliments each other, and provide strong evidence for PN-induced oxidative damage being an important upstream mediator in the secondary cell death cascade. In our study, scavenging PN-derived free radicals with the nitroxide antioxidant tempol produces beneficial effects on mitochondrial function

and probably calcium buffering capacity which in turn reduces downstream calpain-mediated proteolysis and neurodegeneration. However, the complexity of the secondary injury process after TBI challenges the idea that single therapy can achieve optimal neuroprotection and improvement in functional outcome. In the future, it will make sense to investigate combination therapies that simultaneously target PN-induced oxidative damage along with either inhibition of mitochondrial permeability transition or calpain activation or both. Copyright © Ying Deng 2007.

Appendix I

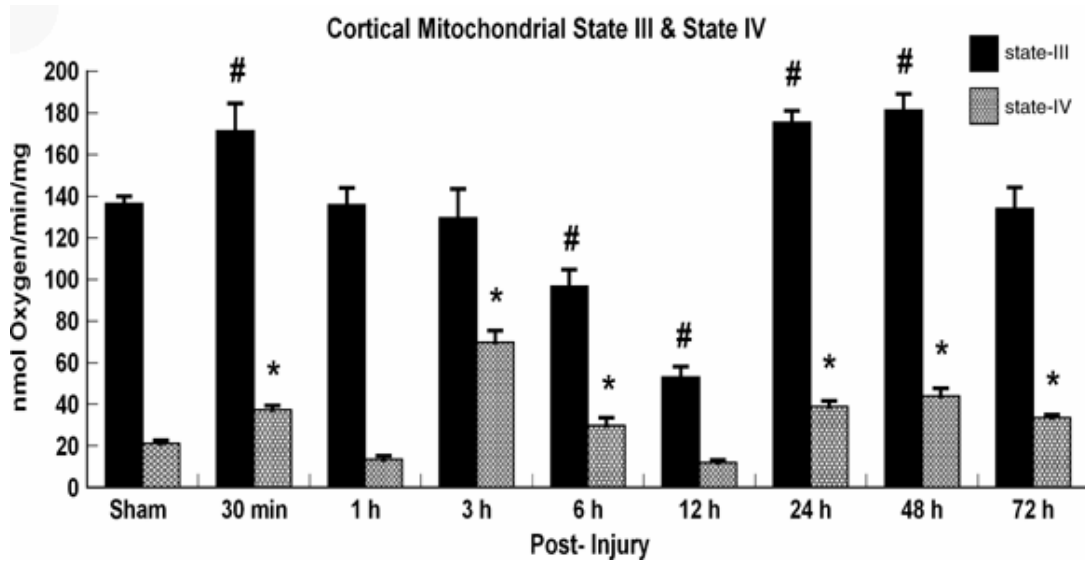


Figure A.1 Time course of mitochondrial states III & IV respiratory rates in mouse ipsilateral cortex after severe (1.0mm) TBI. Mitochondrial oxygen consumption was measured using a Clark-type electrode in a continuously stirred, sealed chamber (Oxygraph System; Hansatech Instruments Ltd). Purified mitochondrial protein (25 to 35 μ g) was suspended in respiration buffer (125mmol/L KCl, 2mmol/L $MgCl_2$, 2.5mmol/L KH_2PO_4 , 0.1% BSA, 20mmol/L HEPES, pH7.2) in a final volume of 250 μ l. Data are presented as mean \pm s.e.m. Statistical differences (one-way ANOVA and Student-Neuman-Keuls post hoc test): * $P < 0.0001$ versus sham; # $P < 0.001$ versus sham.

Appendix II

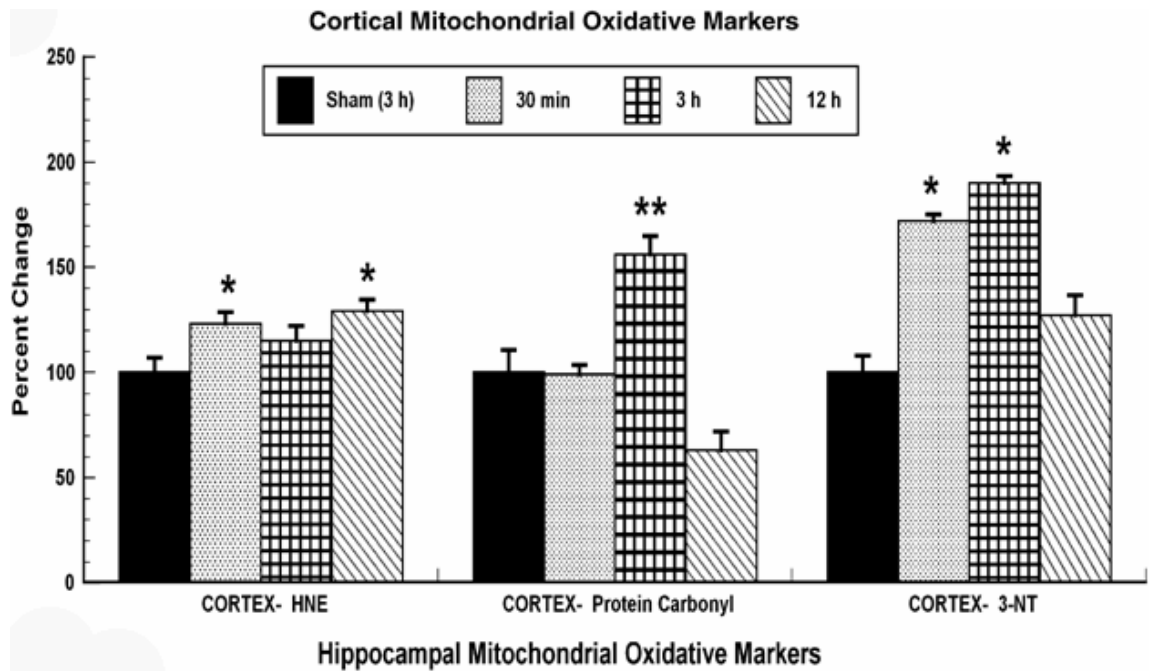


Figure A.2 Time course of lipid (HNE) and protein (protein carbonyl) oxidative damage in percoll-purified mitochondria from the ipsilateral cortex after a severe (1.0mm) TBI. Distribution of HNE, protein carbonyls, and 3NT in cortical mitochondria from mice at 30 min, 3 and 12 hrs after injury and were compared with sham (3 hrs) animals. Approximately 2.5µg of percoll-purified mitochondrial protein isolated from cortical region was applied onto Protran nitrocellulose membrane (Schleicher & Schuell, Dassel, Germany), as described in **Materials and Methods**, and oxidative markers were quantitated using a Minifold II vacuum slot blot apparatus. Data are presented as mean \pm s.e.m. Statistical differences (one-way ANOVA and SNK *post hoc* test): * $P < 0.05$ versus sham; ** $P < 0.001$ versus sham; *** $P < 0.0001$ versus sham; @ $P < 0.005$ versus sham.

Appendix III

Glossary of important terms

$\Delta\Psi_m$	mitochondrial membrane potential	iNOS	inducible nitric oxide synthase
ΔpH	proton force	L-DOPA	dihydroxyphenylalanine
3NT	3-nitrotyrosin	LP	lipid peroxidation
4HNE	4-hydroxynonenal	NADPH	nicotinamide adenine dinucleotide phosphate, reduced form
8-OH-G	8-hydroxyguanine		
8-OHdG	8-hydroxydeoxyguanosine	nNOS	neuronal nitric oxide synthase
ADP	adenosine diphosphate	MAP2	microtubule-associated proteins
AIF	apoptosis inducing factor	MDA	malondialdehyde
ANT	adenine nucleotide translocator	mPTP	mitochondrial permeability transition pore
ASDH	subdural hematoma	MPTP	1-methyl-4-phenyl-1,2,5,6-tetrahydropyridine
ATP	adenosine triphosphate	mtNOS	mitochondrial nitric oxide synthase
BBB	blood-brain barrier	NADH	nicotinamide adenine dinucleotide, reduced form
BDPs	breakdown products	NADPH	nicotinamide adenine dinucleotide phosphate, reduced form
Ca ²⁺	calcium	NF	neurofilament
CCI	controlled cortical impact	NMDA	N-Methyl-D-aspartate
CNS	central nervous system	NO	nitric oxide
CsA	cyclosporine A	NOS	nitric oxide synthase
CypD	cyclophilin D	ONOO [•]	peroxynitrite anion
Cyt c	cytochrome c	ONOO ⁻	peroxynitrite anion
DNPH	2,4-dinitrophenylhydrazine	ONOOH	peroxynitrite acid
eNOS	epithelial nitric oxide synthase	ONOOCO ₂	nitrosoperoxo carbonate
ETC	electron transport chain	PARS	ADP-ribose synthetase
FADH ₂	reduced flavin adenine dinucleotide	PBS	phosphate-buffered saline
FCCP	<i>p</i> -trifluoromethoxy carbonyl cyanide phenyl hydrazone	PGH	prostaglandin hydroperoxidase
FMNH ₂	reduced flavin mononucleotide	PN	peroxynitrite
FPI	fluid percussion injury	PUFAs	polyunsaturated fatty acids
GPX	glutathione peroxidase		
GSH	glutathione		
HPLC	high-performance liquid chromatography		
IMM	inner mitochondrial membrane		

RCR	respiratory control ratio
ROS	reactive oxygen species
RNS	reactive nitrogen species
SBDPs	α -spectrin breakdown products
SCI	spinal cord injury
SOD	superoxide dismutase
XO	xanthine oxidase
TAI	traumatic axonal injury
TBI	traumatic brain injury
TBS	tris-buffered saline
UCPs	uncoupling proteins
UQ	ubiquinone
UQ ^{•-}	semiquinone anion species
UQH ₂	ubiquinol
XDH	xanthine dehydrogenase
XO	xanthine oxidase

References

- Arrigoni, E. and F. Cohadon (1991). "Calcium-activated neutral protease activities in brain trauma." Neurochem Res **16**(4): 483-7.
- Awasthi, D., D. F. Church, et al. (1997). "Oxidative stress following traumatic brain injury in rats." Surg Neurol **47**(6): 575-81; discussion 581-2.
- Azbill, R. D., X. Mu, et al. (1997). "Impaired mitochondrial function, oxidative stress and altered antioxidant enzyme activities following traumatic spinal cord injury." Brain Res **765**(2): 283-90.
- Bartus, R. T., R. L. Dean, et al. (1998). "Temporal ordering of pathogenic events following transient global ischemia." Brain Res **790**(1-2): 1-13.
- Bartus, R. T., P. J. Elliott, et al. (1995). "Calpain as a novel target for treating acute neurodegenerative disorders." Neurol Res **17**(4): 249-58.
- Bartus, R. T., N. J. Hayward, et al. (1994). "Calpain inhibitor AK295 protects neurons from focal brain ischemia. Effects of postocclusion intra-arterial administration." Stroke **25**(11): 2265-70.
- Bates, T. E., A. Loesch, et al. (1995). "Immunocytochemical evidence for a mitochondrially located nitric oxide synthase in brain and liver." Biochem Biophys Res Commun **213**(3): 896-900.
- Beatrice, M. C., J. W. Palmer, et al. (1980). "The relationship between mitochondrial membrane permeability, membrane potential, and the retention of Ca²⁺ by mitochondria." J Biol Chem **255**(18): 8663-71.
- Beckman, J. S. (1994). "Peroxynitrite versus hydroxyl radical: the role of nitric oxide in superoxide-dependent cerebral injury." Ann N Y Acad Sci **738**: 69-75.
- Beckman, J. S. (1996). "Oxidative damage and tyrosine nitration from peroxynitrite." Chem Res Toxicol **9**(5): 836-44.
- Beckman, J. S. and W. H. Koppenol (1996). "Nitric oxide, superoxide, and peroxynitrite: the good, the bad, and ugly." Am J Physiol **271**(5 Pt 1): C1424-37.
- Behringer, W., P. Safar, et al. (2002). "Antioxidant Tempol enhances hypothermic cerebral preservation during prolonged cardiac arrest in dogs." J Cereb Blood Flow Metab **22**(1): 105-17.
- Beit-Yannai, E., R. Zhang, et al. (1996). "Cerebroprotective effect of stable nitroxide radicals in closed head injury in the rat." Brain Res **717**(1-2): 22-8.
- Benuck, M., M. Banay-Schwartz, et al. (1992). "Peroxidative stress effects on calpain activity in brain of young and adult rats." Brain Res **596**(1-2): 296-8.
- Bernardi, P. (1996). "The permeability transition pore. Control points of a cyclosporin A-sensitive mitochondrial channel involved in cell death." Biochim Biophys Acta **1275**(1-2): 5-9.
- Bernardi, P., K. M. Broekemeier, et al. (1994). "Recent progress on regulation of the mitochondrial permeability transition pore; a cyclosporin-sensitive pore in the inner mitochondrial membrane." J Bioenerg Biomembr **26**(5): 509-17.

- Bianca, V. D., S. Dusi, et al. (1999). "beta-amyloid activates the O-2 forming NADPH oxidase in microglia, monocytes, and neutrophils. A possible inflammatory mechanism of neuronal damage in Alzheimer's disease." J Biol Chem **274**(22): 15493-9.
- Bicker, G. (2001). "Nitric oxide: an unconventional messenger in the nervous system of an orthopteroide insect." Arch Insect Biochem Physiol **48**(2): 100-10.
- Blou, N. V. and O. C. Zafiriou (1985) Reaction of superoxide with nitric oxide to form peroxynitrite in alkaline aqueous solution. Inorg. Chem. **24**, 3504-3505.
- Bonini, M. G., R. P. Mason, et al. (2002). "The Mechanism by which 4-hydroxy-2,2,6,6-tetramethylpiperidine-1-oxyl (tempol) diverts peroxynitrite decomposition from nitrating to nitrosating species." Chem Res Toxicol **15**(4): 506-11.
- Bredt, D. S. and S. H. Snyder (1990). "Isolation of nitric oxide synthetase, a calmodulin-requiring enzyme." Proc Natl Acad Sci U S A **87**(2): 682-5.
- Bredt, D. S. and S. H. Snyder (1994). "Nitric oxide: a physiologic messenger molecule." Annu Rev Biochem **63**: 175-95.
- Bringold, U., P. Ghafourifar, et al. (2000). "Peroxynitrite formed by mitochondrial NO synthase promotes mitochondrial Ca²⁺ release." Free Radic Biol Med **29**(3-4): 343-8.
- Brookes, P. S., J. M. Land, et al. (1998). "Peroxynitrite and brain mitochondria: evidence for increased proton leak." J Neurochem **70**(5): 2195-202.
- Brown, M. R., P. G. Sullivan, et al. (2004). "Nitrogen disruption of synaptoneurosomes: an alternative method to isolate brain mitochondria." J Neurosci Methods **137**(2): 299-303.
- Buki, A., O. Farkas, et al. (2003). "Preinjury administration of the calpain inhibitor MDL-28170 attenuates traumatically induced axonal injury." J Neurotrauma **20**(3): 261-8.
- Buki, A., R. Siman, et al. (1999). "The role of calpain-mediated spectrin proteolysis in traumatically induced axonal injury." J Neuropathol Exp Neurol **58**(4): 365-75.
- Butterfield, D. A. and C. M. Lauderback (2002). "Lipid peroxidation and protein oxidation in Alzheimer's disease brain: potential causes and consequences involving amyloid beta-peptide-associated free radical oxidative stress." Free Radic Biol Med **32**(11): 1050-60.
- Carafoli, E. and M. Molinari (1998). "Calpain: a protease in search of a function?" Biochem Biophys Res Commun **247**(2): 193-203.
- Carroll, R. T., P. Galatsis, et al. (2000). "4-Hydroxy-2,2,6,6-tetramethylpiperidine-1-oxyl (Tempol) inhibits peroxynitrite-mediated phenol nitration." Chem Res Toxicol **13**(4): 294-300.
- Castro, L., M. Rodriguez, et al. (1994). "Aconitase is readily inactivated by peroxynitrite, but not by its precursor, nitric oxide." J Biol Chem **269**(47): 29409-15.
- Chakraborti, T., S. Das, et al. (1999). "Oxidant, mitochondria and calcium: an overview." Cell Signal **11**(2): 77-85.

- Chan, P. H., C. J. Epstein, et al. (1995). "Transgenic mice and knockout mutants in the study of oxidative stress in brain injury." J Neurotrauma **12**(5): 815-24.
- Chan, S. L. and M. P. Mattson (1999). "Caspase and calpain substrates: roles in synaptic plasticity and cell death." J Neurosci Res **58**(1): 167-90.
- Chiueh, C. C. (1999). "Neuroprotective properties of nitric oxide." Ann N Y Acad Sci **890**: 301-11.
- Cobbs, C. S., A. Fenoy, et al. (1997). "Expression of nitric oxide synthase in the cerebral microvasculature after traumatic brain injury in the rat." Brain Res **751**(2): 336-8.
- Coyle, J. T. and P. Puttfarcken (1993). "Oxidative stress, glutamate, and neurodegenerative disorders." Science **262**(5134): 689-95.
- Crow, J. P. and J. S. Beckman (1996). "The importance of superoxide in nitric oxide-dependent toxicity: evidence for peroxynitrite-mediated injury." Adv Exp Med Biol **387**: 147-61.
- Cudd, A. and I. Fridovich (1982). "Electrostatic interactions in the reaction mechanism of bovine erythrocyte superoxide dismutase." J Biol Chem **257**(19): 11443-7.
- Cuzzocrea, S., M. C. McDonald, et al. (2000). "Effects of tempol, a membrane-permeable radical scavenger, in a gerbil model of brain injury." Brain Res **875**(1-2): 96-106.
- Davis, M. D., S. Kaufman, et al. (1988). "The auto-oxidation of tetrahydrobiopterin." Eur J Biochem **173**(2): 345-51.
- Dawson, V. L. and T. M. Dawson (1996). "Nitric oxide in neuronal degeneration." Proc Soc Exp Biol Med **211**(1): 33-40.
- de Olmos, J. S., C. A. Beltramino, et al. (1994). "Use of an amino-cupric-silver technique for the detection of early and semiacute neuronal degeneration caused by neurotoxicants, hypoxia, and physical trauma." Neurotoxicol Teratol **16**(6): 545-61.
- DeGraff, W. G., M. C. Krishna, et al. (1992). "Nitroxide-mediated protection against X-ray- and neocarzinostatin-induced DNA damage." Free Radic Biol Med **13**(5): 479-87.
- Deng, Y., B. M. Thompson, et al. (2007). "Temporal relationship of peroxynitrite-induced oxidative damage, calpain-mediated cytoskeletal degradation and neurodegeneration after traumatic brain injury." Exp Neurol **205**(1): 154-65.
- DeRidder, M. N., M. J. Simon, et al. (2006). "Traumatic mechanical injury to the hippocampus in vitro causes regional caspase-3 and calpain activation that is influenced by NMDA receptor subunit composition." Neurobiol Dis **22**(1): 165-76.
- Echtay, K. S., T. C. Esteves, et al. (2003). "A signalling role for 4-hydroxy-2-nonenal in regulation of mitochondrial uncoupling." Embo J **22**(16): 4103-10.
- Edmunds, T., P. A. Nagainis, et al. (1991). "Comparison of the autolyzed and unautolyzed forms of mu- and m-calpain from bovine skeletal muscle." Biochim Biophys Acta **1077**(2): 197-208.

- Elfering, S. L., T. M. Sarkela, et al. (2002). "Biochemistry of mitochondrial nitric-oxide synthase." J Biol Chem **277**(41): 38079-86.
- Faddis, B. T., M. J. Hasbani, et al. (1997). "Calpain activation contributes to dendritic remodeling after brief excitotoxic injury in vitro." J Neurosci **17**(3): 951-9.
- Faden, A. I., P. Demediuk, et al. (1989). "The role of excitatory amino acids and NMDA receptors in traumatic brain injury." Science **244**(4906): 798-800.
- Gadelha, F. R., L. Thomson, et al. (1997). "Ca²⁺-independent permeabilization of the inner mitochondrial membrane by peroxynitrite is mediated by membrane protein thiol cross-linking and lipid peroxidation." Arch Biochem Biophys **345**(2): 243-50.
- Gahm, C., S. Holmin, et al. (2000). "Temporal profiles and cellular sources of three nitric oxide synthase isoforms in the brain after experimental contusion." Neurosurgery **46**(1): 169-77.
- Gao, H. M., J. Jiang, et al. (2002). "Microglial activation-mediated delayed and progressive degeneration of rat nigral dopaminergic neurons: relevance to Parkinson's disease." J Neurochem **81**(6): 1285-97.
- Garcia, M., V. Bondada, et al. (2005). "Mitochondrial localization of mu-calpain." Biochem Biophys Res Commun **338**(2): 1241-7.
- Garthwaite, J. and C. L. Boulton (1995). "Nitric oxide signaling in the central nervous system." Annu Rev Physiol **57**: 683-706.
- Garthwaite, J., S. L. Charles, et al. (1988). "Endothelium-derived relaxing factor release on activation of NMDA receptors suggests role as intercellular messenger in the brain." Nature **336**(6197): 385-8.
- Ghafourifar, P. and C. Richter (1997). "Nitric oxide synthase activity in mitochondria." FEBS Lett **418**(3): 291-6.
- Ghafourifar, P., U. Schenk, et al. (1999). "Mitochondrial nitric-oxide synthase stimulation causes cytochrome c release from isolated mitochondria. Evidence for intramitochondrial peroxynitrite formation." J Biol Chem **274**(44): 31185-8.
- Gibson, G. E. and H. M. Huang (2004). "Mitochondrial enzymes and endoplasmic reticulum calcium stores as targets of oxidative stress in neurodegenerative diseases." J Bioenerg Biomembr **36**(4): 335-40.
- Giulivi, C. (1998). "Functional implications of nitric oxide produced by mitochondria in mitochondrial metabolism." Biochem J **332** (Pt 3): 673-9.
- Giulivi, C. (2003). "Characterization and function of mitochondrial nitric-oxide synthase." Free Radic Biol Med **34**(4): 397-408.
- Globus, M. Y., O. Alonso, et al. (1995). "Glutamate release and free radical production following brain injury: effects of posttraumatic hypothermia." J Neurochem **65**(4): 1704-11.
- Green, D. R. and G. Kroemer (2004). "The pathophysiology of mitochondrial cell death." Science **305**(5684): 626-9.
- Grijalba, M. T., A. E. Vercesi, et al. (1999). "Ca²⁺-induced increased lipid packing and domain formation in submitochondrial particles. A possible early step in the mechanism of Ca²⁺-stimulated generation of reactive oxygen species by the respiratory chain." Biochemistry **38**(40): 13279-87.

- Grune, T., T. Reinheckel, et al. (1997). "Degradation of oxidized proteins in mammalian cells." Faseb J **11**(7): 526-34.
- Gunter, T. E. and D. R. Pfeiffer (1990). "Mechanisms by which mitochondria transport calcium." Am J Physiol **258**(5 Pt 1): C755-86.
- Gutteridge, J. M. and B. Halliwell (1989). "Iron toxicity and oxygen radicals." Baillieres Clin Haematol **2**(2): 195-256.
- Guttmann, R. P., J. S. Elce, et al. (1997). "Oxidation inhibits substrate proteolysis by calpain I but not autolysis." J Biol Chem **272**(3): 2005-12.
- Guttmann, R. P. and G. V. Johnson (1998). "Oxidative stress inhibits calpain activity in situ." J Biol Chem **273**(21): 13331-8.
- Hahn, S. M., C. M. Krishna, et al. (1994). "Potential use of nitroxides in radiation oncology." Cancer Res **54**(7 Suppl): 2006s-2010s.
- Halestrap, A. P. and C. Brennerb (2003). "The adenine nucleotide translocase: a central component of the mitochondrial permeability transition pore and key player in cell death." Curr Med Chem **10**(16): 1507-25.
- Hall, E. D., P. K. Andrus, et al. (1993). "Brain hydroxyl radical generation in acute experimental head injury." J Neurochem **60**(2): 588-94.
- Hall, E. D., P. K. Andrus, et al. (1994). "Generation and detection of hydroxyl radical following experimental head injury." Ann N Y Acad Sci **738**: 15-24.
- Hall, E. D. and J. M. Braugher (1993). "Free radicals in CNS injury." Res Publ Assoc Res Nerv Ment Dis **71**: 81-105.
- Hall, E. D., M. R. Detloff, et al. (2004). "Peroxynitrite-mediated protein nitration and lipid peroxidation in a mouse model of traumatic brain injury." J Neurotrauma **21**(1): 9-20.
- Hall, E. D., T. R. Gibson, et al. (2005). "Lack of a gender difference in post-traumatic neurodegeneration in the mouse controlled cortical impact injury model." J Neurotrauma **22**(6): 669-79.
- Hall, E. D., N. C. Kupina, et al. (1999). "Peroxynitrite scavengers for the acute treatment of traumatic brain injury." Ann N Y Acad Sci **890**: 462-8.
- Hall, E. D., J. A. Oostveen, et al. (1997). "Immunocytochemical method for investigating in vivo neuronal oxygen radical-induced lipid peroxidation." J Neurosci Methods **76**(2): 115-22.
- Hall, E. D. and S. L. Smith (1991). "The 21-aminosteroid antioxidant tirilazad mesylate, U-74006F, blocks cortical hypoperfusion following spreading depression." Brain Res **553**(2): 243-8.
- Hall, E. D., P. G. Sullivan, et al. (2005). "Spatial and temporal characteristics of neurodegeneration after controlled cortical impact in mice: more than a focal brain injury." J Neurotrauma **22**(2): 252-65.
- Halliwell, B. and J. M. C. Gutteridge (1999) "Free radicals in biology and medicine (3rd)." Oxford Science Publications
- Hamakubo, T., R. Kannagi, et al. (1986). "Distribution of calpains I and II in rat brain." J Neurosci **6**(11): 3103-11.
- Hausladen, A. and I. Fridovich (1994). "Superoxide and peroxynitrite inactivate aconitases, but nitric oxide does not." J Biol Chem **269**(47): 29405-8.

- Herrero, A. and G. Barja (1997). "Sites and mechanisms responsible for the low rate of free radical production of heart mitochondria in the long-lived pigeon." Mech Ageing Dev **98**(2): 95-111.
- Hillard, V. H., H. Peng, et al. (2004). "Tempol, a nitroxide antioxidant, improves locomotor and histological outcomes after spinal cord contusion in rats." J Neurotrauma **21**(10): 1405-14.
- Huh, J. W., H. L. Laurer, et al. (2002). "Rapid loss and partial recovery of neurofilament immunostaining following focal brain injury in mice." Exp Neurol **175**(1): 198-208.
- Huie, R. E. and S. Padmaja (1993). "The reaction of NO with superoxide." Free Radic Res Commun **18**(4): 195-9.
- Ischiropoulos, H. and J. S. Beckman (2003). "Oxidative stress and nitration in neurodegeneration: cause, effect, or association?" J Clin Invest **111**(2): 163-9.
- Ischiropoulos, H., L. Zhu, et al. (1992). "Peroxynitrite-mediated tyrosine nitration catalyzed by superoxide dismutase." Arch Biochem Biophys **298**(2): 431-7.
- Jiang, D., P. G. Sullivan, et al. (2001). "Zn(2+) induces permeability transition pore opening and release of pro-apoptotic peptides from neuronal mitochondria." J Biol Chem **276**(50): 47524-9.
- Kamatari, M., H. Yasui, et al. (2002). "Local pharmacokinetic analysis of a stable spin probe in mice by in vivo L-band ESR with surface-coil-type resonators." Free Radical Research **36**(10): 1115-1125.
- Kampfl, A., R. Posmantur, et al. (1996). "mu-calpain activation and calpain-mediated cytoskeletal proteolysis following traumatic brain injury." J Neurochem **67**(4): 1575-83.
- Kampfl, A., R. M. Posmantur, et al. (1997). "Mechanisms of calpain proteolysis following traumatic brain injury: implications for pathology and therapy: implications for pathology and therapy: a review and update." J Neurotrauma **14**(3): 121-34.
- Kasprzak, H. A., A. Wozniak, et al. (2001). "Enhanced lipid peroxidation processes in patients after brain contusion." J Neurotrauma **18**(8): 793-7.
- Katayama, Y., D. P. Becker, et al. (1990). "Massive increases in extracellular potassium and the indiscriminate release of glutamate following concussive brain injury." J Neurosurg **73**(6): 889-900.
- Kato, N., K. Yanaka, et al. (2003). "Stable nitroxide Tempol ameliorates brain injury by inhibiting lipid peroxidation in a rat model of transient focal cerebral ischemia." Brain Res **979**(1-2): 188-93.
- Kehrer, J. P. (2000). "The Haber-Weiss reaction and mechanisms of toxicity." Toxicology **149**(1): 43-50.
- Keller, J. N., R. J. Mark, et al. (1997). "4-Hydroxynonenal, an aldehydic product of membrane lipid peroxidation, impairs glutamate transport and mitochondrial function in synaptosomes." Neuroscience **80**(3): 685-96.
- Kontos, H. A. and J. T. Povlishock (1986). "Oxygen radicals in brain injury." Cent Nerv Syst Trauma **3**(4): 257-63.

- Kontos, H. A. and E. P. Wei (1986). "Superoxide production in experimental brain injury." J Neurosurg **64**(5): 803-7.
- Kowaltowski, A. J., R. F. Castilho, et al. (1995). "Ca(2+)-induced mitochondrial membrane permeabilization: role of coenzyme Q redox state." Am J Physiol **269**(1 Pt 1): C141-7.
- Kowaltowski, A. J., L. E. Netto, et al. (1998). "The thiol-specific antioxidant enzyme prevents mitochondrial permeability transition. Evidence for the participation of reactive oxygen species in this mechanism." J Biol Chem **273**(21): 12766-9.
- Kowaltowski, A. J. and A. E. Vercesi (1999). "Mitochondrial damage induced by conditions of oxidative stress." Free Radic Biol Med **26**(3-4): 463-71.
- Krishna, M. C., A. Russo, et al. (1996). "Do nitroxide antioxidants act as scavengers of O₂⁻. or as SOD mimics?" J Biol Chem **271**(42): 26026-31.
- Kristian, T., I. B. Hopkins, et al. (2006). "Isolation of mitochondria with high respiratory control from primary cultures of neurons and astrocytes using nitrogen cavitation." J Neurosci Methods **152**(1-2): 136-43.
- Kruman, I., A. J. Bruce-Keller, et al. (1997). "Evidence that 4-hydroxynonenal mediates oxidative stress-induced neuronal apoptosis." J Neurosci **17**(13): 5089-100.
- Kukreja, R. C., H. A. Kontos, et al. (1986). "PGH synthase and lipoxygenase generate superoxide in the presence of NADH or NADPH." Circ Res **59**(6): 612-9.
- Kupina, N. C., M. R. Detloff, et al. (2003). "Cytoskeletal protein degradation and neurodegeneration evolves differently in males and females following experimental head injury." Exp Neurol **180**(1): 55-73.
- Kupina, N. C., M. R. Detloff, et al. (2002). "Neuroimmunophilin ligand V-10,367 is neuroprotective after 24-hour delayed administration in a mouse model of diffuse traumatic brain injury." J Cereb Blood Flow Metab **22**(10): 1212-21.
- Kupina, N. C., R. Nath, et al. (2001). "The novel calpain inhibitor SJA6017 improves functional outcome after delayed administration in a mouse model of diffuse brain injury." J Neurotrauma **18**(11): 1229-40.
- Kwon, T. H., D. L. Chao, et al. (2003). "Tempol, a novel stable nitroxide, reduces brain damage and free radical production, after acute subdural hematoma in the rat." J Neurotrauma **20**(4): 337-45.
- Lacza, Z., M. Puskar, et al. (2001). "Mitochondrial nitric oxide synthase is constitutively active and is functionally upregulated in hypoxia." Free Radic Biol Med **31**(12): 1609-15.
- Lang-Rollin, I. C., H. J. Rideout, et al. (2003). "Mechanisms of caspase-independent neuronal death: energy depletion and free radical generation." J Neurosci **23**(35): 11015-25.
- Lau, A., M. Arundine, et al. (2006). "Inhibition of caspase-mediated apoptosis by peroxynitrite in traumatic brain injury." J Neurosci **26**(45): 11540-53.
- Lehninger, A. L., A. Vercesi, et al. (1978). "Regulation of Ca²⁺ release from mitochondria by the oxidation-reduction state of pyridine nucleotides." Proc Natl Acad Sci U S A **75**(4): 1690-4.

- Leker, R. R., A. Teichner, et al. (2002). "The nitroxide antioxidant tempol is cerebroprotective against focal cerebral ischemia in spontaneously hypertensive rats." Exp Neurol **176**(2): 355-63.
- Lighthall, J. W., C. E. Dixon, et al. (1989). "Experimental models of brain injury." J Neurotrauma **6**(2): 83-97.
- Liu, Y., G. Fiskum, et al. (2002). "Generation of reactive oxygen species by the mitochondrial electron transport chain." J Neurochem **80**(5): 780-7.
- Lopez-Figueroa, M. O., C. Caamano, et al. (2000). "Direct evidence of nitric oxide presence within mitochondria." Biochem Biophys Res Commun **272**(1): 129-33.
- Ludin, B. and A. Matus (1993). "The neuronal cytoskeleton and its role in axonal and dendritic plasticity." Hippocampus **3 Spec No**: 61-71.
- Marklund, N., T. Lewander, et al. (2001). "Effects of the nitron radical scavengers PBN and S-PBN on in vivo trapping of reactive oxygen species after traumatic brain injury in rats." J Cereb Blood Flow Metab **21**(11): 1259-67.
- Marshall, L. F., A. I. Maas, et al. (1998). "A multicenter trial on the efficacy of using tirilazad mesylate in cases of head injury." J Neurosurg **89**(4): 519-25.
- Martin, E., R. E. Rosenthal, et al. (2005). "Pyruvate dehydrogenase complex: metabolic link to ischemic brain injury and target of oxidative stress." J Neurosci Res **79**(1-2): 240-7.
- Matthews, R. T., P. Klivenyi, et al. (1999). "Novel free radical spin traps protect against malonate and MPTP neurotoxicity." Exp Neurol **157**(1): 120-6.
- Maxwell, W. L., J. T. Povlishock, et al. (1997). "A mechanistic analysis of nondisruptive axonal injury: a review." J Neurotrauma **14**(7): 419-40.
- McCord, J. M. (1987). "Oxygen-derived radicals: a link between reperfusion injury and inflammation." Fed Proc **46**(7): 2402-6.
- McIntosh, T. K., R. Vink, et al. (1989). "Traumatic brain injury in the rat: characterization of a lateral fluid-percussion model." Neuroscience **28**(1): 233-44.
- McStay, G. P., S. J. Clarke, et al. (2002). "Role of critical thiol groups on the matrix surface of the adenine nucleotide translocase in the mechanism of the mitochondrial permeability transition pore." Biochem J **367**(Pt 2): 541-8.
- Mesenge, C., C. Charriaut-Marlangue, et al. (1998). "Reduction of tyrosine nitration after N(omega)-nitro-L-arginine-methylester treatment of mice with traumatic brain injury." Eur J Pharmacol **353**(1): 53-7.
- Mesenge, C., C. Verrecchia, et al. (1996). "Reduction of the neurological deficit in mice with traumatic brain injury by nitric oxide synthase inhibitors." J Neurotrauma **13**(4): 209-14.
- Michel, R. P. and L. M. Cruz-Orive (1988). "Application of the Cavalieri principle and vertical sections method to lung: estimation of volume and pleural surface area." J Microsc **150**(Pt 2): 117-36.

- Mikawa, S., H. Kinouchi, et al. (1996). "Attenuation of acute and chronic damage following traumatic brain injury in copper, zinc-superoxide dismutase transgenic mice." J Neurosurg **85**(5): 885-91.
- Mohanakumar, K. P., I. Hanbauer, et al. (1998). "Neuroprotection by nitric oxide against hydroxyl radical-induced nigral neurotoxicity." J Chem Neuroanat **14**(3-4): 195-205.
- Monyer, H., D. M. Hartley, et al. (1990). "21-Aminosteroids attenuate excitotoxic neuronal injury in cortical cell cultures." Neuron **5**(2): 121-6.
- Mori, T., T. Kawamata, et al. (1998). "Antioxidant, OPC-14117, attenuates edema formation, and subsequent tissue damage following cortical contusion in rats." Acta Neurochir Suppl **71**: 120-2.
- Mota-Filipe, H., M. C. McDonald, et al. (1999). "A membrane-permeable radical scavenger reduces the organ injury in hemorrhagic shock." Shock **12**(4): 255-61.
- Murai, H., J. E. Pierce, et al. (1998). "Twofold overexpression of human beta-amyloid precursor proteins in transgenic mice does not affect the neuromotor, cognitive, or neurodegenerative sequelae following experimental brain injury." J Comp Neurol **392**(4): 428-38.
- Murphy, M. P., M. A. Packer, et al. (1998). "Peroxynitrite: a biologically significant oxidant." Gen Pharmacol **31**(2): 179-86.
- Neely, M. D., K. R. Sidell, et al. (1999). "The lipid peroxidation product 4-hydroxynonenal inhibits neurite outgrowth, disrupts neuronal microtubules, and modifies cellular tubulin." J Neurochem **72**(6): 2323-33.
- Neumar, R. W., F. H. Meng, et al. (2001). "Calpain activity in the rat brain after transient forebrain ischemia." Exp Neurol **170**(1): 27-35.
- Nicolli, A., E. Basso, et al. (1996). "Interactions of cyclophilin with the mitochondrial inner membrane and regulation of the permeability transition pore, and cyclosporin A-sensitive channel." J Biol Chem **271**(4): 2185-92.
- Nicholls, D. G. and S. J. Ferguson (2001) "Bioenergetics 3 (2nd)." Academic Press.
- Nieminen, A. L., A. M. Byrne, et al. (1997). "Mitochondrial permeability transition in hepatocytes induced by t-BuOOH: NAD(P)H and reactive oxygen species." Am J Physiol **272**(4 Pt 1): C1286-94.
- Nishio, S., M. Yunoki, et al. (1997). "Detection of lipid peroxidation and hydroxyl radicals in brain contusion of rats." Acta Neurochir Suppl **70**: 84-6.
- Nixon, R. A. (1989). "Calcium-activated neutral proteinases as regulators of cellular function. Implications for Alzheimer's disease pathogenesis." Ann N Y Acad Sci **568**: 198-208.
- Okabe, E., Y. Tsujimoto, et al. (2000). "Calmodulin and cyclic ADP-ribose interaction in Ca²⁺ signaling related to cardiac sarcoplasmic reticulum: superoxide anion radical-triggered Ca²⁺ release." Antioxid Redox Signal **2**(1): 47-54.
- Okonkwo, D. O., E. H. Pettus, et al. (1998). "Alteration of the neurofilament sidearm and its relation to neurofilament compaction occurring with traumatic axonal injury." Brain Res **784**(1-2): 1-6.

- Onyszchuk, G., B. Al-Hafez, et al. (2007). "A mouse model of sensorimotor controlled cortical impact: characterization using longitudinal magnetic resonance imaging, behavioral assessments and histology." J Neurosci Methods **160**(2): 187-96.
- Opii, W. O., V. N. Nukala, et al. (2007). "Proteomic identification of oxidized mitochondrial proteins following experimental traumatic brain injury." J Neurotrauma **24**(5): 772-89.
- Orihara, Y., K. Ikematsu, et al. (2001). "Induction of nitric oxide synthase by traumatic brain injury." Forensic Sci Int **123**(2-3): 142-9.
- Packer, M. A. and M. P. Murphy (1994). "Peroxynitrite causes calcium efflux from mitochondria which is prevented by Cyclosporin A." FEBS Lett **345**(2-3): 237-40.
- Packer, M. A. and M. P. Murphy (1995). "Peroxynitrite formed by simultaneous nitric oxide and superoxide generation causes cyclosporin-A-sensitive mitochondrial calcium efflux and depolarisation." Eur J Biochem **234**(1): 231-9.
- Pandya, J. D., J. R. Pauly, et al. (2007). "Post-Injury Administration of Mitochondrial Uncouplers Increases Tissue Sparing and Improves Behavioral Outcome following Traumatic Brain Injury in Rodents." J Neurotrauma **24**(5): 798-811.
- Posmantur, R., R. L. Hayes, et al. (1994). "Neurofilament 68 and neurofilament 200 protein levels decrease after traumatic brain injury." J Neurotrauma **11**(5): 533-45.
- Posmantur, R., A. Kampfl, et al. (1997). "A calpain inhibitor attenuates cortical cytoskeletal protein loss after experimental traumatic brain injury in the rat." Neuroscience **77**(3): 875-88.
- Posmantur, R. M., A. Kampfl, et al. (1996). "Cytoskeletal derangements of cortical neuronal processes three hours after traumatic brain injury in rats: an immunofluorescence study." J Neuropathol Exp Neurol **55**(1): 68-80.
- Povlishock, J. T., A. Buki, et al. (1999). "Initiating mechanisms involved in the pathobiology of traumatically induced axonal injury and interventions targeted at blunting their progression." Acta Neurochir Suppl **73**: 15-20.
- Radi, R. (1998). "Peroxynitrite reactions and diffusion in biology." Chem Res Toxicol **11**(7): 720-1.
- Radi, R., J. S. Beckman, et al. (1991). "Peroxynitrite-induced membrane lipid peroxidation: the cytotoxic potential of superoxide and nitric oxide." Arch Biochem Biophys **288**(2): 481-7.
- Radi, R., A. Cassina, et al. (2002). "Peroxynitrite reactions and formation in mitochondria." Free Radic Biol Med **33**(11): 1451-64.
- Radi, R., M. Rodriguez, et al. (1994). "Inhibition of mitochondrial electron transport by peroxynitrite." Arch Biochem Biophys **308**(1): 89-95.
- Raghupathi, R., S. C. Fernandez, et al. (1998). "BCL-2 overexpression attenuates cortical cell loss after traumatic brain injury in transgenic mice." J Cereb Blood Flow Metab **18**(11): 1259-69.

- Rak, R., D. L. Chao, et al. (2000). "Neuroprotection by the stable nitroxide Tempol during reperfusion in a rat model of transient focal ischemia." J Neurosurg **92**(4): 646-51.
- Ringger, N. C., P. J. Tolentino, et al. (2004). "Effects of injury severity on regional and temporal mRNA expression levels of calpains and caspases after traumatic brain injury in rats." J Neurotrauma **21**(7): 829-41.
- Roberts-Lewis, J. M., M. J. Savage, et al. (1994). "Immunolocalization of calpain I-mediated spectrin degradation to vulnerable neurons in the ischemic gerbil brain." J Neurosci **14**(6): 3934-44.
- Roveri, A., M. Coassin, et al. (1992). "Effect of hydrogen peroxide on calcium homeostasis in smooth muscle cells." Arch Biochem Biophys **297**(2): 265-70.
- Saatman, K. E., D. Bozyczko-Coyne, et al. (1996). "Prolonged calpain-mediated spectrin breakdown occurs regionally following experimental brain injury in the rat." J Neuropathol Exp Neurol **55**(7): 850-60.
- Saatman, K. E., D. I. Graham, et al. (1998). "The neuronal cytoskeleton is at risk after mild and moderate brain injury." J Neurotrauma **15**(12): 1047-58.
- Saatman, K. E., H. Murai, et al. (1996). "Calpain inhibitor AK295 attenuates motor and cognitive deficits following experimental brain injury in the rat." Proc Natl Acad Sci U S A **93**(8): 3428-33.
- Saido, T. C., S. Nagao, et al. (1992). "Autolytic transition of mu-calpain upon activation as resolved by antibodies distinguishing between the pre- and post-autolysis forms." J Biochem (Tokyo) **111**(1): 81-6.
- Saito, K., J. S. Elce, et al. (1993). "Widespread activation of calcium-activated neutral proteinase (calpain) in the brain in Alzheimer disease: a potential molecular basis for neuronal degeneration." Proc Natl Acad Sci U S A **90**(7): 2628-32.
- Samuni, A., C. M. Krishna, et al. (1990). "Superoxide reaction with nitroxides." Free Radic Res Commun **9**(3-6): 241-9.
- Samuni, A., C. M. Krishna, et al. (1989). "Superoxide reaction with nitroxide spin-adducts." Free Radic Biol Med **6**(2): 141-8.
- Saran, M., C. Michel, et al. (1990). "Reaction of NO with O₂⁻. implications for the action of endothelium-derived relaxing factor (EDRF)." Free Radic Res Commun **10**(4-5): 221-6.
- Schinder, A. F., E. C. Olson, et al. (1996). "Mitochondrial dysfunction is a primary event in glutamate neurotoxicity." J Neurosci **16**(19): 6125-33.
- Schraufstatter, I. U., D. B. Hinshaw, et al. (1986). "Oxidant injury of cells. DNA strand-breaks activate polyadenosine diphosphate-ribose polymerase and lead to depletion of nicotinamide adenine dinucleotide." J Clin Invest **77**(4): 1312-20.
- Sen, S., H. Goldman, et al. (1994). "alpha-Phenyl-tert-butyl-nitron inhibits free radical release in brain concussion." Free Radic Biol Med **16**(6): 685-91.
- Sen, S. and J. W. Phillis (1993). "alpha-Phenyl-tert-butyl-nitron (PBN) attenuates hydroxyl radical production during ischemia-reperfusion injury of rat brain: an EPR study." Free Radic Res Commun **19**(4): 255-65.

- Sensi, S. L., D. Ton-That, et al. (2003). "Modulation of mitochondrial function by endogenous Zn²⁺ pools." Proc Natl Acad Sci U S A **100**(10): 6157-62.
- Serbest, G., M. F. Burkhardt, et al. (2007). "Temporal Profiles of Cytoskeletal Protein Loss following Traumatic Axonal Injury in Mice." Neurochem Res.
- Shigenaga, M. K., T. M. Hagen, et al. (1994). "Oxidative damage and mitochondrial decay in aging." Proc Natl Acad Sci U S A **91**(23): 10771-8.
- Singh, I. N. and P. G. Sullivan, et al. (2006a) "Time course of post-traumatic mitochondrial oxidative damage and dysfunction in a mouse model of focal traumatic brain injury: implications for neuroprotective therapy." J Cereb Blood Flow Metab Mar 15.
- Singh, I. N. K. M. Carrico, et al. (2006b) "Protective effects of neuroprotective antioxidants penicillamine and tempol against peroxynitrite-induced dysfunction in isolated brain mitochondria." J Neurotrauma **23**:991.
- Skulachev, V. P. (1996). "Why are mitochondria involved in apoptosis? Permeability transition pores and apoptosis as selective mechanisms to eliminate superoxide-producing mitochondria and cell." FEBS Lett **397**(1): 7-10.
- Smith, S. L., P. K. Andrus, et al. (1994). "Direct measurement of hydroxyl radicals, lipid peroxidation, and blood-brain barrier disruption following unilateral cortical impact head injury in the rat." J Neurotrauma **11**(4): 393-404.
- Sorimachi, H., S. Ishiura, et al. (1997). "Structure and physiological function of calpains." Biochem J **328 (Pt 3)**: 721-32.
- Stewart, V. C., M. A. Sharpe, et al. (2000). "Astrocyte-derived nitric oxide causes both reversible and irreversible damage to the neuronal mitochondrial respiratory chain." J Neurochem **75**(2): 694-700.
- Sugioka, K., M. Nakano, et al. (1988). "Mechanism of O₂- generation in reduction and oxidation cycle of ubiquinones in a model of mitochondrial electron transport systems." Biochim Biophys Acta **936**(3): 377-85.
- Sullivan, P. G., A. J. Bruce-Keller, et al. (1999). "Exacerbation of damage and altered NF-kappaB activation in mice lacking tumor necrosis factor receptors after traumatic brain injury." J Neurosci **19**(15): 6248-56.
- Sullivan, P. G., C. Dube, et al. (2003). "Mitochondrial uncoupling protein-2 protects the immature brain from excitotoxic neuronal death." Ann Neurol **53**(6): 711-7.
- Sullivan, P. G., J. D. Geiger, et al. (2000). "Dietary supplement creatine protects against traumatic brain injury." Ann Neurol **48**(5): 723-9.
- Sullivan, P. G., J. N. Keller, et al. (2002). "Cytochrome c release and caspase activation after traumatic brain injury." Brain Res **949**(1-2): 88-96.
- Sullivan, P. G., A. G. Rabchevsky, et al. (2004). "Intrinsic differences in brain and spinal cord mitochondria: Implication for therapeutic interventions." J Comp Neurol **474**(4): 524-34.
- Sullivan, P. G., J. E. Springer, et al. (2004). "Mitochondrial uncoupling as a therapeutic target following neuronal injury." J Bioenerg Biomembr **36**(4): 353-6.

- Sullivan, P. G., M. Thompson, et al. (2000). "Continuous infusion of cyclosporin A postinjury significantly ameliorates cortical damage following traumatic brain injury." Exp Neurol **161**(2): 631-7.
- Sullivan, P. G., M. B. Thompson, et al. (1999). "Cyclosporin A attenuates acute mitochondrial dysfunction following traumatic brain injury." Exp Neurol **160**(1): 226-34.
- Switzer, R. C., 3rd (2000). "Application of silver degeneration stains for neurotoxicity testing." Toxicol Pathol **28**(1): 70-83.
- Taft, W. C., K. Yang, et al. (1992). "Microtubule-associated protein 2 levels decrease in hippocampus following traumatic brain injury." J Neurotrauma **9**(3): 281-90.
- Tatoyan, A. and C. Giulivi (1998). "Purification and characterization of a nitric-oxide synthase from rat liver mitochondria." J Biol Chem **273**(18): 11044-8.
- Thompson, S. N., T. R. Gibson, et al. (2006). "Relationship of calpain-mediated proteolysis to the expression of axonal and synaptic plasticity markers following traumatic brain injury in mice." Exp Neurol **201**(1): 253-65.
- Thurman, D. J., C. Alverson, et al. (1999). "Traumatic brain injury in the United States: A public health perspective." J Head Trauma Rehabil **14**(6): 602-15.
- Turrens, J. F. and A. Boveris (1980). "Generation of superoxide anion by the NADH dehydrogenase of bovine heart mitochondria." Biochem J **191**(2): 421-7.
- Vicente, S., R. Perez-Rodriguez, et al. (2006). "Nitric oxide and peroxynitrite induce cellular death in bovine chromaffin cells: Evidence for a mixed necrotic and apoptotic mechanism with caspases activation." J Neurosci Res **84**(1): 78-96.
- Volbracht, C., B. T. Chua, et al. (2005). "The critical role of calpain versus caspase activation in excitotoxic injury induced by nitric oxide." J Neurochem **93**(5): 1280-92.
- Wada, K., K. Chatzipanteli, et al. (1998). "Role of nitric oxide in traumatic brain injury in the rat." J Neurosurg **89**(5): 807-18.
- Wada, K., K. Chatzipanteli, et al. (1998). "Inducible nitric oxide synthase expression after traumatic brain injury and neuroprotection with aminoguanidine treatment in rats." Neurosurgery **43**(6): 1427-36.
- Wang, K. K. (2000). "Calpain and caspase: can you tell the difference?" Trends Neurosci **23**(1): 20-6.
- Wang, K. K. (2000). "Calpain and caspase: can you tell the difference?, by Kevin K.W. Wang Vol. 23, pp. 20-26." Trends Neurosci **23**(2): 59.
- Watson, B. D. (1993). "Evaluation of the concomitance of lipid peroxidation in experimental models of cerebral ischemia and stroke." Prog Brain Res **96**: 69-95.
- Whiteman, M., J. S. Armstrong, et al. (2004). "Peroxyntirite mediates calcium-dependent mitochondrial dysfunction and cell death via activation of calpains." Faseb J **18**(12): 1395-7.

- Wrogemann, K. and S. D. Pena (1976). "Mitochondrial calcium overload: A general mechanism for cell-necrosis in muscle diseases." Lancet **1**(7961): 672-4.
- Xiong, Y., A. G. Rabchevsky, et al. (2007). "Role of peroxynitrite in secondary oxidative damage after spinal cord injury." J Neurochem **100**(3): 639-49.
- Young, W. (1992). "Role of calcium in central nervous system injuries." J Neurotrauma **9 Suppl 1**: S9-25.
- Zamzami, N., T. Hirsch, et al. (1997). "Mitochondrial implication in accidental and programmed cell death: apoptosis and necrosis." J Bioenerg Biomembr **29**(2): 185-93.
- Zeltcer, G., E. Berenshtein, et al. (1997). "Nitroxide radicals prevent metal-aggravated reperfusion injury in isolated rat heart." Free Radic Res **27**(6): 627-35.
- Zhang, R., E. Shohami, et al. (1998). "Mechanism of brain protection by nitroxide radicals in experimental model of closed-head injury." Free Radic Biol Med **24**(2): 332-40.
- Zhang, Y., O. Marcillat, et al. (1990). "The oxidative inactivation of mitochondrial electron transport chain components and ATPase." J Biol Chem **265**(27): 16330-6.
- Zhou, F., Z. Xiang, et al. (2001). "Neuronal free Ca(2+) and BBB permeability and ultrastructure in head injury with secondary insult." J Clin Neurosci **8**(6): 561-3.

Vita

Ying Deng-Bryant

Date of Birth: August 23, 1978

Place of Birth: Guangzhou/Canton, P.R. China

Education: Bachelor of Science (2001)
Department of Biochemistry
Zhongshan/Sun Yat-Sen University, P.R. China

Research and Professional Experience:

2002 – present Doctoral Degree Candidate
Department of Anatomy and Neurobiology,
The Graduate School at the University of Kentucky

2003 – present Research Assistant
Department of Anatomy and Neurobiology,
University of Kentucky, with Dr. Edward D Hall

2005 – 2005 Teaching Assistant (Anatomy and Physiology, ANA110)
Department of Anatomy and Neurobiology,
University of Kentucky, with Dr. Pamela A Stein

Awards and Professional Honors:

2006 Dissertation Year Fellowship Recipient; University of
Kentucky

- 2007 Finalist, Student Top Poster; 25th Annual National Neurotrauma Society Symposium, Kansas city, MO
- 2007 Travel Grant Recipient; 25th Annual National Neurotrauma Society Symposium, Kansas city, MO
- 2007 Invited Speaker, Open Communication Session; 25th Annual National Neurotrauma Society Symposium, Kansas city, MO
- 2007 Invited Young Investigator Speaker; 8th Annual University of California Symposium, Santa Barbara, CA

Publications:

S.N. Thompson, T.G. Hurst, B.M. Thompson, **Y. Deng**, and E.D. Hall

Changes in Synaptic and Axonal Plasticity following Controlled Cortical Impact Traumatic Brain Injury in Mice, *Exp. Neurol*; 201(1):253-65, September 2006

I.N. Singh*, P.G. Sullivan*, **Y. Deng**, L.H. Mbye and E.D. Hall

Time Course of Post-Traumatic Mitochondrial Oxidative Damage Dysfunction in a Mouse Model of Focal Traumatic Brain Injury, *J. Cereb, Blood Flow & Metab*; 26(11):1407-18, November 2006

Y. Deng, B.M. Thompson, X. Gao and E.D. Hall

Temporal Relationship of Peroxynitrite-Induced Oxidative Damage, Calpain-Mediated Cytoskeletal Degradation and Neurodegeneration after Traumatic Brain Injury, *Exp. Neurol*; 205(1):154-65, May 2007

E.D. Hall, **Y. Deng**, W. Cho and P. G. Sullivan

Evolution of Post-Traumatic Neurodegeneration after Controlled Cortical
Impact Traumatic Brain Injury in Mice and Rats, *submitted for publication*

W. Cho, **Y. Deng**, X. Gao, K.M. Carrico, E.D. Hall* and J. Chen*

Regional and Cell-Type Specific Hippocampal Cell Death Following
Experimental Traumatic Brain Injury, *submitted for publication*

Manuscript in Preparation:

Y. Deng-Bryant, I.N. Singh and E.D. Hall

Neuroprotective Effects of Tempol, a Catalytic Scavenger of Peroxynitrite-
Derived Free Radicals, in the Mouse Controlled Cortical Impact Injury
Model, *in preparation*

Abstracts:

Y. Deng, B.M. Thompson, T.G. Hurst and E.D. Hall

Relationship of Calpain-Mediated Cytoskeletal Degradation and
Neurodegeneration in the Mouse Controlled Cortical Impact Traumatic
Brain Injury Model
Journal of Neurotrauma; 22:1255, 2005

I.N. Singh, P.G. Sullivan, K.M. Day, T.G. Hurst, **Y. Deng**, L.H. Mbye, E.D. Hall

Relationship of Oxidative Damage, Mitochondrial Dysfunction and
Neurodegeneration in the Mouse Controlled Cortical Impact Traumatic
Brain Injury Model

Journal of Neurotrauma; 22:1187, 2005

Y. Deng, B.M. Thompson, T.G. Hurst and E.D. Hall

Peroxynitrite-Induced Oxidative Damage Precedes Cytoskeletal
Degradation and Neurodegeneration after Traumatic Brain Injury

Journal of Neurotrauma; 23:1031, 2006

Y. Deng-Bryant, K.M. Carrico, I.N. Singh and E.D. Hall

Neuroprotective Effects of Tempol, a Catalytic Scavenger of Peroxynitrite-
Derived Free Radicals, in the Mouse Controlled Cortical Impact Injury
Model

Journal of Neurotrauma; 24:1232, 2007

Poster Presentations:

Y. Deng, B.M. Thompson, T.G. Hurst and E.D. Hall

Relationship of Calpain-Mediated Cytoskeletal Degradation and
Neurodegeneration in the Mouse Controlled Cortical Impact Traumatic

Brain Injury Model, 11th Annual Kentucky Spinal Cord & Head Injury

Symposium (KSCHIRT), Louisville, KY; June, 2005

Y. Deng, B.M. Thompson, T.G. Hurst and E.D. Hall

Relationship of Calpain-Mediated Cytoskeletal Degradation and Neurodegeneration in the Mouse Controlled Cortical Impact Traumatic Brain Injury Model, 17th Annual Physical Medicine & Rehabilitation Research Day, Cardinal Hill Rehabilitation Center, Lexington, KY; June, 2005

Y. Deng, B.M. Thompson, T.G. Hurst and E.D. Hall

Relationship of Calpain-Mediated Cytoskeletal Degradation and Neurodegeneration in the Mouse Controlled Cortical Impact Traumatic Brain Injury Model, 2005 Frontiers in Spinal Cord Regeneration Symposium, Seelbach Hilton Hotel Medallion Room, Lexington, KY; June, 2005

Y. Deng, B.M. Thompson, T.G. Hurst and E.D. Hall

Relationship of Calpain-Mediated Cytoskeletal Degradation and Neurodegeneration in the Mouse Controlled Cortical Impact Traumatic Brain Injury Model, 23rd Annual National Neurotrauma Society Symposium, Washington D.C.; November, 2005

Y. Deng, B.M. Thompson, T.G. Hurst and E.D. Hall

Relationship of Calpain-Mediated Cytoskeletal Degradation and Neurodegeneration in the Mouse Controlled Cortical Impact Traumatic Brain Injury Model, Mitochondrial Symposium, Life & Death: the Mitochondrial Perspective, University of Kentucky, Lexington, KY; November, 2005

Y. Deng, B.M. Thompson, T.G. Hurst and E.D. Hall

Peroxynitrite-Induced Oxidative Damage Precedes Cytoskeletal Degradation and Neurodegeneration after Traumatic Brain Injury, 12th Annual Kentucky Spinal Cord & Head Injury Symposium (KSCHIRT), Lexington, KY; June, 2006

Y. Deng, B.M. Thompson, T.G. Hurst and E.D. Hall

Peroxynitrite-Induced Oxidative Damage Precedes Cytoskeletal Degradation and Neurodegeneration after Traumatic Brain Injury, 24th Annual National Neurotrauma Society Symposium, St. Louis, MO; July, 2006

Y. Deng, B.M. Thompson, T.G. Hurst and E.D. Hall

Peroxynitrite-Induced Oxidative Damage Precedes Cytoskeletal Degradation and Neurodegeneration after Traumatic Brain Injury, Bluegrass Chapter Society for Neuroscience – Neuroscience Day, Lexington Conventional Center, Lexington, KY; March, 2007

Y. Deng-Bryant, K.M. Carrico, I.N. Singh and E.D. Hall

Neuroprotective Effects of Tempol, a Catalytic Scavenger of Peroxynitrite-Derived Free Radicals, in the Mouse Controlled Cortical Impact Injury Model, 19th Annual Physical Medicine & Rehabilitation Research Day, Cardinal Hill Rehabilitation Center, Lexington, KY; June, 2007

Y. Deng-Bryant, K.M. Carrico, I.N. Singh and E.D. Hall

Neuroprotective Effects of Tempol, a Catalytic Scavenger of Peroxynitrite-Derived Free Radicals, in the Mouse Controlled Cortical Impact Injury Model, 13th Annual Kentucky Spinal Cord & Head Injury Symposium (KSCHIRT), Louisville, KY; June, 2007

Y. Deng-Bryant, K.M. Carrico, I.N. Singh and E.D. Hall

Neuroprotective Effects of Tempol, a Catalytic Scavenger of Peroxynitrite-Derived Free Radicals, in the Mouse Controlled Cortical Impact Injury Model, Clinical & Translational Science Spring Conference, Civic Center, Lexington, KY; June, 2007

Y. Deng-Bryant, K.M. Carrico, I.N. Singh and E.D. Hall

Neuroprotective Effects of Tempol, a Catalytic Scavenger of Peroxynitrite-Derived Free Radicals, in the Mouse Controlled Cortical Impact Injury Model, 25th Annual National Neurotrauma Society Symposium, Kansas city, MO; July, 2007

